

REMARKS/ARGUMENTS

Status of the claims

With entry of the instant amendment, claims 10, 16, and 17 have been amended and claims 13, 15, 18, and 20-28 have been cancelled. Cancellation of subject matter is without prejudice to subsequent revival for prosecution in a continuation or divisional filing.

The amendments to the claims add no new matter.

Claims 10-12, 14, and 16, 17, 19, and 20 are under examination.

Sequence listing

Applicants have provided a substitute sequence listing. The amendments to the specification add no new matter. The format for the sequence listing of the nucleic acid entered as SEQ ID NO:9 and the polypeptide entered as SEQ ID NO:10 has been corrected. The "FEATURE" for SEQ ID NO:9 found on page 66 of the original Sequence Listing submitted on April 16, 2004, and on page 21 of the Substitute Sequence Listing submitted on October 15, 2004, respectively, included the "/note= "N signifies gap in sequence". Similarly, the "FEATURE" for SEQ ID NO:10 found on page 67 and page 22, respectively, included the "/note= "Xaa signifies gap in sequence". As such, the inclusion of a "gap" in these sequences does not conform to 37 C.F.R. § 1.822(e) which states that "A sequence with a gap or gaps shall be presented as a plurality of separate sequences, with separate sequence identifiers...". For this reason, the nucleic acid originally presented as SEQ ID NO:9 has been assigned SEQ ID NOS:9, 15 and 16, and the polypeptide originally presented as SEQ ID NO:10 has been assigned SEQ ID NOS:10, 17 and 18. This change is reflected in the amendments to paragraphs beginning on pages 4, 13, 14 and 19, where the additional respective SEQ ID NOS: have been inserted.

Amendments to Tables beginning on pages 15, 17 and 18 were made to correct typographical errors. The Table beginning on page 15 has been renumbered from "Table 5" to "Table 6", as there is already a "Table 5" beginning on page 11. Similarly, on page 17, "Table 6" and "Table 7" have been amended to "Table 7" and "Table 8", respectively, and on page 18, "Table 8" has been renumbered as "Table 9".

This amendment is accompanied by a floppy disk containing the above named sequences, SEQ ID NOS:1-92, in computer readable form, and a paper copy of the sequence information which has been printed from the floppy disk.

The information contained in the computer readable disk was prepared through the use of the software program "PatentIn" and is identical to that of the paper copy.

Claim objection

The objection to claim 17 has been addressed by the amendment to remove the period that inadvertently was included in the middle of the claim.

Rejection under 35 U.S.C. § 101, utility

Claims 10-19 are rejected as allegedly lacking utility. The Examiner alleges that there is no immediately obvious patentable use for Robo 1 antibodies, because, according to the Examiner, the specification fails to describe a biological function of human Robo 1. The Examiner contends that that the function of Robo-1 in axon growth that is disclosed in the specification is based only on homology and as such, is not credible. Applicants respectfully traverse this rejection.

First, the specification does in fact provide support for a biological function for Robo in the regulation of nerve cell function and morphology (page 3, line 4). The specification describes a new family of neuronal guidance receptors, robo proteins, and characterizes *robo* across various species including *Drosophila*, *C. elegans*, human, and mouse. The specification teaches that antibodies can be used, *e.g.*, in applications where pathology relates to improper or undesirable axon outgrowth, orientation or inhibition thereof (*e.g.*, page 13, lines 10-19). and that Robo inhibitors can be used to promote nerve cell growth (*e.g.*, page 3, line 10, first full paragraph). The specification also provides experimental evidence that robo is involved in axon growth. For example, the examples provide experiments showing that robo is expressed on longitudinally-projecting growth cones and axons (page 29, lines 12-17 of the first complete paragraph). The application additionally provides evidence that *robo1* is involved in mammalian nerve cell growth. The application demonstrates that rat *robo1* RNA is expressed in the rat

embryonic spinal cord (see, e.g., the last paragraph on page 31 bridging to page 32. This indicates that it encodes the function equivalent of Drosophila Robo1 (page 32, lines 11-13).

Robo compositions, e.g., robo-specific binding agents such as antibodies, therefore have a utility for diagnostic and therapeutic applications involving nerve growth. In addition, Robo antibodies have a readily apparent use in a laboratory setting, explained in detail below. These utilities meet the standards set forth in the MPEP at § 2107: they are credible, substantial, and specific.

Guidelines For Utility--MPEP § 2107

A. An Asserted Utility Must be Specific and Substantial

"[A] disclosure that identifies a particular biological activity of a compound and explains how that activity can be utilized in a particular therapeutic application of the compound does contain an assertion of specific and substantial utility for the invention." (MPEP § 2107.02.II.A)

The robo-related compositions have utility for the treatment of diseases or conditions related to abnormal axon orientation or growth

As indicated above, assertions of utility are present in the specification. Exemplary passages are also detailed below. Briefly, the specification teaches that Robo is involved in axon guidance, e.g., midline crossing (e.g., last paragraph of page 2, bridging to page 3) and that Robo polypeptides and antibodies can be used to modulate neuronal cell growth. For example, the inventors teach that Robo-specific binding agents can be used for pharmaceutical development and diagnostic and therapeutic purposes, e.g., to promote nerve cell growth (page 3, lines 9-15; page 4, lines 13-16) and/or for the treatment of pathology, wound repair incompetency or prognosis that is associated with improper or undesirable axon outgrowth, orientation or inhibition thereof (e.g., page 13, lines 10-19).

The application therefore identifies a particular biological activity of a Robo compound and explains how that activity can be utilized, e.g., in a pathological condition involving neuronal cell growth. Accordingly, the biological utility is a specific and substantial utility as set forth in the MPEP.

B. An Asserted Utility Creates a Presumption of Utility

"If the asserted utility is credible (i.e., believable based on the record or the nature of the invention), a rejection based on "lack of utility" is not appropriate." (MPEP § 2107.02.III.B)

"[T]o overcome the presumption of truth that an assertion of utility by the applicants enjoys, Office personnel must establish that it is more likely than not that one of ordinary skill in the art would doubt (i.e., "question") the truth of the statement of utility." (MPEP § 2107.02.III.B)

There is no evidence that one of skill would doubt the asserted utility

The biological utility is also credible. The Patent Office must treat as true a statement of fact made by an applicant in relation to an asserted utility, unless countervailing evidence can be provided that shows that one of ordinary skill in the art would have a legitimate basis to doubt the credibility of such a statement. The rejection appears to assert that the utility is not believable, because, according to the Examiner, the asserted utility is only based on homology among the Robo family members. However, as noted above, the specification in fact provides experimental evidence supporting the asserted utility. Furthermore, provided herewith is additional evidence to support the contention that one of skill would believe that the robo-related compositions are useful for identifying modulators that can be used in disease or conditions involving axon growth. Appendices A-D provide exemplary gene expression data showing that robo is expressed in adult tissues and is associated with conditions or diseases involving neuronal growth.

Marillat *et al.*, *J. Comp Neur.* 442:130-155, 2002 (Appendix A) provides evidence that robo is also expressed in adult mammalian tissues. Marillat describes robo expression in the rat central nervous system from embryonic stages to adult age. The abstract of Marillat *et al.*, teaches that slit (a robo ligand) and robo expression are upregulated postnatally. Page 152, second column, first full paragraph further teaches that the maintained high level expression of slit proteins and their receptors, *i.e.*, robo proteins, in adult neurons suggest that the function of

the robo and slit proteins is not restricted to the control of axonal pathfinding and neuronal migration, but they are involved in synaptic plasticity.

Robo is also expressed in the human adult central nervous system. Appendix B provides data from the online database expression source Gene Normal Tissue Expression (GeneNote, http://bioinfo2.weizmann.ac.il/cgi-bin/genenote/home_page.pl). These data are from 1) hybridization studies using an array to obtain expression profiles of polyA+ RNA from twelve normal human tissues and 2) electronic Northern analysis. The array data and electronic northern are generated as described in the GeneNote methodology section, also provided in Appendix B. In brief, the data in the electronic northern is based on the origin and number of ESTs in Genbank that represent a locus. The data are derived from the Unigene dataset, which was mined for information about the number of unique clones per gene. Both the array analysis and electronic expression analysis show that robo is expressed in normal adult nervous tissue.

Further, enclosed is a paper showing the robo is expressed in injured central nervous system and spinal cord (Wehrle, *et al.*, *Eur J Neurosci.* 22:2134-44, 2005, Appendix C, see, *e.g.*, the abstract).

In summary, the supplemental material provided in Appendices A-D provide additional evidence supporting Applicants' assertion that robo proteins, including robo 1, play a role in the biological process of axon guidance and axon outgrowth, and that the claimed compositions have diagnostic and therapeutic utilities, *e.g.*, use for identifying modulators of robo function, which modulators can be used for treating conditions relating to abnormalities of axon growth. "If the record as a whole would make it more likely than not that the asserted utility for the claimed invention would be considered credible by a person of ordinary skill in the art, the Office cannot maintain the rejection" (MPEP §2107.02.VI). Thus, in order to apply a utility rejection to the instant claims, the Examiner must provide additional evidence that one of skill, in considering the totality of the evidence, would not be likely to believe the asserted utility. In the absence of such evidence, the asserted utility meets the requirements for credibility.

C. Many Research Tools Have a Clear, Specific, and Unquestionable Utility

"Some confusion can results when one attempts to label certain types of inventions as not being capable of having a specific and substantial utility based on the setting in which the invention is to be used. One example is inventions to be used in a research or laboratory setting. Many research tools... have a clear, specific and unquestionable utility.... An assessment that focuses on whether an invention is useful only in a research setting...does not address whether the invention is in fact "useful" in a patent sense." (MPEP § 2107.01)

The claimed subject matter has specific and substantial utility in a laboratory setting

Robo proteins, robo binding agents, and modulators of robo also have utility in a laboratory setting as a research tool for studies involving neuron growth. As indicated above, the MPEP explicitly cautions against labeling inventions as lacking specific and substantial utility based on the setting, such as a laboratory, in which the invention is to be used. In the case of robo and its associated compositions, utility in a laboratory setting is both specific and substantial.

A utility is specific if it is not applicable to a broad category in general (MPEP § 2107.01.I). As noted above, robo proteins play a role in axon guidance, for example, they are important in controlling midline crossing. This function is not applicable to a broad category, *i.e.*, proteins, in general. Common sense dictates that one of skill in the art employing robo antibodies (or other robo-related reagents) in a laboratory is in fact likely using robo compositions because of the role of robo in axon outgrowth and guidance, not simply non-specific reagents. Accordingly, in light of the guidelines provided in the MPEP, the utility is specific to the subject matter claimed.

The use of robo proteins and related compositions in a laboratory setting is also a substantial utility. The MPEP (§2107) defines a substantial utility as a real world use. Robo proteins and related compositions, *e.g.*, antibodies, have a practical use, real-world use. For example, antibodies to robo proteins are offered for sale by Santa Cruz Biotechnology, Inc. s (see, Appendix D, a printout of available antibodies to various robo proteins). Although this is of course a post-filing listing of the antibodies, such antibodies must have a real-world use, or

there would be no market for them. Even though this market exists within the context of research, rather than diagnostics or therapeutics, this does not negate the utility of the claimed subject matter. A simple search of the literature shows that axon guidance is an active area of investigation, and hence, provides a practical and specific context for using robo antibodies in a laboratory setting..

Last, this is a credible utility. In order to find to the contrary, the Office personnel would have to establish that it would be more likely than not that one of ordinary skill in the art would doubt the truth of the utility. (MPEP § 2107.02.III.A). The rejection does not provide evidence that an ordinary artisan would believe that this utility is not real.

In view of the foregoing, the invention meets the requirements for utility. Applicants therefore respectfully request withdrawal of the rejection.

Rejection under 35 U.S.C. § 112, first paragraph written description

Claims 10-12, 14, 15, 18, and 19 are rejected as allegedly lacking written descriptive support. In particular, the Examiner alleges that the specification does not properly describe an antibody that binds to a polypeptide that has at least 95% identity to SEQ ID NO:8. Although Applicants disagree, in the interests of expediting prosecution, claim 10 has been amended to recite that the antibody specifically binds to SEQ ID NO:8.

In view of the foregoing, Applicants respectfully request withdrawal of the rejection.

Rejections under 35 U.S.C. § 112, second paragraph

Claims 10-19 are rejected as allegedly indefinite over the recitation of "Robo" in the terms "Rob-specific" and "Robo-mediated signaling" in claims 10 and 18, respectively. Although Applicants disagree, as the claims recite specific structural features that allow one of skill to determine the metes and bounds of the inventions, in the interests of expediting prosecution, the claims have been amended to delete the term "Robo". Applicants therefore respectfully request withdrawal of the rejection.

Rejection under 35 U.S.C. § 102(e)

Claims 10-19 are rejected as allegedly anticipated by McCarthy *et al.* in U.S. Patent Publication No. 2002/0150988. The Examiner contends that McCarthy discloses a polypeptide having 100% identity to the polypeptide 68-167 of SEQ ID NO:8. The sequence at issue in McCarthy, depicted in Figure 3, was first included in provisional application 60/062,017, filed October 10, 1997. Submitted herewith is a Rule 131 Declaration establishing that the invention was made in the United States prior to October 10, 1997, thus removing McCarthy *et al.* as prior art.

In Exhibit A to the attached Declaration, Applicants provide evidence that they obtained the sequence to human Robo-1 before October 10, 1997. Exhibit A, with dates redacted therefrom, is a printout of laboratory records showing the amino acid sequence of human Robo-1. The raw sequence file data were saved to an optical disk. The pages in Exhibit A show a computer analysis of sequence data comparing the human Robo-1 (H-Robo1 pep) sequence to those of other Robo proteins. The amino acid sequence was determined based on nucleic acid sequence. H-Robo1 pep includes the extracellular domain (five immunoglobulin domains and three fibronectin domains). Amino acids 68-167 of H-Robo1 pep are the first immunoglobulin domain and correspond to amino acids 68-167 of SEQ ID NO:8 in the application.

In view of the foregoing, it is respectfully submitted that the evidence provided in Exhibit A unequivocally establishes that the basic inventive concept of the claimed invention was conceived of and reduced to practice prior to October 10, 1997. Withdrawal of the rejection is respectfully requested.

Double patenting

This potential objection is moot in view of the cancellation of claim 15.

Additional Species

In view of the foregoing, Applicants respectfully request that the Examiner extend examination to additional species.

Appl. No. 10/826,812
Amdt. dated August 13, 2007
Reply to Office Action of February 12, 2007


PATENT

CONCLUSION

Applicants believe all claims now pending in this Application are in condition for allowance. The issuance of a formal Notice of Allowance at an early date is respectfully requested.

If the Examiner believes a telephone conference would expedite prosecution of this application, please telephone the undersigned at 415-576-0200.

Respectfully submitted,



Jean M. Lockyer
Reg. No. 44,879

TOWNSEND and TOWNSEND and CREW LLP
Two Embarcadero Center, Eighth Floor
San Francisco, California 94111-3834
Tel: 415-576-0200
Fax: 415-576-0300
JML:jml
61098022 v1

Appendix A

Spatiotemporal Expression Patterns of *slit* and *robo* Genes in the Rat Brain

VALÉRIE MARILLAT,¹ OLIVER CASES,¹ KIM TUYEN NGUYEN-BA-CHARVET,¹ MARC TESSIER-LAVIGNE,² CONSTANTINO SOTELO,¹ AND ALAIN CHÉDOTAL^{1*}

¹INSERM U106, Bâtiment de Pédiatrie, Hôpital de la Salpêtrière, 75013 Paris, France

²Howard Hughes Medical Institute, Department of Anatomy and Department of Biochemistry and Biophysics, University of California, San Francisco, California 94143-0452

ABSTRACT

Diffusible chemorepellents play a major role in guiding developing axons toward their correct targets by preventing them from entering or steering them away from certain regions. Genetic studies in *Drosophila* revealed a repulsive guidance system that prevents inappropriate axons from crossing the central nervous system midline; this repulsive system is mediated by the secreted extracellular matrix protein Slit and its receptors Roundabout (Robo). Three distinct *slit* genes (*slit1*, *slit2*, and *slit3*) and three distinct *robo* genes (*robo1*, *robo2*, *rig-1*) have been cloned in mammals. However, to date, only Robo1 and Robo2 have been shown to be receptors for Slits. In rodents, Slits have been shown to function as chemorepellents for several classes of axons and migrating neurons. In addition, Slit can also stimulate the formation of axonal branches by some sensory axons. To identify Slit-responsive neurons and to help analyze Slit function, we have studied, by in situ hybridization, the expression pattern of *slits* and their receptors *robo1* and *robo2*, in the rat central nervous system from embryonic stages to adult age. We found that their expression patterns are very dynamic: in most regions, *slit* and *robo* are expressed in a complementary pattern, and their expression is up-regulated postnatally. Our study confirms the potential role of these molecules in axonal pathfinding and neuronal migration. However, the persistence of *robo* and *slit* expression suggests that the couple *slit/robo* may also have an important function in the adult brain. *J. Comp. Neurol.* 442: 130–155, 2002. © 2002 Wiley-Liss, Inc.

Indexing terms: olfactory system; hippocampus; thalamus; cerebellum; axon guidance; migration

In the past decade, a large number of axon guidance molecules has been characterized (Tessier-Lavigne and Goodman, 1996). Remarkably, many of these novel molecules are diffusible, secreted by cells located at a distance from the growth cones they are acting on. The *slit* family is the most recently discovered family of chemotropic factors (Brose and Tessier-Lavigne, 2000). The first *slit* was identified in *Drosophila* embryo as a gene involved in the patterning of larval cuticle (Nusslein-Volhard et al., 1984). Subsequently, it was shown that Slit is synthesized in the central nervous system by midline glia cells and that, in its absence, longitudinal and commissural axons converge and coalesce abnormally at the midline (Rothberg et al., 1988, 1990; Sonnenfeld and Jacobs, 1994). More recent studies have shown that Slit is a chemorepulsive factor and a key regulator of midline crossing and axonal fasciculation (Battye et al., 1999; Rajagopalan et al., 2000a,b; Simpson et al., 2000a,b). Vertebrate homologues have since been found in virtually all taxa, from amphibians (Li

et al., 1999), fishes (Halloran et al., 2000; Yeo et al., 2001), birds (Vargesson et al., 2001), to rodents and humans (Holmes et al., 1998; Itoh et al., 1998; Brose et al., 1999; Yuan et al., 1999). In mammals, three *slit* genes (*slit1*–*slit3*) have been cloned. All *slits* encode large extracellular matrix proteins, composed from their N-terminus to their C-terminus of a long stretch of leucine-rich repeats, seven (in flies) to nine (in vertebrates) EGF repeats, flanking a domain named ALPS (Rothberg and Artavanis-Tsakonas,

Grant sponsor: Institut de la Santé et de la Recherche Médicale; Grant sponsor: Ministère de la Recherche et de la Technologie (ACI); Grant sponsor: Association pour la Recherche sur le Cancer; Grant number: 5249.

*Correspondence to: Alain Chédotal, INSERM U106, Bâtiment de Pédiatrie, Hôpital de la Salpêtrière, 47 Bd de l'Hôpital, 75013 Paris, France. E-mail: chedotal@infobiogen.fr

Received 22 June 2001; Revised 16 August 2001; Accepted 29 September 2001

1992), LNS (Rudenko et al., 1999), or LG module (Hohe-
nester et al., 1999). Human Slit2 and *Drosophila* Slit are
cleaved in vitro and in vivo into two fragments, a 140-kDa
N-terminal one and a 60-kDa C-terminal one (Brose et al.,
1999; Kidd et al., 1999; Wang et al., 1999). These frag-
ments have different biochemical characteristics. The
C-terminal fragment is more diffusible than the larger
N-terminal and full-length fragments, which are more
tightly associated to the cell membrane (see below). In the
vertebrate central nervous system (CNS) Slits have also
been shown to be repulsive factors for developing axons
projecting from the spinal cord (Brose et al., 1999), the
olfactory bulb (Li et al., 1999; Nguyen-Ba-Charvet et al.,
1999), the dentate gyrus (Nguyen-Ba-Charvet et al.,
1999), the retina (Erskine et al., 2000; Niclou et al., 2000;
Ringstedt et al., 2000), and the cortex (Shu and Richards,
2001). Interestingly, in rodents *slit2* can stimulate axonal
elongation and branch formation of sensory axons from
the dorsal root ganglia (Wang et al., 1999). Moreover, in
vivo and in vitro experiments suggest that Slit proteins
control the migration of muscle precursors in fly embryos
(Kidd et al., 1999; Kramer et al., 2001), of mesodermal
cells in zebrafish embryos (Halloran et al., 2000; Yeo et al.,
2001) and of several categories of tangentially migrating

telencephalic interneurons in organotypic cultures (Hu,
1999; Wu et al., 1999; Zhu et al., 1999). Structure-function
studies have shown that Slit's repulsive activities are
associated with the leucine-rich repeats (Chen et al., 2001;
Nguyen-Ba-Charvet et al., 2001a).

One major breakthrough toward the understanding of
Slit function has been the recent discovery that the
Roundabout (Robo) proteins are Slit receptors (Brose et
al., 1999; Kidd et al., 1999; Li et al., 1999). The first *robo*
gene, *robo1*, was identified in *Drosophila* with a compre-
hensive screen for genes controlling CNS midline crossing
(Seeger et al., 1993). In *robo1* mutants, ipsilateral axons
that normally avoid the midline cross it and commissural
axons cross and recross it repeatedly (Seeger et al., 1993).
Robo is an evolutionary conserved family of transmem-
brane receptors (Zallen et al., 1998; Kidd et al., 1999;
Rajagopalan et al., 2000b; Simpson et al., 2000b). They
define a small subgroup within the immunoglobulin su-
perfamily characterized by the presence of five immuno-
globulin (Ig)-like domains followed by three fibronectin
type III (FNIII) repeats, a transmembrane portion, and a
long cytoplasmic tail containing robo-specific motifs (Kidd
et al., 1998a; Rajagopalan et al., 2000b; Simpson et al.,
2000b). To date, three *robo* genes have been found in flies

Abbreviations

Ac	accumbens nuclei	LRN	lateral reticular nucleus
AH	anterior hypothalamic nucleus	LS	lateral septum
AOB	accessory olfactory bulb	LSO	lateral superior olive
AON	anterior olfactory nucleus	m	mitral cell layer
AONe	anterior olfactory nucleus pars externalis	MA	medial nucleus of the amygdala
AONI	anterior olfactory nucleus pars lateralis	MAO	medial accessory olive
Aq	aqueduct	mes	mesencephalon
Ar	arcuate hypothalamic nucleus	MG	medial geniculate nucleus
BM	basomedial nucleus of the amygdala	MGv	ventral medial geniculate nucleus
CA1	cornu ammonii 1 field	mHb	medial habenula
CA3	cornu ammonii 3 field	OB	olfactory bulb
CL	central lateral nucleus	oe	olfactory epithelium
CM	central median nucleus	PAG	periaqueductal gray
ChP	choroid plexus	Pavh	paraventricular hypothalamic nucleus
CPu	caudate putamen	Pe	periventricular hypothalamic area
Cu	cuneate nucleus	pn	pontine nucleus
DAO	dorsal accessory olive	PO	principal olive
DB	diagonal band of Broca	PV	paraventricular thalamic nucleus
DG	dentate gyrus	Rho	rhombencephalon
di	diencephalon	RMC	red magnocellularis nucleus
dLG	dorsal lateral geniculate nucleus	RMS	rostral migratory stream
Dmh	dorsomedial hypothalamic nucleus	Rt	reticular nucleus
DN	deep cerebellar nuclei	S	septum
dTH	dorsal thalamus	SC	superior colliculus
egl	external granular layer	SN	substantia nigra
ep	external plexiform layer	Sth	subthalamic nucleus
Et	epithalamus	SVZ	subventricular zone
fp	floor plate	tel	telencephalon
g	glomerular layer	Tu	olfactory tubercle
GCL	granular cell layer	Tz	trapezoid body nucleus
ge	ganglionic eminence	vLG	ventral lateral geniculate nucleus
Gr	gracile nucleus	VM	ventromedial thalamic nucleus
hil	hilus	VMH	ventromedial hypothalamic nucleus
IC	inferior colliculus	VNO	vomeroneasal organ
ic	islands of Calleja	VP	ventral pallidum
ig	indusium griseum	VPL	ventral posterior lateral nucleus
IP	interpeduncular nucleus	VPM	ventral posterior medial nucleus
IO	inferior olive	Vs	spinal trigeminal nucleus
LA	lateral nucleus of the amygdala	VTA	ventral tegmental area
LD	laterodorsal thalamic nucleus	vTH	ventral thalamus
lge	lateral ganglionic eminence	VZ	ventricular zone
LH	lateral hypothalamic nucleus	XII	hypoglossal nucleus
IHb	lateral habenula	Zi	zona incerta
LL	lateral lemniscus	zli	zona limitans intrathalamica
LP	lateroposterior thalamic nucleus		

(Kidd et al., 1998a; Rajagopalan et al., 2000a; Simpson et al., 2000b) and in mammals (Brose et al., 1999; Li et al., 1999; Yuan et al., 1999). In *Drosophila*, genetic and biochemical evidence indicates that Slit is a ligand of the robo1–robo3 receptors (Kidd et al., 1999; Rajagopalan et al., 2000b; Simpson et al., 2000b). Similarly, in vitro studies have shown that, in mammals, Slit1 (Yuan et al., 1999), Slit2 (Brose et al., 1999), and Slit3 (M.T.L. and A.C., unpublished data) bind with a similar affinity to Robo1 and Robo2 and that Slit binding is mediated in its N-terminal portion (Nguyen-Ba-Charvet et al., 2001a). However, it is not known whether Rig-1 (Yuan et al., 1999), the third vertebrate Robo-like protein, which lacks some cytoplasmic domains found in Robo1 and Robo2, is a receptor for Slit. It also remains to be determined whether in mammals Slit functions are mediated by Robos. Despite the importance of these molecules, the spatiotemporal expression of vertebrate *robo* and *slit* genes has only been partially reported, mostly at early embryonic stages (Holmes et al., 1998; Itoh et al., 1998; Brose et al., 1999; Liang et al., 1999; Nguyen-Ba-Charvet et al., 1999; Yuan et al., 1999; Erskine et al., 2000; Niclou et al., 2000; Ringstedt et al., 2000; Shu and Richards, 2001). In this study, we have performed an extensive in situ hybridization analysis of the expression patterns of *slits* and their receptors *robo1* and *robo2*, in an attempt to identify neurons that could respond to Slits and also to gain further insights into Slit function in the developing and adult brain.

MATERIALS AND METHODS

Animals

Wistar (IFFA-Credo, Lyon, France) and Sprague-Dawley rats (Janvier, Le Genest Saint Isle, France) were analyzed at different prenatal (embryonic day [E] 12, E15, E18, and E20) and postnatal ages (postnatal day [P] 1, P3, P5, P10, and adult). The day of the vaginal plug was counted as embryonic day 0 (E0), and the day of birth as postnatal day 0 (P0). Pregnant dams were anesthetized with chloral hydrate (350 mg/kg). All animal procedures were conducted in strict compliance with approved institutional protocols.

E12–E15 embryos were fixed by immersion in 4% paraformaldehyde in 0.1 M phosphate buffer, pH 7.4 (PFA). Embryos from E20 and postnatal rats until P5 were perfused transcardially with 4% PFA. Whole embryos or brains were postfixed overnight in the same fixative, cryoprotected in 10% sucrose, frozen in isopentane (–55°C), and stored at –80°C until sectioning. P10 and adults were anesthetized and decapitated, and brains were immediately frozen in isopentane and stored at –80°C. Serial coronal, horizontal, and sagittal sections (25 µm) were cut with a cryostat and stored at –80°C before hybridization.

Cloning of rat Slit3 cDNA

Total RNAs from E15 brain were extracted with Trizol procedures (Invitrogen, Cergy-Pontoise, France). cDNAs were synthesized by using the first strand cDNA synthesis kit (Amersham, Orsay, France). cDNAs were used as template in a polymerase chain reaction (PCR) reaction. By using the following primers in PCR: primer 1, 5'-CTGGAGACCATGCACGGACGCATGTTC-3', and primer 2, 5'-AGTGGGCTCCTGCTGTACCACAATGCA-3', a single

1,749-bp fragment was yielded. This PCR product was identified by sequencing as a 1,749-bp partial rat slit3 sequence (nucleotides 1,777 to 3,426) and was cloned into pCR-II-topo vector (Invitrogen, Groningen, The Netherlands).

Riboprobes synthesis

cDNAs encoding rat *slit1*, *slit2*, *robo1*, and *robo2* were described elsewhere (Brose et al., 1999). The in vitro transcription was carried out by using the Promega kit (Promega, Charbonnières, France) and probes were labeled either with digoxigenin-11-d-UTP (Roche Diagnostics, Meylan, France) or ³⁵S-UTP (>1,000 Ci/mM; Amersham).

In situ hybridization with digoxigenin-labeled riboprobes

Tissue sections from E12 to E20 embryos and postnatal rats until P5 were hybridized with digoxigenin-labeled riboprobes. Tissue sections were postfixed for 10 minutes in 4% PFA, washed in PBS (pH 7.4), treated with proteinase K (10 µg/ml; Invitrogen) for 7 minutes 30 seconds, postfixed for 5 minutes in 4% PFA, washed in PBS, acetylated, washed in PBS 1% Triton X-100. Slides were incubated 2 hours at room temperature with hybridization buffer (50% formamide, 5× SSC, 1× Denhardt's, 250 µg/ml yeast tRNA, and 500 µg/ml herring sperm DNA, pH 7.4). Then, tissue sections were hybridized overnight at 72°C with riboprobes (1/200). After hybridization, sections were rinsed for 2 hours in 2× SSC at 72°C, and blocked in 0.1 M Tris, pH 7.5, 0.15 M NaCl (B1) containing 10% normal goat serum (NGS) for 1 hour at room temperature. After blocking, slides were incubated overnight at room temperature with anti-DIG antibody conjugated with the alkaline phosphatase (1/5,000, Roche Diagnostics) in B1 containing 1% NGS. After washing in B1 buffer, the alkaline phosphatase activity was detected by using nitroblue tetrazolium chloride (337.5 µg/ml) and 5-bromo-4-chloro-3-indolyl phosphate (175 µg/ml) (Roche Diagnostics). Sections were mounted in Mowiol (Calbiochem/Merck, Carlsbad, Germany).

In situ hybridization with ³⁵S-labeled riboprobes

Tissue sections of P10 and adult brains were hybridized with ³⁵S-labeled riboprobes. Sections were post-fixed 15 minutes in 4% PFA, washed in PBS, acetylated, washed in PBS, dehydrated in graded ethanols and air-dried. Sections were covered with hybridization buffer containing 5.10⁵ cpm/µl of riboprobes (50% formamide, 0.3 M NaCl, 20 mM Tris-HCl pH 7.4, 5 mM EDTA, 1× Denhardt's, 10% dextran sulfate, 10 mM DTT, 10 mM NaH₂PO₄, pH 8.0 and 250 µg/ml yeast tRNA, pH 7.4). Slides were hybridized overnight at 48°C in humid chamber. After hybridization, sections were rinsed for 30 minutes in 5× SSC at 48°C and for 20 minutes in 2.5× SSC at 60°C. Sections were then treated for 30 minutes with 20 mg/ml Rnase A at 37°C, washed in 2× SSC and in 0.1× SSC for 15 minutes each, dehydrated, and air-dried. Autoradiograms were obtained by apposing the sections to hyperfilms (βmax, Amersham) for 3 days. For histologic analyses, the slides were dipped in photographic emulsion (NTB2, Kodak) and exposed for approximately 12 days. Then, slides were developed at 14°C D19 (Kodak), fixed in AL4 (Ilford) and subsequently rinsed, dehydrated, and mounted with cyto seal 60 (Stephens Scientific, Riverdale,

TABLE 1. Spatiotemporal Distribution of *robo1* (1) and *robo2* (2) mRNA in the Telencephalon¹

Telencephalon	E15	E18	E20	P0	P5	P10	Adult
Olfactory system							
Olfactory epithelium	-2	-2	nd	nd	nd	nd	-2
Mitral cells	-2	-2	12	12	12	12	12
Anterior olfactory n.		12	12	12	12	12	12
Accessory olfactory bulb	-2	-2	-2	-2	12	12	12
Cortex							
Marginal zone	-2	--	--	--	--	--	--
Cortical plate	1-	12	12				
Intermediate zone	-2	-2	-2				
Subventricular zone ²	-2	12	12				
II-III				-2	12	12	12
IV				--	--	--	--
V				12	12	12	12
VI				-2	-2	12	12
Entorhinal	--	12	12	12	12	12	12
Piriform	-2	-2	-2	-2	12	12	12
Retrosplenial	--	--	--	1-	1-	1-	1-
Induseum griseum	--	1-	1-	1-	1-	1-	1-
Tenia tecta	--	1-	1-	1-	1-	12	12
Hippocampal system							
CA1	1-	1-	12	12	12	12	12
CA3	1-	1-	12	12	12	12	12
Dentate gyrus	--	--	--	1-	12	12	12
Subiculum	--	-2	-2	-2	-2	-2	-2
Basal ganglia							
Caudate putamen	12	12	12	12	12	12	12
Accumbens n.	12	12	12	12	12	12	12
Globus pallidus (lateral)	12	12	12	12	12	12	12
Basal telencephalon							
Septum	--	--	--	--	--	--	--
Islands of Calleja	--	1-	1-	1-	1-	1-	1-
Olfactory tubercle	-2	12	12	12	12	1-	1-
Amygdaloid complex	--	1-	12	12	12	12	12

¹ E, embryonic day; P, postnatal day; n., nucleus; nd, not determined; --, not detected.² From P0, we refer to the anterior subventricular zone.

NJ). For the determination of labeled structures, we mostly used the nomenclature of Paxinos et al. (1991), for embryos, and from Paxinos and Watson (1986) for postnatal ages. Images were captured with a Zeiss Axiophot microscope, scanned with Nikon Coolsan II, and processed with Photoshop 6.0 (Adobe).

RESULTS

Olfactory system

slit's and *robo*'s mRNAs were detected in every component of the olfactory system, but in most cases, each neuronal population expressed only one of the receptors or one of the ligands (Tables 1 and 2).

Main olfactory system. Olfactory neurons in the olfactory epithelium were found to express high levels of *robo2* mRNAs, as early as E12–E13 (Fig. 1A,B), shortly after they have sent their first axons toward the olfactory bulb (Lopez-Mascaraque et al., 1996). This pattern of *robo2* expression was maintained at E18 (Fig. 1E; Table 1) and in the adult olfactory epithelium (Fig. 1C; Table 1). *slit1* mRNA was first detected in olfactory neurons from E18 (Fig. 1F; Table 2). The comparison of *robo2* and *slit1* expression pattern on adjacent sections showed that *slit1* was only expressed in restricted zones of the olfactory epithelium, although we did not try to determine whether these correspond to known olfactory projection zones (Yoshihara et al., 1997). *robo1*, *slit2*, and *slit3* transcripts were not detected in the olfactory epithelium at all embryonic stages (Fig. 1D; Table 1 and data not shown). However, at E18, *slit2* was highly expressed in mesenchymal cells surrounding the olfactory epithelium (not shown). Olfactory axons are known to contain mRNAs, and at P5, *slit3* mRNAs could be found in olfactory axons ending in

the glomeruli, indicating that olfactory receptor neurons also expressed *slit3* at this stage (Fig. 2I).

In the olfactory bulb, *robo1* expression was detected around birth in mitral cells (Fig. 2A; Table 1). In the adult, mitral cells still expressed high levels of *robo1* mRNAs, but also periglomerular cells in the glomerular layer and some neurons in the external plexiform layer, corresponding probably to tufted cells (Fig. 2B). Similarly, mitral cells and most interneurons in the olfactory bulb expressed *robo2* from E13 onward (Figs. 1E, 2C,D; Table 1). From P5, it became clear that *robo2* transcripts were found in all OB neurons to the exception of periglomerular cells (compare Fig. 2C,D with 2B). From E15 to E18, only *slit1* was found in the olfactory bulb, whereas *slit2* and *slit3* were not detected. During this period *slit1* was expressed in subsets of mitral cells and in scattered cells around the granular cell layer (Fig. 1F; see also Nguyen-Ba-Charvet et al., 1999). It decreased at later stages and was not detected in the olfactory bulb of newborns (Fig. 2E). However, in the adult, *slit1* was highly expressed in the granule cell layer, and at a lower level in mitral cells, periglomerular cells, and neurons of the external plexiform layer (Fig. 2F). *slit2* was still absent from the OB at P5 (Fig. 2G; Table 2), but in the adult, it was weakly expressed in granule cells and periglomerular cells (Fig. 2H). *slit3* expression appeared around birth, and at P5 *slit3* was found in the mitral cells (Fig. 2I; Table 2). From P10, *slit3* expression decreased and it was not detected in the adult olfactory bulb (Fig. 2J).

In organotypic cultures, Slit1 and Slit2 proteins can repel OB interneurons migrating through the rostral migratory stream (RMS) from the subventricular zone (SVZ) to the OB (Hu, 1999; Wu et al., 1999). Moreover, Robo ectodomain can block this repulsive effect. However, the

TABLE 2. Spatiotemporal Distribution of *slit1* (1), *slit2* (2), and *slit3* (3) mRNA in the Telencephalon¹

Telencephalon	E15	E18	E20	P0	P5	P10	Adult
Olfactory system							
Olfactory epithelium	1--	1--	nd	nd	nd	nd	nd
Mitral cells	1--	1--	--3	--3	--3	--	--
Anterior olfactory n.		--3	-23	-23	-23	123	123
Accessory olfactory bulb	---	---	---	---	1-3	1-3	1-3
Cortex							
Marginal zone	--3	---	---				
Cortical plate	1--	1--	12-				
Intermediate zone	---	---	---				
Subventricular zone ²	---	---	---				
II-III				---	1--	1--	1--
IV				---	--3	--3	--3
V				123	123	123	123
VI				1--	1-3	1-3	1-3
Entorhinal	123	123	123	123	123	123	123
Piriform	--3	1-3	1-3	1-3	123	123	123
Retrosplenial	---	---	---	1-3	1-3	1-3	1-3
Induseum griseum	---	1-3	1-3	1-3	1-3	1-3	1-3
Tenia tecta	---	1-3	1-3	1-3	1-3	1-3	1-3
Hippocampal system							
CA1	1-3	1-3	1-3	-23	-23	123	1-3
CA3	123	123	123	123	123	123	123
Dentate gyrus	-2-	-23	-23	-23	-23	123	123
Subiculum	1-	1-3	1-3	1-3	1-3	1-3	1-3
Basal ganglia							
Caudate putamen	1--	1--	1--	---	--3	--3	1-3
Accumbens n.	---	---	---	---	--3	--3	--3
Globus pallidus (medial)	---	---	---	---	1--	1--	1--
Basal telencephalon							
Septum	12-	12-	12-	12-	12-	12-	12-
Islands of Calleja	---	---	---	---	---	---	--3
Olfactory tubercle	---	---	---	--3	--3	--3	-23
Bed stria terminalis n.	1-3	1-3	1-3	1-3	1-3	1-3	1-3
Amygdaloid complex	---	---	--3	123	123	123	123

¹ E, embryonic day; P, postnatal day; n., nucleus; nd, not determined; --, not detected.² From P0, we refer to the anterior subventricular zone.

expression of Robo in cells migrating in the RMS had never been determined. We found that in the adult, cells migrating in the RMS express high levels of *robo2* and low levels of *robo1* mRNAs (Fig. 2B,D and not shown). These migrating cells were also found to express very high levels of *slit1* transcripts (Fig. 2F), which is difficult to reconcile with the actual model of Slit/Robo function in this system (see Discussion section).

Accessory olfactory system. At E18, we found that *slit1* and *robo2* were expressed in the vomeronasal organ (VNO). However, both genes were found in distinct layers: *robo2* was detected in the basal part of the VNO, whereas *slit1* was restricted to the apical part of the VNO (Fig. 1E,F). These neurons project to distinct domains in the accessory olfactory bulb (see Discussion section; Mori et al., 2000). *slit2*, *slit3*, and *robo1* were not expressed in the embryonic VNO (Fig. 1D and not shown). From E15 to birth, only *robo2* was detected in the accessory olfactory bulb (AOB) the target of VNO axons (Table 1 and not shown). This expression pattern evolves rapidly after P0, such as by P5 *robo1*, *robo2*, *slit1*, and *slit3* were all detected in the AOB (Fig. 2A,C,E,I; Tables 1 and 2). *robo1*, *robo2*, and *slit3* were found in the mitral and external plexiform cell layers (Fig. 2A,C,I). At that stage, *slit1* and *slit3* were also present in the glomerular layer, most likely in VNO axons (Fig. 2E,I). *Slit2* was not expressed in the AOB (Fig. 2G; Table 2).

Other olfactory structures. At E13–E15, cells migrating from the olfactory epithelium toward the forebrain strongly expressed *robo2* mRNA (Figs. 1B, 3D). These cells are most likely neurons secreting luteinizing hormone-releasing hormone (LHRH), on their way from the olfactory epithelium to the septal preoptic nuclei and the hypothalamus (Schwanzel-Fukuda and Pfaff, 1989; Schwarting et al.,

2001). However, they might also be glial ensheathing cells of the olfactory nerve, which start migrating from the olfactory epithelium at that stage (De Carlos et al., 1995).

Mitral, middle, and deep tufted cells in the olfactory bulb, project ipsilaterally to the anterior olfactory nucleus (AON) and to higher olfactory centers, including the piriform cortex, the olfactory tubercle, and some amygdaloid nuclei, collectively referred to as the primary olfactory cortex (for a review see Shipley and Ennis, 1996). By E18, *robo* and *slit* genes were present in all these regions (Figs. 2, 3; Tables 1 and 2).

The AON is a laminated structure that can be subdivided in different regions based on their connections and cytoarchitecture. Neurons from the AON send axons to other components of the olfactory cortex and to the contralateral OB, this projection constituting a large part (the anterior arm) of the anterior commissure. In the AON, *robo1*, *robo2*, and *slit3* expression started at E18, whereas *slit1* and *slit2* expression started, respectively, at P10 and E20 (Tables 1 and 2). At P5, all genes to the exception of *slit1* were detected in the AON (Fig. 2). *robo1* and *slit2* were found in the internal part of the AON, whereas *robo2* and *slit3* were both expressed in the external and internal part. This expression was unchanged in the adult except for *slit1*, which was up-regulated and became highly expressed in the AON.

In the piriform cortex, only *robo2* was detected from E15 to adulthood (Fig. 3D–F), whereas *robo1* was not detected (Fig. 3A–C). *slit1* and *slit2* were also expressed in some of these structures such as the amygdala (see below). The taenia tecta (Tables 1 and 2 and not shown), which projects to the OB, and the indusium griseum (a structure just dorsal to the corpus callosum and related to the hippocampus, see Figs. 4H, 5C,D; Tables 1 and 2), which

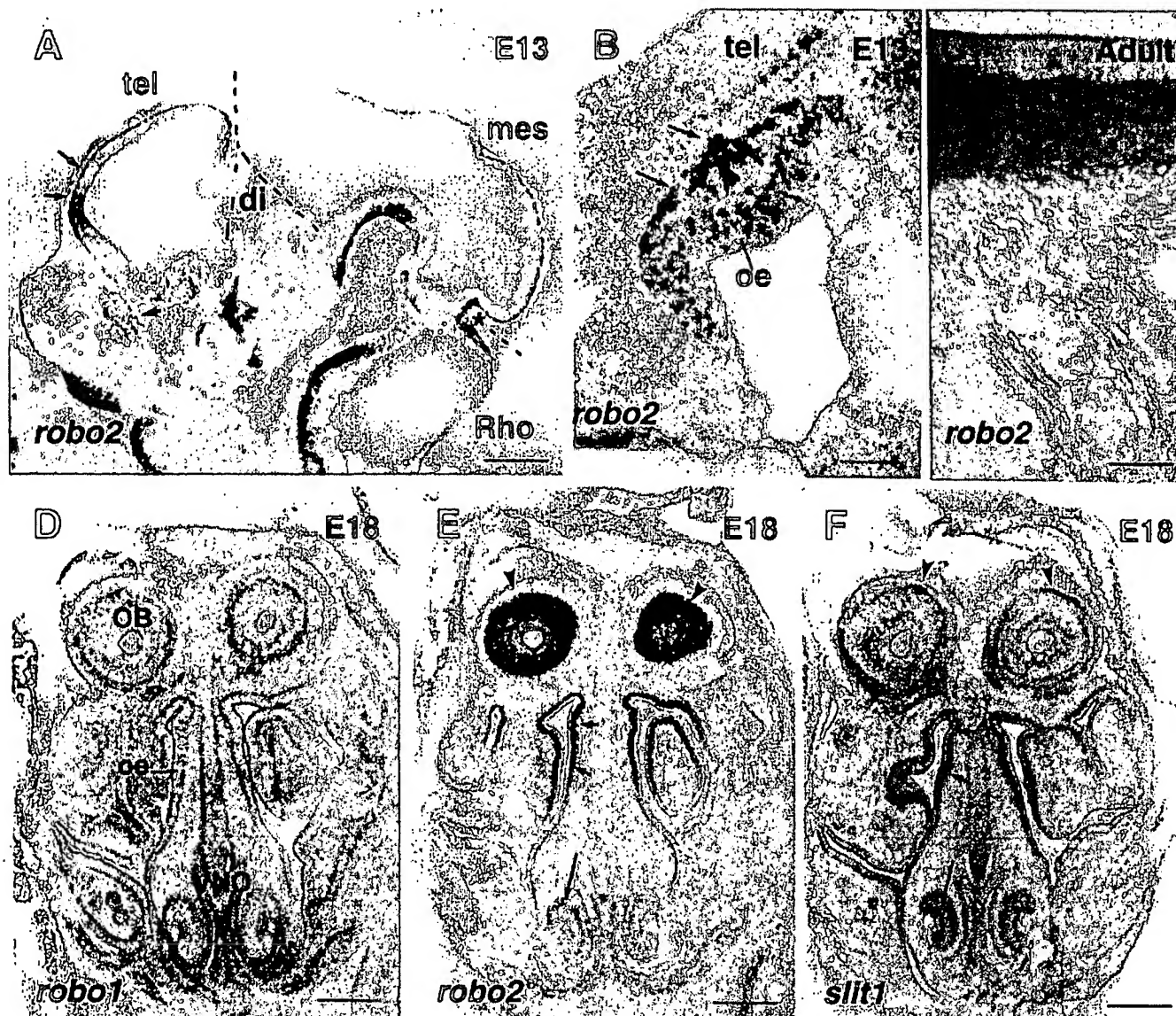


Fig. 1. *robo1*, *robo2*, and *slit1* expression in the embryonic rat olfactory system. Sagittal (A) and coronal (B–F) sections were hybridized with digoxigenin-labeled riboprobes for *robo1* (D), *robo2* (A, B, C, E) and *slit1* (F). A,B: At embryonic day (E) 13, *robo2* is already detected in the telencephalon (tel), the alar and basal plates of the diencephalon (di) and the mesencephalon (mes). *robo2* is also expressed in the cortical plate (arrows), in the cerebellar anlage (asterisk). In the olfactory epithelium (short arrow in A), *robo2* is expressed in olfactory receptor neurons of the olfactory epithelium (oe) and in migrating cells (arrows in B) possibly LHRH neurons or glial ensheathing cells. C: In the adult, *robo2* is still expressed in the olfactory receptor neurons of the olfactory epithelium (oe). D–F: At E18, *robo1*

(D) is not expressed in the olfactory system, whereas *robo2* (E) is highly expressed in the mitral cell layer of the olfactory bulb (arrowheads) and in olfactory receptor neurons (short arrows). *robo2* is also detected in the basal part of the vomeronasal epithelium (long arrow in E). In the olfactory bulb, *slit1* (F) is present in a subset of mitral cells (arrowheads) and in scattered cells throughout the granular cell layer (asterisk). *slit1* is also weakly expressed in olfactory receptor neurons (short arrows in F) and in the apical part of the vomeronasal epithelium (long arrow). OB, olfactory bulb; Rho, rhombencephalon; VNO, vomeronasal organ. Scale bars = 1 mm in A, 220 μ m in B, 31 μ m in C, 500 μ m in D–F.

receives direct projections from the olfactory bulb, both expressed from E18 to adult, *robo1*, *slit1*, and *slit3* mRNAs. At E15, the olfactory tubercle only expressed *robo2* (Fig. 3D), then both *robo1* and *robo2* from E18 to P5 (Fig. 3B,E), and only *robo1* from P10 to the adult (Fig. 3C). In contrast, no *slits* expression could be observed in this region before birth, when *slit3* started to be detected (Table 2 and not shown). This expression of *slit3* was main-

tained at a high level in the adult (Fig. 4I), and at this stage, neurons of the olfactory tubercle also expressed a low level of *slit2* (Fig. 4F).

Basal telencephalic structures

From E15 to the adult stage, we found that only *robo1* is expressed in the Islands of Calleja (Fig. 3C; Table 1),

whereas both *slit1* and *slit3* were present in the basal striatal terminalis (not shown, Table 2).

Septum. Olfactory bulb axons have also been shown to be repelled by a chemorepulsive factor released by the sep-

tum (Pini, 1993). Interestingly, we found that from E14, *slit1* and *slit2* were expressed in the septum with *slit1* more highly and broadly distributed than *slit2* (Fig. 4A,D; Table 2). In the adult, *slit1* was expressed in the dorsal part of the lateral septum and the triangular nucleus. *slit3* mRNA was never detected in the septum (Table 2). A low expression of *robo1* and *robo2* were also found in the septum at E14, but it was not detected at E18 (Fig. 3A,B).

Striatum. At E15, *robo1* was expressed in the entire striatal anlage (Fig. 3A), whereas *robo2* expression was restricted to a dorsal domain (Fig. 3D). From E18, *robo1* and *robo2* were expressed in postmitotic neurons of the caudate putamen and the nucleus accumbens (Fig. 3B,C,E,F; Table 1). At E15, *slit1* was expressed in the striatal anlage at the level of the ventricular and subventricular zones of the ganglionic eminences (Fig. 4A). At E18, *slit1* expression was still detected in the striatal SVZ (Fig. 4B). From birth, *slit1* was restricted in the caudate-putamen to scattered large neurons, probably cholinergic interneurons (Fig. 4C). *slit2* was never detected in the striatum (Fig. 4D–F). *slit3* expression appeared late in development from P5 (Table 2) in the lateral part of the caudate-putamen (Fig. 4G–I). From P0, *slit1* was expressed in the medial globus pallidus (Table 2 and not shown), whereas *robo1* and *robo2* were expressed in the lateral globus pallidus (Table 1 and not shown).

Amygdala. *slits* and *robos* genes exhibited a distinctive pattern of expression in the developing amygdala. All *slit* genes were expressed from birth in the lateral and medial nuclei (Fig. 7G,H,J; Table 2 and not shown), which correspond, respectively, to the pallial and pallidal components of the amygdaloid complex (Puelles et al., 2000). On the contrary, *robo1* was expressed at high levels only in the basomedial nucleus (Fig. 7E and not shown), whereas in this nucleus, *robo2* exhibited a low level of expression (Fig.

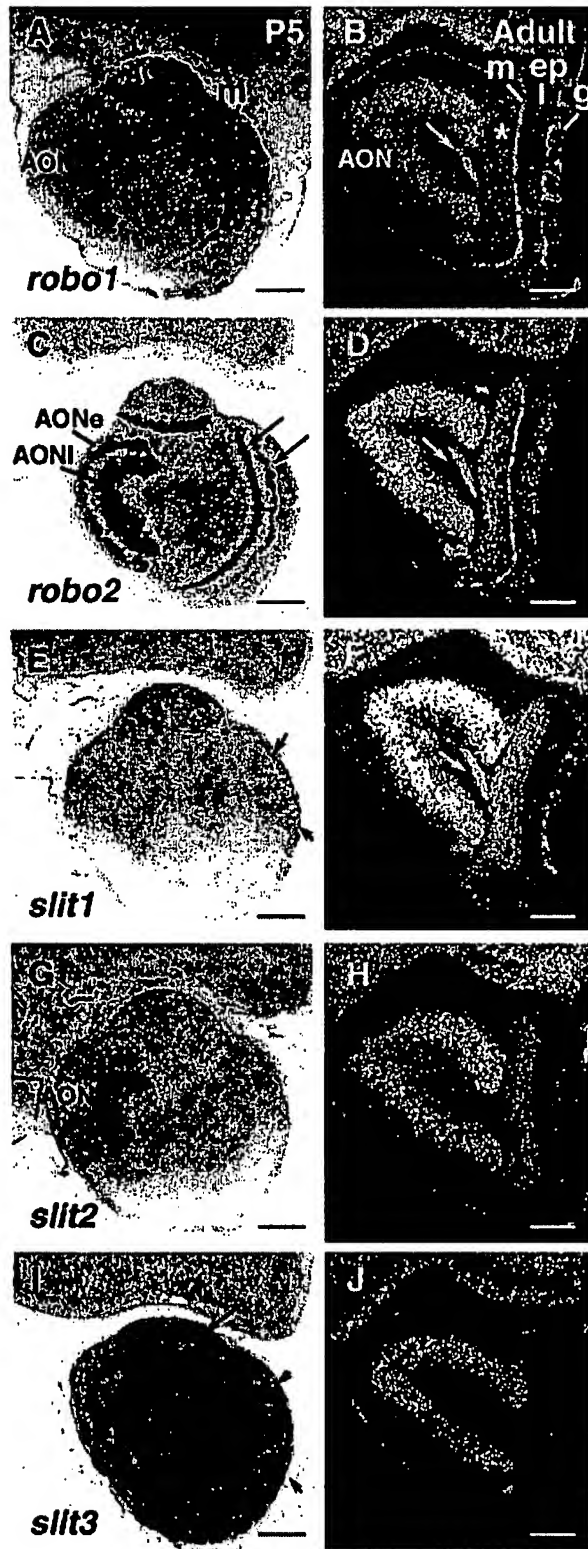


Fig. 2. *robos* and *slits* expression in the postnatal rat olfactory bulb. Coronal sections were hybridized with digoxigenin-labeled riboprobes (A,C,E,G,I), or 35 S-labeled riboprobes (B,D,F,H,J), for *robo1* (A,B), *robo2* (C,D), *slit1* (E,F), *slit2* (G,H), and *slit3* (I,J). A: At postnatal day (P) 5, *robo1* is highly expressed in the mitral cell layer of the accessory olfactory bulb (AOB) and in the lateral part of the accessory olfactory nuclei (AONI). In the olfactory bulb, *robo1* is only found in the mitral cell layer (m), in periglomerular cells of the glomerular layer (g), in neurons of the external plexiform layer (ep), and at a weak level in the granular cell layer (asterisk). *robo1* is also detected in the subventricular zone (arrow). C: At P5, *robo2* is highly expressed in the mitral cell layer of the AOB and in the lateral part (AONI) and the external part (AONe) of the accessory olfactory nuclei. In the olfactory bulb, *robo2* is strongly expressed in mitral cells and in the external plexiform layer (arrows). D: In the adult, *robo2* expression is maintained in the AON, in all olfactory bulb neurons except in periglomerular cells. *robo2* is also highly expressed in the subventricular zone (arrow). E: At P5, *slit1* expression is weak in olfactory glomeruli (arrows) and in the olfactory bulb and AOB, probably in axons from the olfactory epithelium and VNO. F: In the adult, *slit1* is found in the AON, the subventricular zone (arrow), the granular cell layer and at a low level in mitral, external plexiform, and periglomerular cell layers. G: At P5, *slit2* is only detected in the AONI. H: In the adult, *slit2* is still expressed in the AON and is also detected at a low level in the granular cell layer. I: At P5, *slit3* is expressed in mitral cells of the olfactory bulb, in the glomeruli (short arrows), in the mitral and glomerular layers of the AOB (long arrow), and in the AONI and AONe. J: In the adult, *slit3* expression is down-regulated except in the AON. Scale bars = 440 μ m in A,C,E,G,I, 750 μ m in B,D,F,H,J.

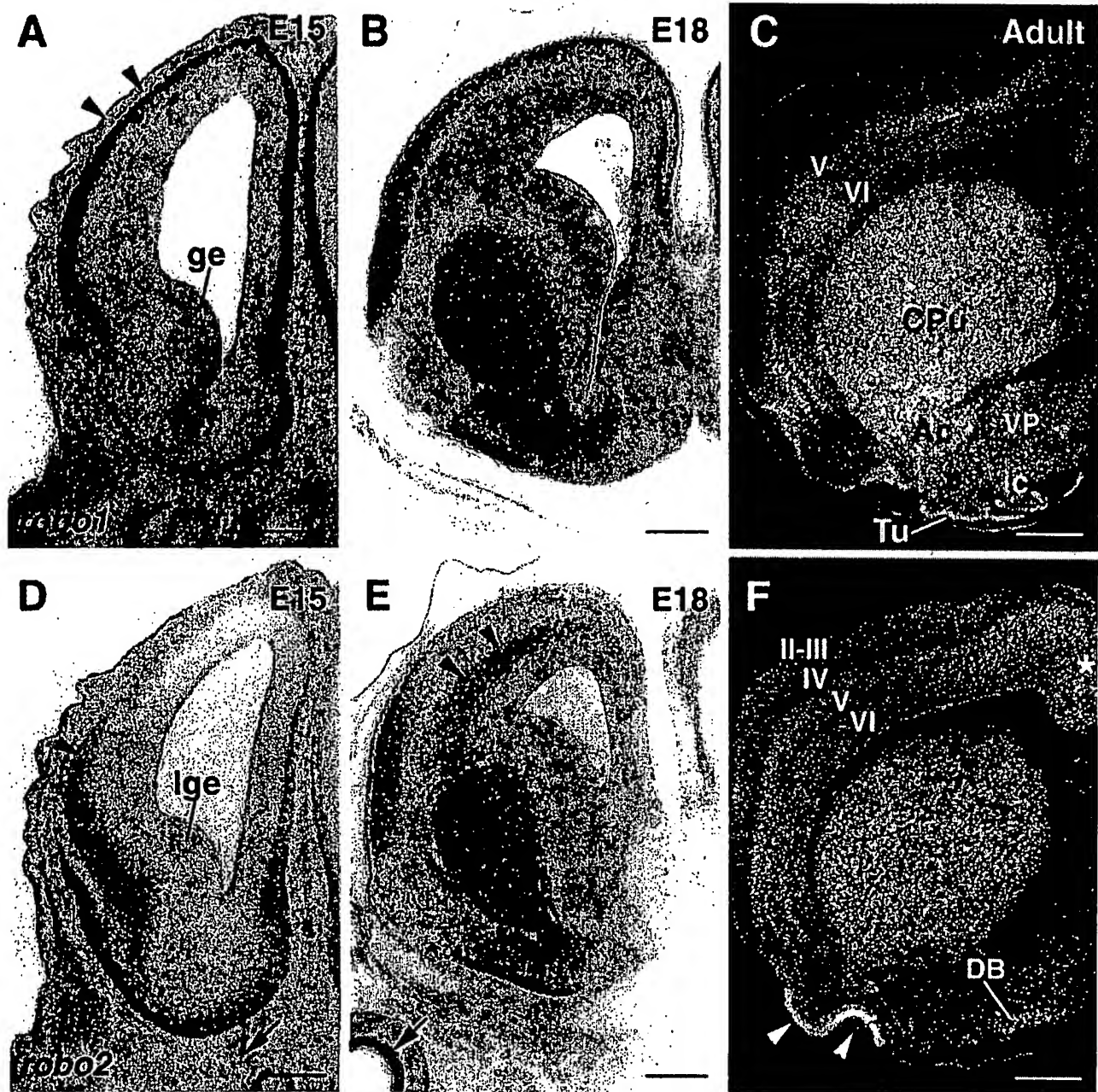


Fig. 3. Expression pattern of *robos* in the developing rostral telencephalon. Coronal sections were hybridized with digoxigenin-labeled riboprobes (A,B,D,E), or with ^{35}S -labeled riboprobes (C,F) for *robo1* (A–C) and *robo2* (D–F). A–C: At embryonic day (E) 15 (A), *robo1* is highly expressed in the cortical plate (arrowheads) and in the ventricular zone of the ganglionic eminence (ge). From embryonic day (E) 18 (B) until adult (C), *robo1* is expressed in the cortex, the caudate putamen (CPu), the accumbens nucleus (Ac), the olfactory tubercle (Tu), the islands of Calleja (ic), and the ventral pallidum (VP). In the adult cortex, *robo1* is restricted to layers V–VI. D: At E15, *robo2* expression is restricted to the cortical plate of the limbic cortex (ar-

rowhead), the lateral part of the ganglionic eminence (lge), the piriform cortex, and the olfactory tubercle. Likewise, *robo2* is expressed in putative LHRH migrating neurons (arrow). E,F: From E18 (E) to adult (F), *robo2* is highly expressed in the caudate putamen and the accumbens nucleus. At E18, *robo2* is detected in the intermediate zone of the neocortex (arrowheads), and in the retinal ganglion cells (arrow in E). In the adult neocortex (F), *robo2* is found in cortical layers II–III, Va, and VI, the piriform cortex (arrowheads), in the diagonal band of Broca (DB), and in the cingulate cortex (asterisk). Scale bars = 1,400 μm in A,D, 550 μm in B,E, 1,200 μm in C,F.

7B,F; Table 1; and not shown). This basomedial nucleus belongs to the striatal portion of the amygdaloid complex. In addition, *robo2* was also expressed in scattered neurons in the anterior amygdala area (not shown).

Cerebral cortex

All five genes were expressed in the cortex but often in different layers. *robo1* and *robo2* were first detected in the telencephalic vesicles from E13 (Fig. 1A, not shown, see

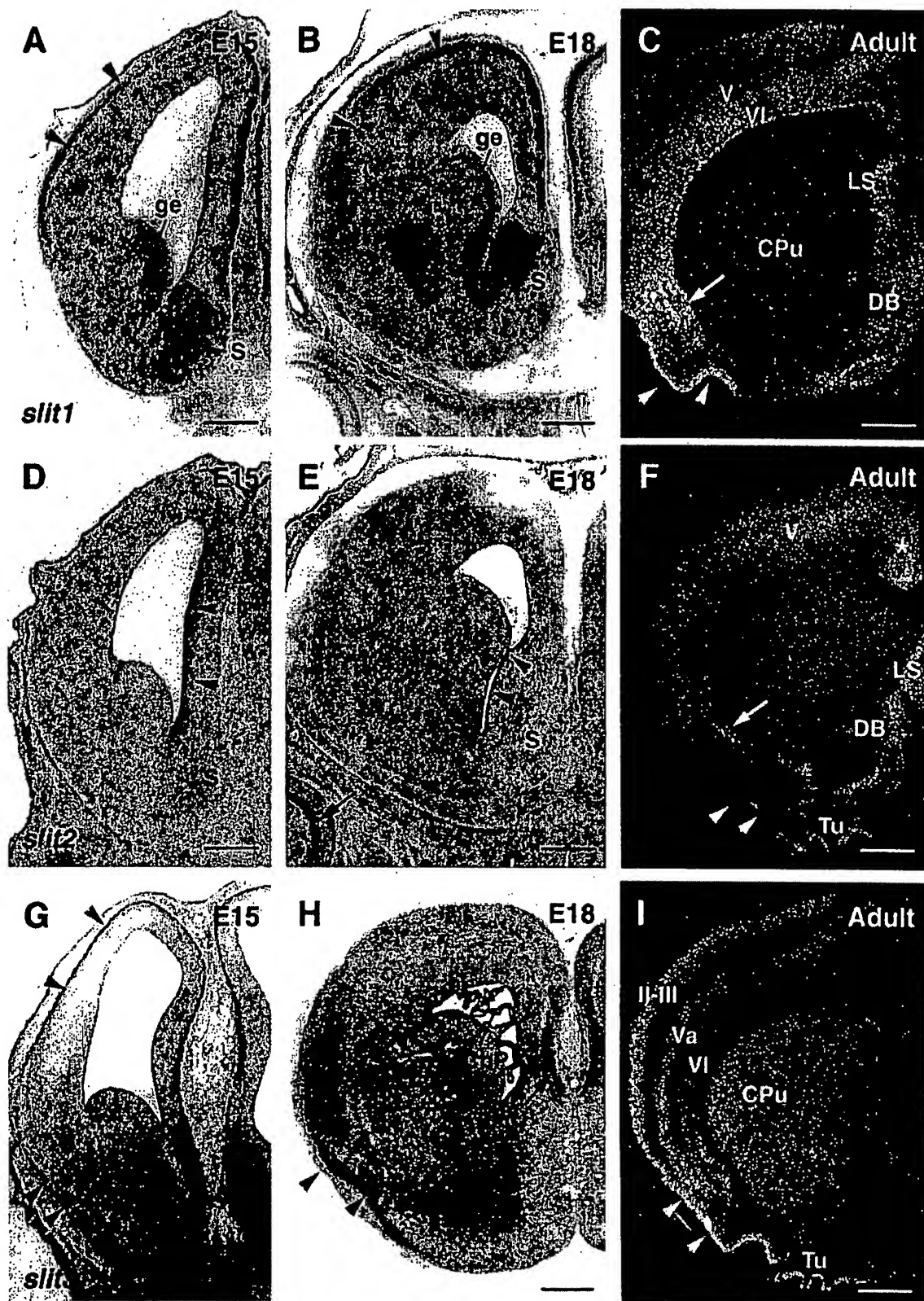


Fig. 4. Expression pattern of *slits* in the developing rostral telencephalon. Coronal sections were hybridized with digoxigenin-labeled riboprobes (A,B,D,E,G,H), or with ^{35}S -labeled riboprobes (C,F,I) for *slit1* (A–C), *slit2* (D–F), and *slit3* (G–I). A–C: From embryonic day (E) 15 (A) to E18 (B), *slit1* expression is restricted to the cortical plate of the cortex (arrowheads in A and B), the ventricular zone and subventricular zone of the ganglionic eminence (ge), and the septum (S). In the adult (C), *slit1* is detected in cortical layer VI, the piriform cortex (arrowheads), and the claustrum (arrow). *slit1* is also expressed in the lateral septum (LS), the diagonal band of Broca (DB), and some dispersed interneurons in the caudate putamen (CPu). D–F: From E15 (D) to E18 (E), *slit2* is weakly detected in the ventricular zone (arrowheads) and in postmitotic neurons of the septum (S). At E18 (E), *slit2* is also present in the retina (arrow). In the adult (F), *slit2* is

detected in the layer V of the cortex and is at the highest level in the cingulate cortex (asterisk). It is also detected in cells of the lateral septum (LS) and in the diagonal band of Broca (DB). A weak expression of *slit2* is also observed in the piriform cortex (arrowheads), the claustrum (arrow), and the olfactory tubercle (Tu). G–I: At E15 (G), *slit3* is highly expressed in the superficial cortical plate of the cortex and in the piriform cortex (arrowheads). At E18 (H), *slit3* expression decreased in the cortex but is maintained in the piriform cortex until adult (arrowheads in H and I). *slit3* is also expressed in the indusium griseum (arrow in H). In the adult cortex, *slit3* is highly detected in the layers II–III and Va. *slit3* is also expressed in the caudate putamen (CPu) and in the olfactory tubercle (Tu). ChP, choroid plexus. Scale bars = 1,400 μm in A,D,G, 550 μm in B,E,H, 1,200 μm in C,F,I.

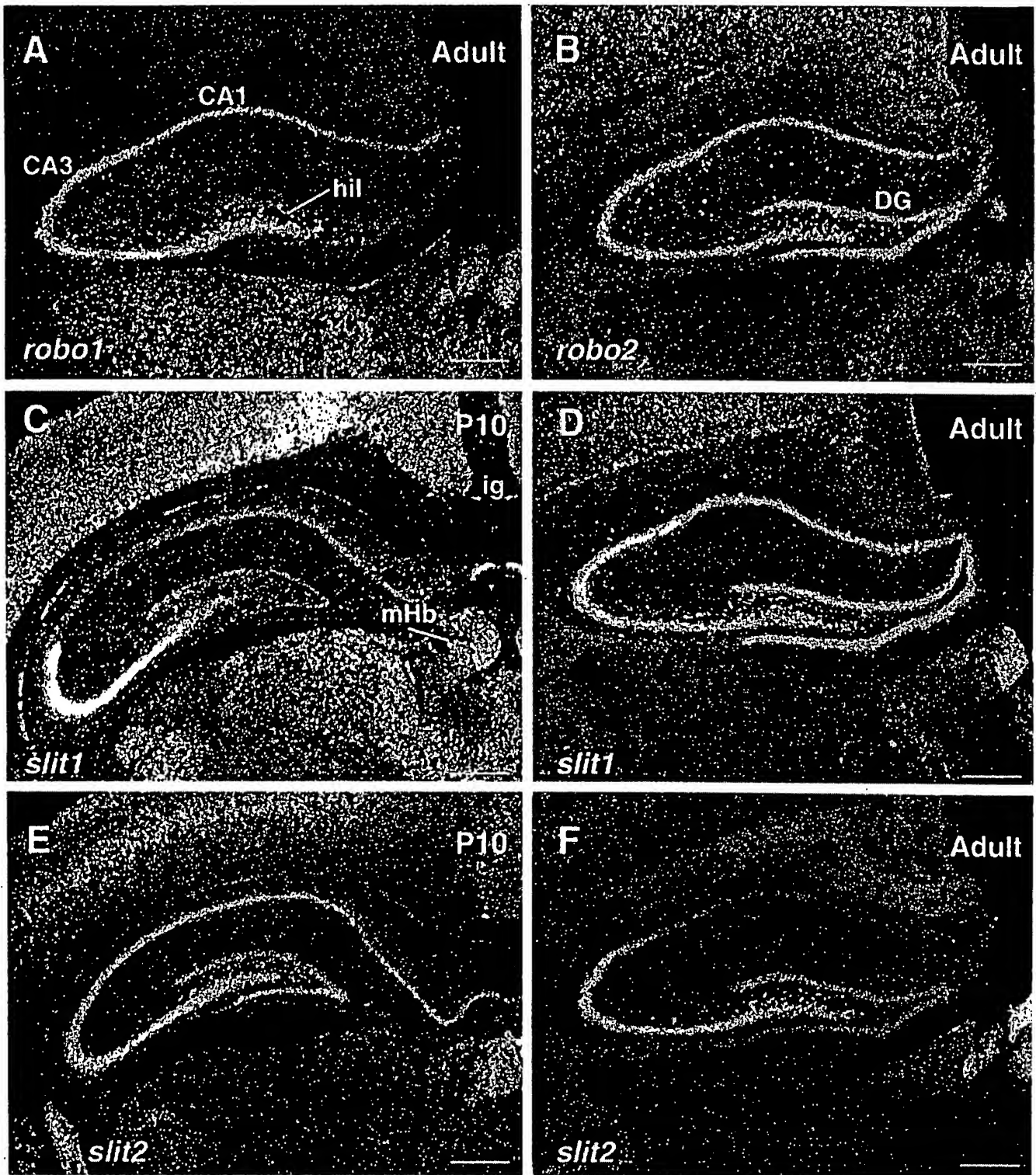


Fig. 5. *robos* and *slits* expression in the postnatal hippocampus. Coronal sections (A–F) were hybridized with 35 S-labeled riboprobes for *robo1* (A), *robo2* (B), *slit1* (C,D), and *slit2* (E,F). A,B: In the adult, a strong expression of *robo1* was detected in the pyramidal cell layer of CA3 and in scattered neurons of the hilus (hil). A lower expression was detected in the pyramidal cell layer of CA1. *robo2* (B) is strongly expressed in the pyramidal cell layer of CA1 and CA3 and in the granular cell layer of the dentate gyrus (DG). *robo2* is also detected in scattered cells outside the pyramidal cell layer. C,D: At postnatal day

(P) 10 (C), *slit1* labeling is intense in CA3 pyramidal neurons and weaker in CA1 pyramidal neurons and in the dentate gyrus, whereas in the adult (D), *slit1* expression is up-regulated in CA1 pyramidal neurons and in the DG. E,F: At P10 (E), *slit2* is highly expressed in the pyramidal neurons of CA1–CA3 subfields and in the granular cell layer of the DG, whereas in the adult (F) *slit2* expression is down-regulated in CA1 pyramidal neurons and in the DG. ig, indusium griseum; mHb, median habenula. Scale bars = 500 μ m in A,B,D,F, 450 μ m in C,E.

also Yuan et al., 1999). At E15, *robo1* mRNA was expressed in the entire cortical plate (Fig. 3A), whereas *robo2* was restricted to the cortical plate of the presumptive limbic cortex (Fig. 3D). By E18, the expression patterns of *robo* genes was unchanged in the cortical plate (Fig. 3B, E). *robo1* remained in the superficial layers of the lateral, dorsal, and medial cortex, whereas *robo2* was expressed in internal cortical layers and in the ventral pallidum (claustrum and piriform cortex). In addition, *robo2* was also found in the intermediate zone. The neocortical lamination is clearly settled by P5, and from this stage to the adult, *robo2* was expressed at various levels in all cortical layers except in layer IV (Fig. 3F; Table 1). Interestingly, *robo2* was strongly expressed in the remaining subplate neurons (layer VIb). *robo1* expression became restricted to layers V and VI (Fig. 3C; Table 1), the most superficial neurons of neocortical layer II and pyramidal neurons of layer II in the retrosplenial and cingulate cortices. *slits* were also all expressed in the cortex but each with a distinct spatiotemporal pattern. From E13, *slit1* mRNA was expressed in the entire cortical plate, *slit3* was only detected in the cortical and hippocampal marginal zone from E15 and *slit2* was not detected at this time (Figs. 4A,D,G, 6A,B, and not shown). By E18, *slit3* expression disappeared from the neocortex, whereas *slit1* was still expressed in the cortical plate (Fig. 4B,E,H). This pattern was maintained until E20, when *slit2* started to be detected at a low level in the cortical plate (not shown). From P5, all three *slits* were expressed, and their expression pattern was maintained to the adult. *slit1* was confined to layers Va and VI (Fig. 4C), *slit2* to layer V of the entire cortex and layers II and III of the cingulate cortex (Fig. 4F), whereas *slit3* was more broadly expressed in layers II–III, Va, and at a lower level in layer VI (Fig. 4I; Table 2).

Hippocampal formation

We previously described some aspects of the expression pattern of *slit1*, *slit2*, *robo1*, and *robo2* in the developing hippocampus, until P5 (Nguyen-Ba-Charvet et al., 1999; see also Tables 1 and 2). We found that these four genes were still expressed in this structure later on. *robo1* and *robo2* expression was unchanged from P5 to the adult (Table 1). Both genes were highly expressed in pyramidal neurons of the CA1–CA3 subfields and in scattered neurons of the hilus (Fig. 5A,B). However, only *robo2* was present in granule cells of the dentate gyrus (Fig. 5B) and in the subiculum (not shown). In contrast *slit1* and *slit2* expression pattern changed drastically between P10 and the adult. At P10, although *slit1* was expressed at very high levels in the CA3 subfield (Fig. 5C) and weakly in other hippocampal regions, *slit2* expression was strong in all hippocampal subfields (Fig. 5E). In the adult, *slit1* expression was up-regulated throughout the hippocampus (Fig. 5D). In contrast, *slit2* expression was down-regulated to very low levels except in the CA3 subfield (Fig. 5F). Therefore, *slit1* and *slit2* expression pattern switches between P10 and the adult. We also studied *slit3* expression that had never been reported. Interestingly, from E13 to the adult, *slit3* was highly expressed in the hippocampal formation (Fig. 6; Table 2). At E13, apart from the floor plate and the skin (Fig. 6A), *slit3* expression in the forebrain was restricted to the primordium of the hippocampus (Fig. 6A). At E15, this expression has increased, but neurons were also labeled in the entorhinal cortex (Fig.

6B). At P1, it was clear that *slit3* was expressed at very high levels in all the hippocampal formation (Fig. 6C). This expression pattern was maintained in the adult (Fig. 6D), although by this stage, *slit3*-expressing neurons were found also outside the hippocampal formation.

Hypothalamus

Most cells in the hypothalamus become postmitotic between E13 to E18 (Altman and Bayer, 1978). During this period, *robo* and *slit* genes were not detected in ventricular (VZ) or subventricular (SVZ) zones. *robo* genes had a very restricted pattern of expression throughout the hypothalamus (Table 3): *robo2* was only detected in the paraventricular hypothalamic nucleus (Pavh) from E15 (Fig. 7B), whereas *robo1* was slightly expressed in Pavh from E20 and the ventromedial hypothalamic nucleus (VMH) from P10 (Fig. 7E). *Slit* genes have a more extended pattern of expression in the hypothalamus (Table 4) than *robo* genes. Particularly, *slit1* was widely expressed in scattered cells of the preoptic, anterior, and lateral areas of the developing and adult hypothalamus (Fig. 7C,G). A high *slit1* expression was also detected in the dorsomedial and dorsal part of VMH. In contrast, *slit2* and *slit3* were expressed in a restricted pattern. *slit2* was detected in Pavh, VMH, and the ventricular lining where tanycytes are localized (Fig. 7D,H). Robust *slit3* expression was detected at the level of the VMH, the arcuate nucleus, and tuberomammillary areas (Fig. 7I–K). In summary, *robo* and *slit* genes have distinct and overlapping patterns of expression in the hypothalamus.

Thalamus

Most cells in the dorsal thalamus (dTH) and ventral thalamus (vTH) become postmitotic between E13 and E17 (Altman and Bayer, 1988). E13 is the onset of neurogenesis for cells in the caudal dTH nuclei, whereas cells in rostral and medial dTH nuclei are generated 1–3 days later. Cells in the vTH are generated between E13 and E15 (Altman and Bayer, 1988). Although dTH has undergone some architectonic differentiation by E15, dTH nuclei cannot be easily distinguished. At this stage, most of the medial and anterior nuclei have not been generated, whereas posterior (median geniculate, MG), ventral (ventroposterior lateral and ventromedial nuclei, VPL, and VPM), and lateral (dorsal lateral geniculate, dLG) structures begins to parcellate. A strong *robo2* expression was detected in the entire dTH, except in the VZ and SVZ (Fig. 7B), whereas robust *robo1* expression was detected in VZ, SVZ, and the most medial domain of the dTH (Fig. 7A). As development proceeds, dTH nuclei can be distinguished. A high level of *robo2* expression was maintained in most dTH nuclei until birth. Then, *robo2* expression decreased sharply in sensory thalamic nuclei, while it is maintained in intralaminar and ventral nuclei (Fig. 7F). Whereas *robo1* expression disappeared from VZ and SVZ, its expression was maintained in the intralaminar and paraventricular nuclei (Table 3). During the period of neurogenesis in vTH, *robo* genes were not detected in mitotic cells of the thalamic neuroepithelium. By E15, vTH has undergone considerable architectonic differentiation and it is possible to histologically distinguish vTH nuclei: the reticular nucleus (Rt), the zona incerta (Zi), the ventral lateral geniculate (vLG), and the subthalamic nucleus (StH). Already at this stage, *robo1* and *robo2* were differentially expressed in patterns similar to those observed in

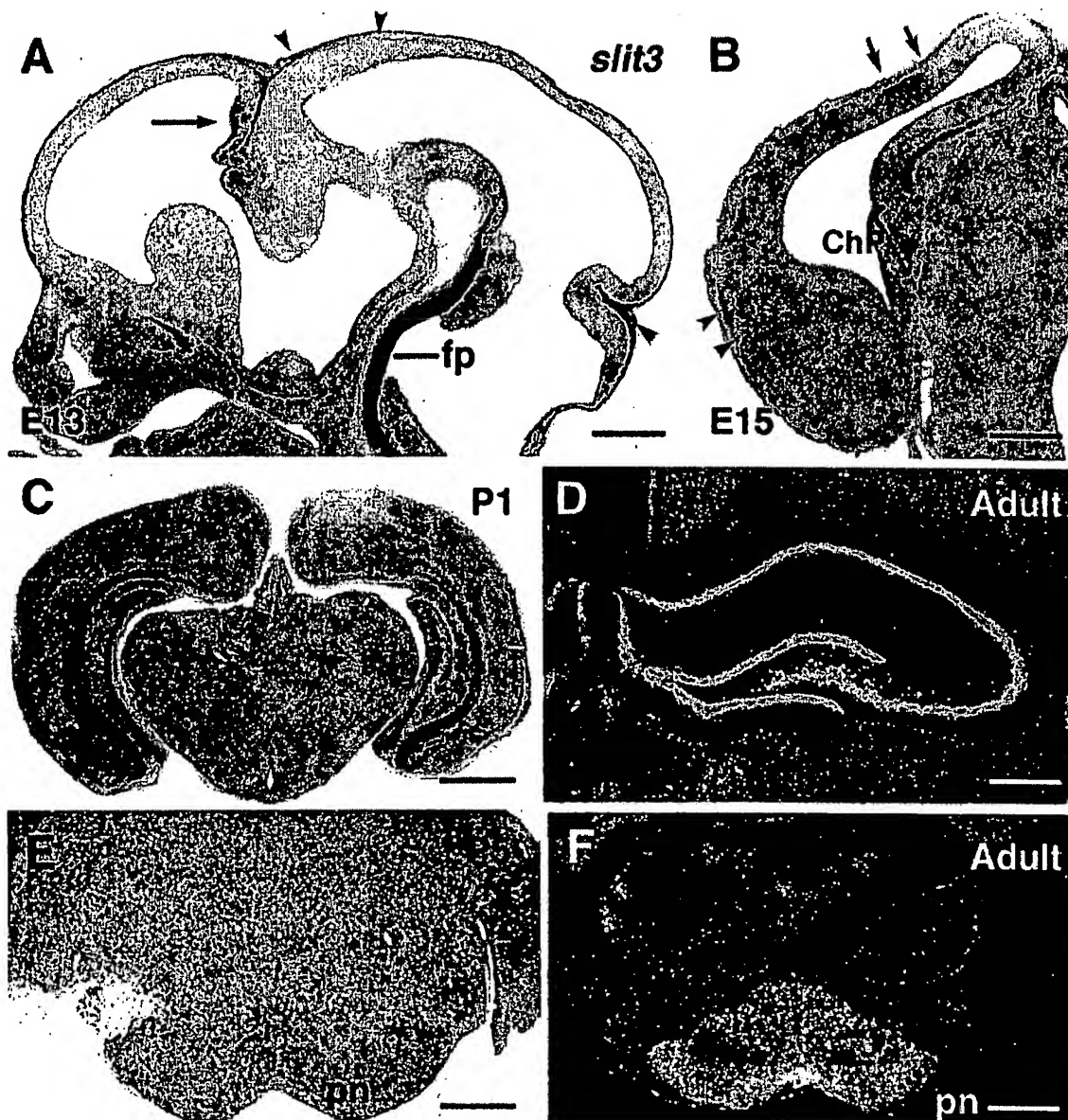


Fig. 6. *slit3* expression in the developing hippocampal formation. Sagittal section (A) and coronal sections (B,C,E,F) were hybridized with digoxigenin-labeled riboprobes, whereas coronal sections (D,F) were hybridized with 35 S-labeled riboprobes. A: At embryonic day (E) 13, *slit3* is expressed in the skin (arrowheads), the craniofacial mesenchyme (asterisk), the hippocampal primordium (arrow) and the floor plate (fp). B: At E15, *slit3* is highly expressed in the developing hippocampus, the choroid plexus (ChP), the marginal zone of the

cortex (arrows) and the entorhinal cortex (arrowheads). C: At postnatal day (P) 1, a strong *slit3* expression is detected in all the hippocampal system, including the entorhinal cortex. D: In the adult hippocampus, *slit3* is strongly expressed in the pyramidal neurons of CA1 and CA3 subfields and in the granular cell layer of the dentate gyrus. E,F: Postnatally, *slit3* is expressed in the pontine nuclei (pn) at P5 (E) and in the adult (F). Scale bars = 330 μ m in A, 380 μ m in B, 1,000 μ m in C,F, 700 μ m in D, 550 μ m in E.

adults. *robo2* was highly expressed in vLG, Rt, Sth nuclei, the rostral part of Zi, and most likely, at the level of A13 dopaminergic neurons (Fig. 7B,F; Table 3). *robo1* expression pattern was far more discrete and was restricted to a subdomain of vLG and Sth (Fig. 7A,E; Table 3).

In summary, *robo* genes have distinct but overlapping expression patterns in subsets of dTH and vTH nuclei; the expression patterns often correlate with the histologically defined borders of nuclei. In addition, potential subdomains within the same nuclei (e.g., vLG) are suggested by some of the more discrete patterns.

Embryonically, *slit* genes had a very restricted pattern of expression in dTH. During the onset of dTH neurogenesis, from E13 to E18, robust *slit1* expression was only detected in the SVZ (Fig. 7C), whereas slight *slit2* expression was specifically detected in the VZ (Fig. 7D), possibly in radial glial cells. Postnatally, after major developmental events, *slit1* expression was detected in intralaminar, ventral, and lateral nuclei (Fig. 7G); *slit2* in anterior and posterior nuclei (Fig. 7H); and *slit3* in MG, dLG, laterodorsal (LD), lateroposterior (LP), and anterior nuclei (Fig. 7G,J,K; Table 4).

TABLE 3. Spatiotemporal Distribution of *robo1* (1) and *robo2* (2) mRNA in the Diencephalon¹

Diencephalon	E15	E18	E20	P0	P5	P10	Adult
Hypothalamus							
Ventromedial hypothalamic n.	--	--	--	--	--	1-	1-
Paraventricular n.	-2	-2	12	12	12	12	12
Eminencia thalamica	1-	--	--	--	--	--	--
Ventral thalamus							
Ventral lateral geniculate n.	1-	1-	12	12	12	12	12
Reticular n.	12	12	12	12	12	12	12
Zona incerta	12	12	12	--	--	--	--
Subthalamic n.	12	12	12	12	12	12	12
Dorsal thalamus							
Medial habenula	12	12	12	12	12	12	12
Intralaminar thalamic n.	1-	12	12	12	12	12	12
Ventral medial n.	--	-2	-2	-2	-2	12	12
Dorsal lateral geniculate n.	-2	-2	--	--	--	1-	1-
Ventral basal n.	-2	-2	--	--	--	--	--
Lateral posterior and dorsal n.	--	-2	-2	--	--	1-	1-
Median geniculate n.	-2	-2	-2	-2	--	1-	1-
Median geniculate dorsal n.	--	-2	-2	-2	--	1-	1-
Paraventricular thalamic n.	1-	1-	12	12	12	12	12
Posterior n.	--	-2	-2	12	12	12	12
Proctum							
Posterior commissure n.	1-	12	1-	--	--	--	--

¹ E, embryonic day; P, postnatal day; n., nucleus; --, not detected.

In vTH, *slit1* mRNA were detected from E15 at the level of A13 in Zi, from birth in Rt, and from P5 in Sth. Curiously, a sequential overlapping expression of *slit* genes was found in Rt (Table 4). Finally, *slit3* was expressed in a subset of cells in vLG. In summary, *slit* genes have a distinct pattern of expression in the developing dTH, and they are most likely implicated in migratory events of newly dTH postmitotic neurons. *robo1* and *robo2* coexpression was also noted from E15 in the median habenula (mHb). From E15, whereas *slit1* was expressed in the entire habenula, *slit2* was only found in the mHb (Fig. 7C,D).

Mesencephalon

The neurons of the pars compacta and pars reticulata of the substantia nigra (SN) are generated between E13 and E15, whereas neurons of the ventral tegmental area (VTA) are produced between E14 and E16. From E15, *robo1* was expressed in most of the postmitotic neurons of the SN-VTA complex, whereas *robo2* was only found in SN neurons (Table 5). The levels of *robo1* and *robo2* expression

increased as development proceeds to reach a maximum by P10 (Fig. 8A,B). Interestingly, *slit1* and *slit2* coexpression began later in SN-VTA neurons (Fig. 8C,D; Table 6). *Robo* genes expression is maintained in adults with the concomitant expression of *slit1* and *slit2*. The cytoarchitecture of the *slits* and *robos* coexpressing cells in the adult SN-VTA complex strongly indicates that these ligands and receptors are coexpressed mainly in dopaminergic neurons: VTA and pars compacta (Fig. 8A-D), as well as in the caudal region of pars reticulata (not shown; Wassef et al., 1981).

Neurons were produced in the red nucleus between E13 and E14; in the periaqueductal gray (PAG) between E13 and E17; in the visual superior (SC) and auditory inferior (IC) colliculus between E14 and birth. We found that *robo1* and *robo2* were coexpressed in postmitotic neurons that form SC and IC. Whereas *robo2* expression was maintained during postnatal life (Figs. 8B, 10B), *robo1* expression stopped between birth and P5 (Figs. 8A, 10A; Table 5). Interestingly, in addition to IC, the other components of the auditory pathway, the cochlear nuclei, the lateral

Fig. 7. *robos* and *slits* expression in the developing diencephalon. Coronal sections were hybridized with digoxigenin-labeled riboprobes (A-D,I), or with ³⁵S-labeled riboprobes (E-H,J,K) for *robo1* (A,E), *robo2* (B,F), *slit1* (C,G), *slit2* (D,H), and *slit3* (I-K). A: At embryonic day (E) 15, *robo1* is detected in the epithalamus (Et), the medial part of the dorsal thalamus (dTH), and the ventral lateral geniculate nuclei (vLG). B: At E15, *robo2* is strongly expressed in the dTH and the ventral thalamus (vTH). Note the lack of expression in the zona limitans (zli). *robo2* is also observed in the paraventricular hypothalamic nuclei (Pavh) and in the dopaminergic cell group A13. C: At E15, *slit1* is expressed in the medial habenula (mHb) and the subventricular zone of the dorsal thalamus (arrowhead). *slit1* is also found in the dopaminergic cell group A13 and in the hypothalamus at the level of the dorsomedial nucleus (Dmh) and the periventricular hypothalamic area (Pe). D: At E15, *slit2* was detected in the medial habenula (mHb) and the paraventricular hypothalamic nuclei (Pavh). E: At postnatal day (p) 10, *robo1* is weakly expressed in the medial habenula (mHb), the central lateral nucleus (CL), the dorsolateral geniculate nuclei (dLG), the paraventricular nucleus of the thalamus (PV), and the subthalamic nucleus (Sth). *robo1* is also detected in the basomedial nucleus of the amygdala (BM). F: At P10, *robo2* is ex-

pressed in the medial part of the habenula (mHb), and in the central lateral (CL), the central medial (CM) and the ventromedial (VM) thalamic nuclei. *robo2* is also highly expressed in the lateroposterior nucleus (LP), the ventral lateral geniculate nucleus (vLG), and the reticular (Rt) and subthalamic (Sth) nuclei. G: At P10, *slit1* is highly expressed in the medial part of the habenula (mHb) and much lower in the lateral part (lHb). *slit1* is also strongly expressed in the laterodorsal nucleus (LD), in all intralaminar thalamic nuclei (PV, CL, VM, and CM), and the Rt. *slit1* is also detected in the anterior (AH) and lateral (LH) area of the hypothalamus and in the lateral (LA) and medial (MA) nuclei of the amygdala. H: At P10, *slit2* is highly expressed in the mHb, the choroid plexus (arrow), the ventromedial (VM) and Rt nuclei. In the hypothalamus, *slit2* is only expressed in the ventromedial nuclei (VMH) and the ventricular zone (arrowhead). *slit2* is also detected in the lateral (LA) and medial (MA) nuclei of the amygdala. I: At E18, *slit3* is not detected in the thalamus and is only found in the VMH. J,K: In the adult, a high *slit3* expression is maintained in the VMH, but *slit3* is also weakly expressed in the arcuate nucleus (Ar). A weak expression of *slit3* in the median geniculate nucleus (MG) is also observed. Scale bars = 400 μ m in A-D, 1,100 μ m in E-H,J,K, 500 μ m in I.

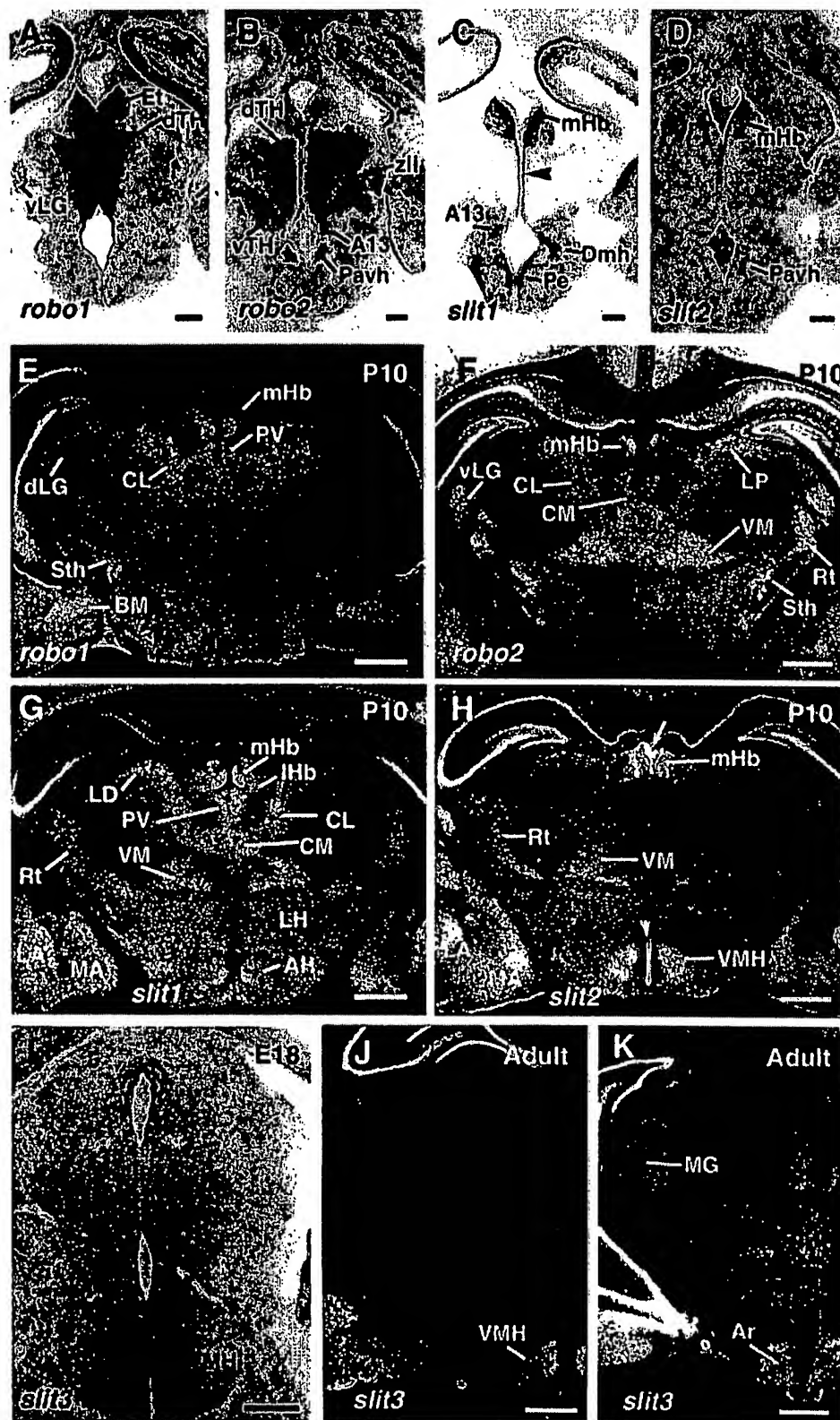


Figure 7

TABLE 4. Spatiotemporal Distribution of *slit1* (1), *slit2* (2), and *slit3* (3) mRNA in the Diencephalon¹

Diencephalon	E15	E18	E20	P0	P5	P10	Adult
Hypothalamus							
Ventromedial hypothalamic n.	-2-	-23	-23	-23	-23	123	123
Paraventricular n.	---	-2-	-2-	-2-	-2-	-2-	-2-
Anterior hypothalamic n.	1--	1--	1--	1--	1--	1-3	1-3
Lateral hypothalamic n.	1--	12	12	12	12	12-	12
Lateral preoptic area	1--	1--	1--	1--	1--	1--	1--
Preoptic n.	-2-	-2-	-2-	-2-	-2-	-2-	-2-
Supraoptic n.	nd	nd	-2-	-2-	-2-	-2-	-2-
Suprachiasmatic n.	nd	nd	-2-	-2-	-2-	-2-	-2-
Ventral thalamus							
Ventral lateral geniculate n.	---	---	---	---	---	-3	-3
Reticular n.	---	---	---	12-	123	123	123
Zona incerta	1--	1--	1--	1-3	1-3	1-3	1-3
Subthalamic n.	---	---	---	---	1--	1--	---
Dorsal thalamus							
Medial habenula	12-	12-	12-	12-	12-	12-	12-
Lateral habenula	1--	1--	1--	1--	1--	1--	1--
Anterior lateral and dorsal n.	---	---	-2-	-23	-23	-23	-2-
Intralaminar thalamic n.	---	---	---	---	---	1--	1--
Ventral medial n.	---	---	---	---	---	123	1-3
Dorsal lateral geniculate n.	---	---	---	---	---	-3	---
Lateral posterior and dorsal n.	---	---	---	---	---	1-3	---
Median geniculate n.	---	---	---	---	---	---	-3
Median geniculate dorsal n.	---	---	---	---	---	---	-3
Paraventricular thalamic n.	---	---	---	---	---	---	-3
Posterior n.	---	---	---	-2-	-2-	-2-	---
Pretectum							
Optic tract n.	nd	nd	nd	-2-	-2-	-2-	-2-

¹ E, embryonic day; P, postnatal day; n., nucleus; nd, not determined; -, not detected.

superior olive, the lemniscal nuclei, and the trapezoid nucleus displayed a robust *robo2* expression (Fig. 8E). We also found *robo2* gene expression in the red nucleus and in PAG (Table 5).

slit genes were expressed in a very limited pattern from E15. *slit1* gene was detected in scattered cells of SC and IC (Fig. 10C), and *slit2* was found in the red nucleus, PAG, and probably the serotonergic neurons of the raphe (Fig. 8F).

Other structures. We found that only *slit2* was expressed in the pineal recess and the subcommissural organ (not shown), whereas both *slit2* and *slit3* were present in the choroid plexus (Figs. 4H, 6B, 10F).

Hindbrain

Cerebellar system. The expression patterns of *slit* and *robo* genes were particularly interesting in the cerebellum, where, to a large extent, they were expressed in different and often complementary structures. At E15, *robo1* (Fig. 9A) and *robo2* (Fig. 9D) expression was detected in zones corresponding, respectively, to masses of migrating deep nuclear neurons and Purkinje cells (Altman and Bayer, 1985; Feirabend, 1990). In contrast, a very low level of *slit1* (Fig. 9G) and a high level of *slit2* (Fig. 9J) mRNAs were expressed in the mantle layer, composed of migrating Purkinje cells (Altman and Bayer, 1985). *Slit1* was also observed in a group of cells adjacent to the cerebellar plate (Fig. 9G) and possibly corresponding to the neurons of the parabrachial nucleus (Cholley et al., 1989). *slit3* was not detectable in the embryonic cerebellum (Fig. 9M,N). At E18, the cerebellar cytoarchitecture was more mature and at that stage *robo1* was still only expressed in deep nuclear neurons (Fig. 9B). In contrast, *robo2* expression was confined to Purkinje cells (Fig. 9E) and, thus, complementary to *robo1* expression. *slit1* and *slit3* were not detectable at E18 in the cerebellar plate (Fig. 9H,N; Table 6), whereas *slit2* was found in subsets of deep nuclear neurons and Purkinje cells (Fig. 9K). This expression pattern was mostly unchanged until birth (Ta-

ble 6). At P5, granule cells have started to migrate from the external granular layer (egl) and oligodendocytes have invaded the white matter. We found that *robo1* was still expressed in the deep nuclei but that, in addition, it could be found in cells in the white matter, most likely glial cells (Fig. 9C; Table 5). *robo1* expression in the white matter was transient and persisted only until P10 (not shown, Table 5). *robo2* was also found from that stage in some deep nuclear neurons, but it was still highly expressed in all Purkinje cells, and at a low level in the granule cell layer (Fig. 9F). *slit1* expression was now discernible but restricted to the deep nuclei (Fig. 9I). In contrast to a previous study (Liang et al., 1999), we could not detect any *slit2* expression in the egl (Fig. 9L). *slit2* mRNA was found in small subsets of deep nuclear neurons and in subsets of Purkinje cells (Fig. 9L) in the vestibulocerebellum (uvula, nodulus, flocculus, and paraflocculus). At this stage, a low level of *slit3* expression started to be detectable in the granule cell layer (Fig. 9O). To a few noticeable exceptions, this expression pattern was maintained in the adult cerebellum. *robo1* and *robo2* were expressed in all subdivisions of the deep nuclei (Fig. 10A,B and not shown). *Robo2* was also expressed in all Purkinje cells but also in Golgi cells in the granule cell layer (Fig. 10B,G). *slit1* expression was very low and restricted to the lateral and interpositus deep nuclei (Fig. 10C, not shown; Table 6). *slit2* was also expressed in the lateral and interpositus nuclei and also in Purkinje cells in the vestibulocerebellum (Fig. 10D,F). In the adult cerebellum, *slit3* was very highly expressed in granule cells (Fig. 10E,H) and in the lateral cerebellar nuclei (not shown, Table 6).

Inferior olive. We studied in detail *slits* and *robos* expression in inferior olivary (IO) neurons, which project as climbing fibers to Purkinje cells and deep nuclear neurons in the cerebellum. At E15, when IO neurons have just finished their tangential migration from the rhombic lip, *robo1* and *robo2* expressions were diffuse in the brainstem. Nevertheless, most IO neurons expressed high level

TABLE 5. Spatiotemporal Distribution of *robo1* (1) and *robo2* (2) mRNA in the Mesencephalon and Rhombencephalon¹

Mesencephalon and rhombencephalon	E15	E18	E20	P0	P5	P10	Adult
Substantia nigra	1 2	1 2	1 2	1 2	1 2	1 2	1 2
Ventral tegmental area	1 -	1 -	1 -	1 -	1 -	1 -	1 -
Superior colliculus	1 2	1 2	1 2	- 2	- 2	- 2	- 2
Deep n.	- nd	- 2	- 2	- 2	- 2	- 2	- 2
Red n.	- nd	- 2	- 2	- 2	- 2	- 2	- 2
Cuneate n.	nd	1 2	1 2	1 2	1 2	1 2	1 2
Gracile n.	nd	1 2	1 2	1 2	1 2	1 2	1 2
Pontine n.	- -	- -	- -	- 2	- 2	- 2	- 2
Motor nuclei							
Oculomotor n. (III)	- -	- -	- -	- -	- -	- -	- -
Trochlear n. (IV)	- -	- -	- -	- -	- -	- -	- -
Trigeminal n. (V)	- -	1 -	1 -	1 -	1 -	1 -	1 -
Abducens n. (VI)	nd	nd	nd	nd	nd	1 -	1 -
Facial n. (VII)	1 -	1 -	1 -	1 -	1 -	1 -	1 -
Vagus n. (X)	1 -	1 -	1 -	- -	- -	- -	- -
Hypoglossal n. (XII)	1 2	1 2	1 2	1 2	1 2	1 2	1 2
Sensory nuclei							
Spinal trigeminal n. (Vs)	nd	- 2	- 2	- 2	- 2	- 2	- 2
Cochlear n. (VIII)	nd	1 2	1 2	1 2	1 2	1 2	1 2
Vestibular n. (VIII)	nd	1 2	1 2	1 2	1 2	1 2	1 2
Auditory pathway							
Inferior colliculus	1 2	1 2	1 2	- 2	- 2	- 2	- 2
Lateral superior olive	- -	- -	- -	- 2	- 2	- 2	- 2
Lemniscal n.	nd	- 2	- 2	- 2	- 2	- 2	- 2
Trapezoid n.	nd	- 2	- 2	- 2	- 2	- 2	- 2
Cerebellum							
Purkinje cells	- 2	- 2	- 2	- 2	- 2	- 2	- 2
Deep nuclei	1 -	1 -	1 2	1 2	1 2	1 2	1 2
Granule cells					- 2	- 2	- 2
White matter					1 -	1 -	- -
Inferior olivary complex							
Medial accessory olivary n.	- 2	- 2	- 2	- 2	- 2	- 2	- 2
Dorsal accessory olivary n.	- 2	- 2	- 2	- 2	1 2	1 2	1 2
Principal olivary n.	- -	- -	- -	- -	- -	- 2	- 2

¹ E, embryonic day; P, postnatal day; n., nucleus; nd, not determined; -, not detected.

of *robo2* mRNA whereas *robo1* labeling was hardly above background (Fig. 11A,D). Similarly, at this stage, *slit1* and *slit3* were weakly expressed in the IO, whereas *slit2* was not detectable (Fig. 11G,J,M). This expression pattern was unchanged until birth, when the olivary cytoarchitecture has already reached a mature appearance, thus, making it possible to determine which IO subnuclei express the different genes. At P1, *robo1* expression was still undetectable (Fig. 11B; Table 5), whereas *robo2* was highly expressed in the medial and dorsal accessory olive (MAO and DAO) and a large portion of the principal olive (PO; see Fig. 11E; Table 6). *slit1* transcripts were found in the PO and rostral MAO (Fig. 11H), *slit2* was not expressed, and *slit3* was detected at a low level throughout the IO (Fig. 11K,N; Table 6). From P10, the expression pattern was unchanged: there was a weak *robo1* expression in the DAO (Fig. 11C), whereas *robo2* was expressed in all IO neurons (Fig. 11F). *slit2* was not expressed in the IO, *slit1* was confined to the DAO and PO, but *slit3* was expressed in all IO subdivisions (Fig. 11I,L,O). In addition, at this stage, other precerebellar nuclei, which send mossy fibers to the cerebellar cortex, also clearly expressed some *slit* and *robo* genes. For instance, the lateral reticular nucleus expressed high levels of *slit2* and *slit3* (Fig. 11L,O), and pontine neurons expressed *slit3* and *robo2* mRNAs from the birth (not shown, and Fig. 6E,F).

Sensory and motor nuclei. In the medulla, cranial motor neurons are generated between E12 and E13 and neurons in brainstem sensory nuclei are generated slightly later between E13 and E15. Cranial motor neuron nuclei project to peripheral targets, whereas sensory nuclei project in a very precise topographic manner to the somatosensory thalamus (VPM and VPL). We also found

that *robo* genes were expressed in a distinct and almost complementary pattern; *robo1* was only expressed in cranial motor nuclei from E13, whereas from E15–E18, *robo2* was expressed by sensory nuclei (Fig. 11B–F; Table 5). However, *robo2* was also expressed by hypoglossal motor neurons (Fig. 11D,E). We found that *slit1*, *slit2*, and *slit3* were expressed in some cranial motor neurons (Fig. 11J–L; Table 6).

DISCUSSION

In this study, we provide the first comprehensive study of *slit* and *robo* gene expression in the developing and adult rat brain. We found that each of these genes is expressed in a unique spatiotemporal pattern. This analysis suggests that Slits and Robos are involved in multiple aspects of the development of many classes of neurons. It also underlines that our understanding of Slit and Robo functions is still incomplete.

To date, Slit and Robo function has been mostly studied in *Drosophila* embryos. In *Drosophila*, Slit is expressed by non-neuronal cells such as midline glia or muscle attachment sites, and regulates midline crossing by developing axons and the migration of muscle precursors (Rothberg et al., 1990; Kramer et al., 2001). For the latest, Slit is bifunctional, i.e., repulsive or attractive (Kramer et al., 2001). We found that in the rat CNS, like in *Drosophila*, *slit* genes are all expressed at the ventral midline in floor plate cells, but unlike *Drosophila*, they do not appear to be in glial cells. (This observation requires further confirmation by double staining with glial cell markers.) Likewise, *robos* are only found in neurons, with no apparent correlation between their temporal expression pattern and the

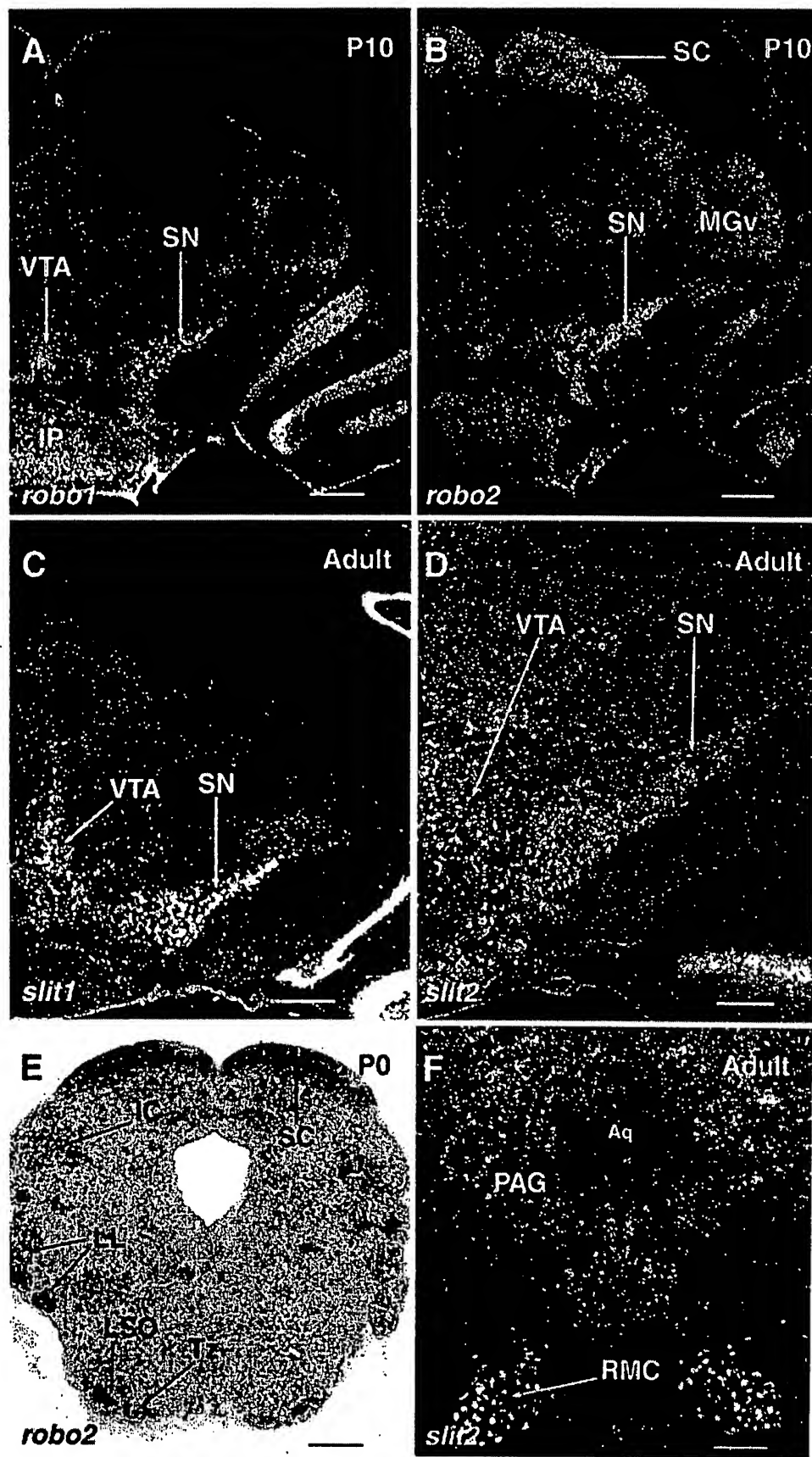


Fig. 8. *robos* and *slits* expression in the developing mesencephalon. Coronal sections were hybridized with digoxigenin-labeled riboprobe (E), or with 35 S-labeled riboprobes (A-D,F) for *robo1* (A), *robo2* (B,E), *slit1* (C), and *slit2* (D,F). A: At postnatal day (P) 10, *robo1* is strongly expressed in the substantia nigra pars compacta (SN), the ventral tegmental area (VTA), and in the interpeduncular nucleus (IP). B: At P10, *robo2* is highly detected in the superior colliculus (SC), the substantia nigra pars compacta (SN), and weakly in the ventral median geniculate nucleus (MGv). C,D: In the adult, *slit1* and *slit2*

are strongly expressed in the SN pars compacta and the ventral tegmental area (VTA). E: At P0, *robo2* is found in all the auditory relays: the inferior colliculus (IC), the lateral lemniscal nucleus (LL), the lateral superior olive (LSO), and the trapezoid body nucleus (Tz). *robo2* is also highly expressed in the superficial layer of the superior colliculus (SC). F: In the adult, *slit2* is detected in the periaqueductal gray (PAG) and the red magnocellularis nucleus (RMC). Aq, aqueduct. Scale bars = 660 μ m in A,B, 320 μ m in C,D,F, 550 μ m in E.

TABLE 6. Regional Distribution of *slit1* (1), *slit2* (2), and *slit3* (3) mRNA in the Mesencephalon and Rhombencephalon¹

Mesencephalon and rhombencephalon	E15	E18	E20	P0	P5	P10	Adult
Substantia nigra	---	---	---	---	---	1--	12-
Ventral tegmental area	---	---	---	---	---	1--	1--
Superior colliculus	1--	1--	1--	1--	1--	1--	1--
Red n.	-2-	-2-	-2-	-2-	-2-	-2-	-2-
Inferior colliculus	1--	1-	1--	1--	1--	1--	1--
Raphe n.	-2-	-2-	-2-	-2-	-2-	12-	12-
Pontine n.	---	---	---	-3	-3	-3	-3
Motor nuclei							
Oculomotor n. (III)	-2 3	-2 3	-2 3	-3	-3	-3	-3
Trochlear n. (IV)	-3	-2 3	-3	-3	-3	-3	-3
Trigeminal n. (V/m)	1 2 3	2 3	2 3	2 3	2 3	2 3	2 3
Abducens n. (VI)	nd	nd	nd	nd	nd	-2 3	-2 3
Facial n. (VII)	-2 3	-2 3	-2 3	-2 3	-2 3	-2 3	-2 3
Vagus n. (X)	-3	-3	-3	-3	-3	-3	-3
Hypoglossal n. (XII)	1 2 3	1 2 3	1 2 3	1 2 3	1 2 3	1 2 3	1 2 3
Sensory nuclei							
Spinal trigeminal n. (Vs)	nd	---	---	---	---	---	---
Cochlear n. (VIII)	nd	1--	1--	1--	1--	1--	1-3
Vestibular n. (VIII)	nd	12-	12-	12-	12-	12 3	12 3
Cerebellum							
Purkinje cells	-2-	-2-	-2-	-2-	-2-	-2-	-2-
Deep nuclei	1--	1--	1--	12-	12 3	12 3	12 3
Granule cells				---	-3	-3	-3
Inferior olivary complex							
Medial accessory olivary n.	1--	1--	1--	1-3	1-3	1-3	1-3
Dorsal accessory olivary n.	1--	1--	1--	1-3	1-3	1-3	1-3
Principal olivary n.	1--	1--	1--	1-3	1-3	1-3	1-3

¹ E, embryonic day; P, postnatal day; n., nucleus; nd, not determined; -, not detected.

crossing or noncrossing of the CNS midline by their axons. This finding suggests that these molecules play multiple roles in the control of CNS development.

Our study revealed that most CNS neurons express at least one *robo* and one *slit* gene during their development. The only noticeable exceptions to this rule being the septum (where no *robos* were detected), layer IV neurons in the neocortex, and dispersed reticular neurons in the brainstem. Some neurons express only one *slit* gene. This is the case for neurons in the olfactory epithelium, the lateral habenula, the hypothalamus, or the superior and inferior colliculi, which express only *slit1*. Similarly, cerebellar Purkinje cells and supraoptic and suprachiasmatic neurons in the hypothalamus express only *slit2*, whereas cerebellar granule cells and motor neurons of the vagus nerve express only *slit3*. Nonetheless, in most systems, neurons express multiple *slit* genes simultaneously, sometimes (e.g., in the hippocampus) at different periods of their development. At the extreme, CA3, entorhinal cortex, hypoglossus, and layer V neurons among others, co-express the three *slit* genes from E15 to the adult. In most cases, *slit* expression is up-regulated after P10 such as the three *slit* genes are simultaneously expressed only when neurons have reached the adult stage.

Likewise, most neurons express a single *robo* gene, either *robo1* (olfactory tubercle, indusium griseum, ventral tegmental area, and so on) or more often *robo2* (most sensory related neurons, Purkinje cells, pons, subiculum, and so on). However, some coexpress, *robo1* and *robo2*, such as in the substantia nigra, hypoglossus, or striatum. Interestingly, *robo*'s expression pattern is less dynamic than *slits*, and with a few exceptions (olfactory tubercle and accessory olfactory bulb), it does not evolve much between E15 and the adult. Another interesting aspect of *slit* and *robo* expression patterns is that in several systems, and particularly at embryonic stages, these genes are expressed in a complementary manner. For instance, in the embryonic cerebellum, Purkinje cells express *robo2*

and *slit2*, whereas their target cells in the cerebellum, the deep nuclear neurons, express *robo1* and *slit1*. Similarly, in the E15 cerebral cortex, *robo1* is in the cortical plate and *robo2* in the intermediate and subventricular zones.

slit3 expression pattern is rather unique. From E13 to birth it is found almost exclusively in the hippocampal formation, whereas other *slits* are more widely expressed. The onset of *slit3* expression coincides with the first delineation of the hippocampal primordium and is maintained in the hippocampal formation until the adult stage. *slit3* is one of the first genes selectively expressed in the embryonic hippocampal formation, suggesting that *Slit3* has an important function in the development of this system. For instance, it might regulate the formation of neuronal connections and/or the specification of the hippocampal region. Several genes also expressed in the embryonic hippocampal primordium have been identified, some of which code for transcription factors (Tole et al., 1997; Grove and Tole, 1999; Tole and Grove, 2001). This finding led to the hypothesis that the pole of the hippocampal primordium close to the midline, the so-called cortical hem, is an organizer of the hippocampal field, producing diffusible inductive factors, and *Slit3* could participate to this process.

Role for Slits and Robos in projection map formation

In the CNS, most axons do not terminate randomly in their target territory but are precisely organized, with a specific topography, and form the so-called projection maps. One of the major conclusions of our study is the spatiotemporal coincidence of *robo* expression in developing structures that project abroad long distances and in a highly ordered pattern. In particular, *robo2* expression is tightly associated to developing sensory systems (olfactory, visual, auditory, and somatosensory) during the critical period of sensory axons outgrowth and pathfinding to the CNS *robo2* is expressed in all sensory-related stations of

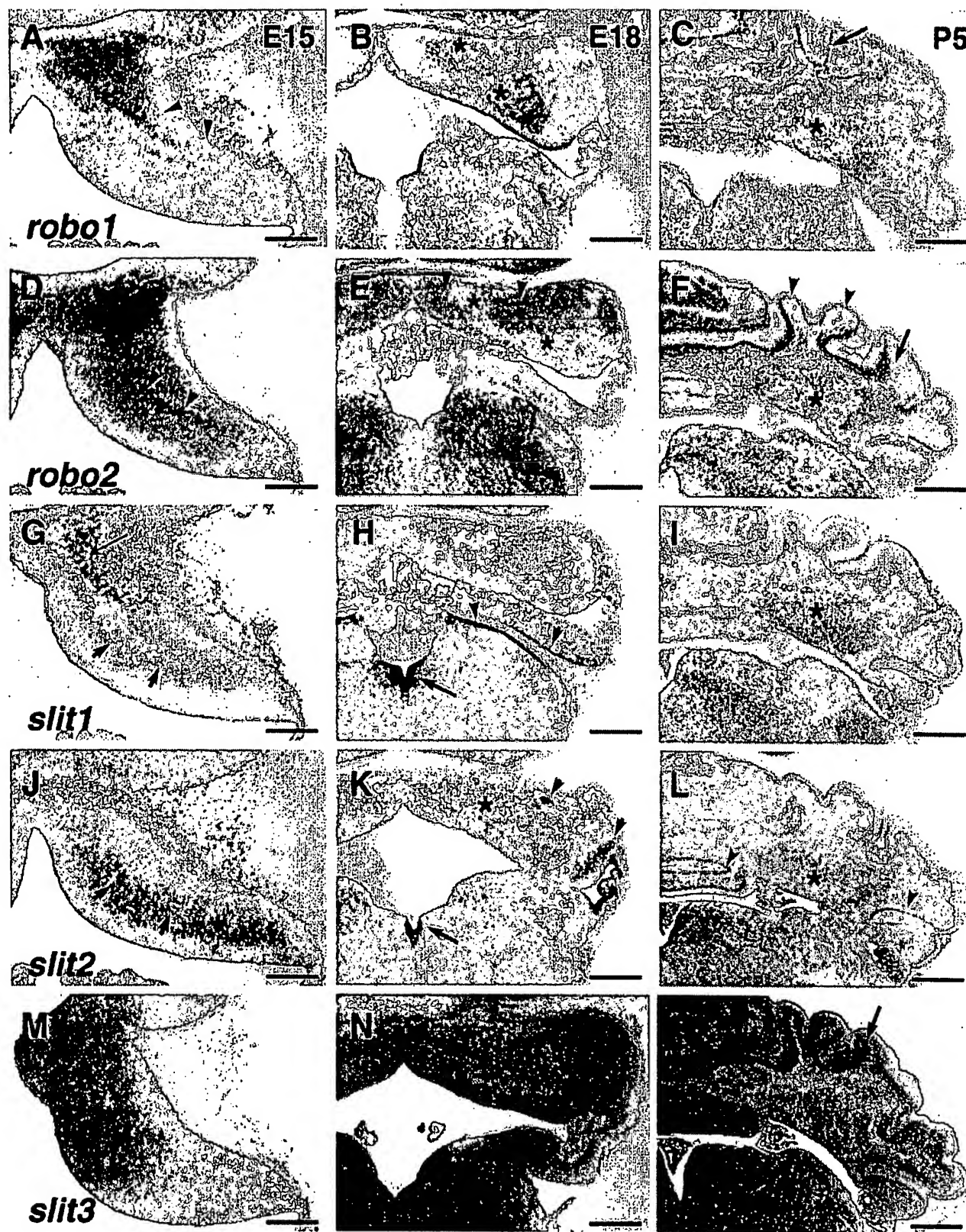


Figure 9

the CNS during their period of axonal pathfinding. For instance, in the visual system, *robo2* is expressed from E15 in retinal ganglion cells, in the primary visual thalamic relay, the dorsal lateral geniculate nucleus and in the superior colliculus. Moreover, in vitro studies have shown that Slit2 repels developing retinal and thalamic axons (Erskine et al., 2000; Niclou et al., 2000; Ringstedt et al., 2000). In the auditory system, we find that *robo2* is expressed during the period of axonal pathfinding of auditory related peripheral and central structures, the cochlea, the cochlear nuclei, the inferior colliculus, the lateral superior olive, the trapezoid body nucleus, and the thalamic median geniculate nucleus. Similarly, in the somatosensory system, *robo2* is expressed during the period of axonal pathfinding of somatosensory-related structures, the trigeminal ganglion, the dorsal root ganglia, the cuneate and gracile nuclei, the three spinal trigeminal nuclei (principalis, oralis, and interpolaris), and the thalamic ventroposterior medial and lateral nuclei. Taken together, we can propose that Robo2 participates to the guidance of all primary sensory and central sensory-related axons. *robo2*, which is also expressed in most components of the motor system (layer V of the motor cortex, basal ganglia, ventromedial nucleus of the thalamus, red nucleus, basilar pons, cerebellum, inferior olive, motor nuclei) could also control the guidance of motor-related axons in the CNS.

In some systems, there is a good correlation between *slits* and *robos* expression. In the accessory olfactory system, where the apical and basal zones of the vomeronasal organ are mapped, respectively, to rostral and caudal domains of the accessory olfactory bulb (Mori et al., 2000), *slit1* and *robo2* are expressed topographically. *robo2* is expressed in the basal zone of the VNO, whereas *slit1* is restricted to the apical part of the VNO, which suggests that these two molecules might participate to the organization of this projection possibly by restricting the mixing

between the two populations of axons. *robo1* and *robo2* are also expressed in the AOB, but it is still unclear whether their expression is restricted to some domains.

Another example is the olivocerebellar system where inferior olivary neurons, in the medulla oblongata, send axons to Purkinje cells in the cerebellar cortex. This projection is arranged according to a precise spatial order resulting from the segregation of olivary axons (the climbing fibers) into distinct compartments of Purkinje cells forming adjacent parasagittal bands. Studies on the development of the olivocerebellar system in vertebrates have revealed that, before the entry of olivary fibers into the cerebellum, there is a simultaneous, independent, and transient biochemical parcellation of the cerebellar cortex and the inferior olive (Sotelo and Chédotal, 1997). Therefore, we have suggested that the major mechanism involved in the formation of the olivocerebellar topography is the existence of matched positional or guidance cues between clusters of PCs and corresponding clusters of IO neurons (Sotelo and Chédotal, 1997). Our results suggest that Slits and Robos could be involved in the targeting of inferior olivary axons. From E15, when inferior olivary axons enter the cerebellar primordium (Wassef et al., 1992), *robo2* is expressed by subsets of inferior olivary neurons, and *slit2* by subsets of Purkinje cells in the vestibulocerebellum. Moreover, deep nuclear neurons, which are the targets of PCs axons and also of inferior olivary axon collaterals, also expressed combination of *slits* and *robos*.

Are Slits and Robos involved in neuronal migration?

In rodents, Slit1 and Slit2 are thought to play a role in the tangential migration of telencephalic interneurons. For instance, in diffusion assays, Slit1 and Slit2 are very potent repellents for neuroblasts produced in the subventricular zone and migrating along the rostral migratory stream (RMS) to the olfactory bulb (Hu, 1999; Wu et al., 1999). Similar studies have shown that GABAergic interneurons, migrating from the medial ganglionic eminence to the neocortex are also repelled by Slit1 and Slit2 (Zhu et al., 1999). In those two cases, if the involvement of Slit proteins seems convincing, the expression of robo receptors by the migrating neurons had not been demonstrated. We found that neuronal cells born in the postnatal telencephalic subventricular zone display a strong *robo2* expression and a weak *robo1* expression from their entrance in RMS to their arrival in the olfactory bulb, which suggests a role of the couple slits/robos in the control of this migration. In the meantime, we found that these migrating cells, specially in the adult brain, also express high levels of *slit1* mRNA, suggesting that Slit1 exerts additional functions in this system, and may act in an autocrine manner (see below), possibly by influencing the proliferation or the differentiation of these cells. Moreover, we could not detect any *robo* expression in cells migrating through the ganglionic eminences to the neocortex, which does not support a role for Robo1 or Robo2 in the control of the migration of these neurons in vivo. A possibility could be that, in this system, *slit* function is mediated by another receptor (see below).

Other expression data support a role for Slit and Robo, and more precisely Robo2, in the control of tangential migration. In the hindbrain, precerebellar neurons, of the inferior olive and pontine nuclei, migrate tangentially to

Fig. 9. *robos* and *slits* expression in the developing cerebellum. Coronal sections were hybridized with digoxigenin-labeled riboprobes for *robo1* (A–C), *robo2* (D–F), *slit1* (G–I), *slit2* (J–L), and *slit3* (M,N). **A:** At embryonic day (E) 15, *robo1* is detected in migrating deep nuclear neurons (arrowheads). **B:** At E15, *robo1* is only expressed in neurons of the deep nuclei (asterisks). **C:** At postnatal day (P) 5, *robo1* is still found in the deep nuclei (asterisk), and in glial cells of the cerebellar white matter (arrow). **D:** At E15, *robo2* is also expressed in migrating Purkinje cells (arrowheads). **E:** At E18, *robo2* is specifically found in Purkinje cells (arrowheads) and is not detected in the deep nuclei (asterisks). **F:** At P5, *robo2* expression is maintained in Purkinje cells (arrowheads). However, *robo2* is also present in some cells of the deep nuclei (asterisk) and at a low level in the granular cell layer (arrow). **G:** At E15, a very low level of *slit1* is found in the migrating Purkinje cells of the mantle layer (short arrows) and in migrating cells (long arrow) probably cells of the parabrachial nucleus. **H:** At E18, *slit1* is not detectable in the cerebellum, but it can be observed in the rhombic lip (arrowheads) and in the floor plate (arrow). **I:** At P5, *slit1* is expressed in the deep nuclei (asterisk). **J:** At E15, at a high level of *slit2* mRNAs is expressed in migrating Purkinje cells of the mantle layer (short arrows). **K:** At E18, *slit2* is expressed in subsets of deep nuclear neurons (asterisk) and subsets of Purkinje cells (arrowheads). *slit2* is also present in the floor plate (arrow). **L:** At P5, *slit2* is expressed in small subsets of deep nuclei (asterisk) and Purkinje cells in the vestibulo-cerebellum (arrowheads). **M,N:** *slit3* is not detected from E15 (M) to E18 (N) in the cerebellum. **O:** At P5, a low level of *slit3* was detectable in the granule cell layer (arrow). Scale bars = 230 μ m in A,D,G,J,M, 420 μ m in B,E,H,K,N, 600 μ m in C,F,I,L,O.

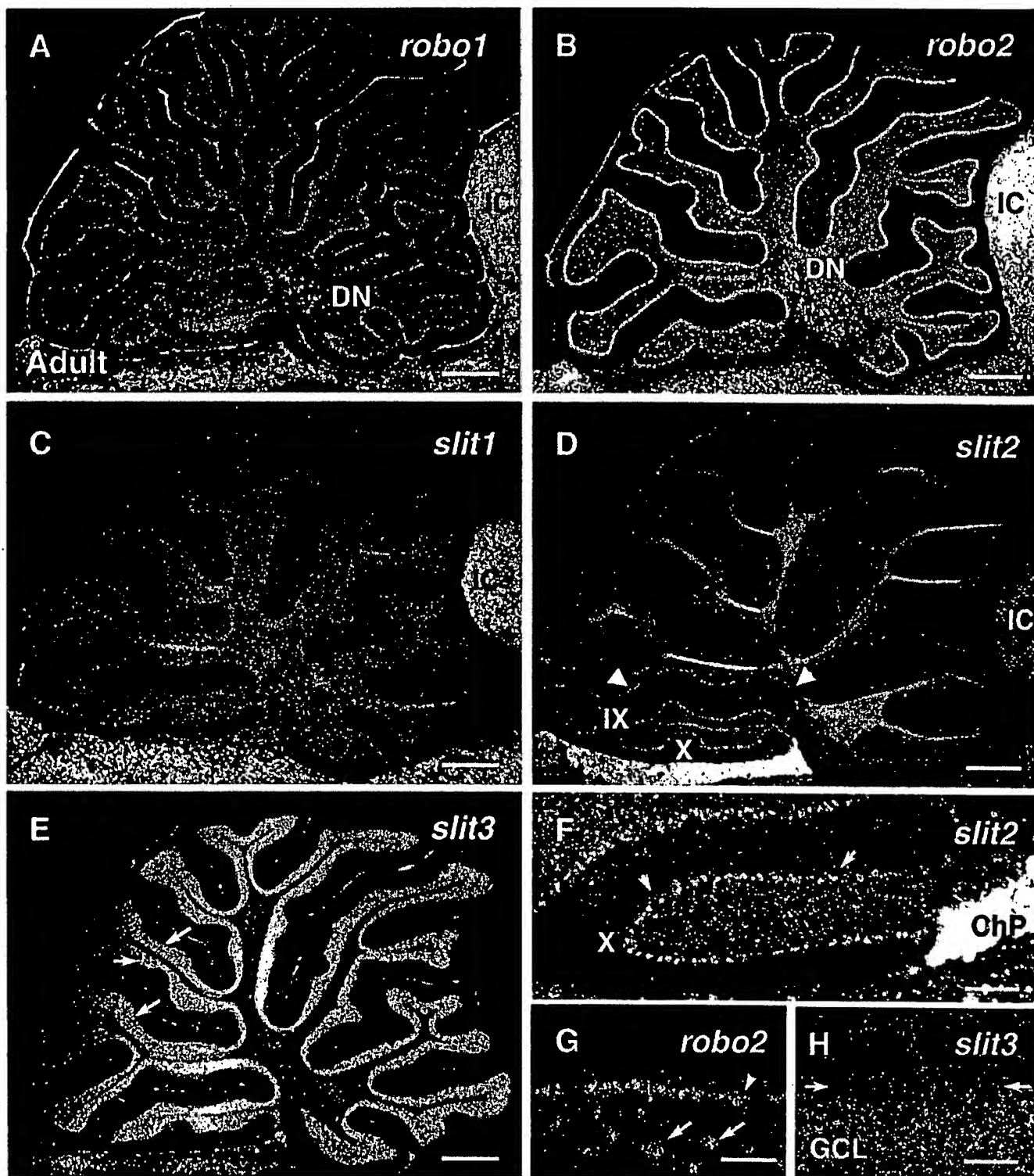


Fig. 10. *robos* and *slits* expression in the adult cerebellum. Sagittal sections (A–H) were hybridized with ^{36}S -labeled riboprobes for *robo1* (A), *robo2* (B,G), *slit1* (C), *slit2* (D,F), and *slit3* (E,H). A: *robo1* is expressed in all the deep nuclear neurons (DN). B: *robo2* is highly expressed in all Purkinje cells, deep nuclear neurons (DN), and Golgi cells. C: *slit1* is absent of the adult cerebellum. D: *slit2* is specifically detected in Purkinje cells of the lobules IX and X (arrowheads). E: *slit3* is highly expressed in the granular cell layer (arrows).

F: Higher magnification of *slit2* expression in Purkinje cells of the lobule X (short arrows). G: Higher magnification of *robo2* expression in Purkinje cells (arrowhead) and Golgi cells (short arrows). H: Higher magnification of *slit3* expression in granular cell layer (GCL) of the cerebellum. The short arrows indicate the Purkinje cell layer. IC, inferior colliculus; ChP, choroid plexus. Scale bars = 890 μm in A–E, 240 μm in F, 180 μm in G, 60 μm in H.

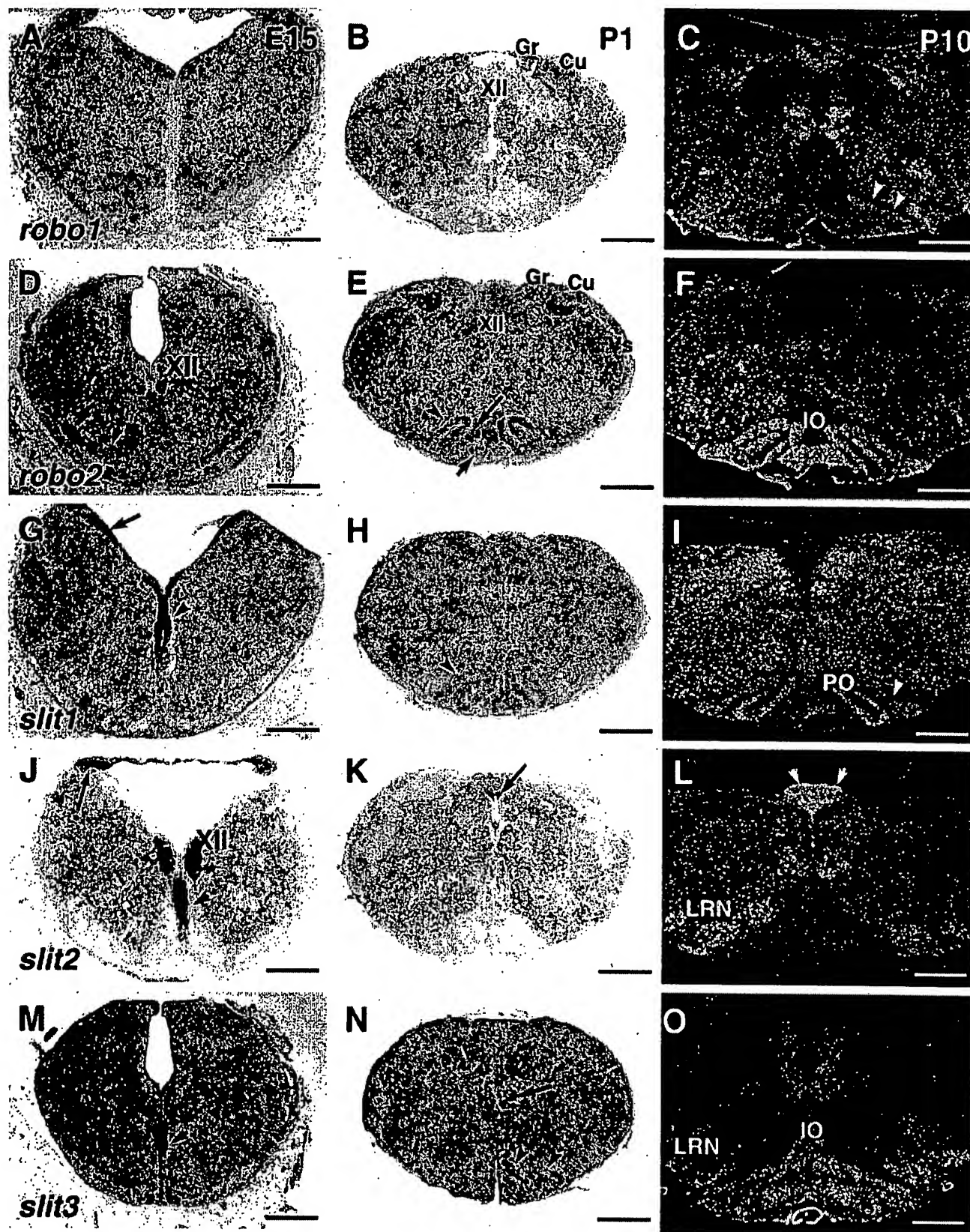


Figure 11

ward the floor plate. During their migration, these neurons express *robo2*, whereas *slit1*, *slit2*, and *slit3* are found in the floor plate. Interestingly, their migration is known to be under the control of netrin-1 (Bloch-Gallego et al., 1999; Yee et al., 1999; Alcantara et al., 2000), another diffusible factor, which can bind to Slit and whose receptor DCC has just been shown to interact with Robo (Stein and Tessier-Lavigne, 2001). It is therefore likely that slits and netrin-1, which are essential for the control of midline crossing by developing axons, cooperate to control the tangential migration of precerebellar neurons.

Our study reveals that *robo2* is expressed in the embryonic olfactory epithelium but also in cells migrating away from this epithelium (De Carlos et al., 1995). During development, three distinct cell types migrate from the olfactory epithelium and, thus, might express *robo2*: the glial ensheathing cells, the LHRH-producing cells, and some olfactory marker protein (OMP)-immunoreactive cells (De Carlos et al., 1995). Glial ensheathing cells contribute to the development of olfactory glomeruli (De Carlos et al., 1995). LHRH neurons migrate through the forebrain to their final destination in the septal preoptic nuclei and hypothalamus (Schwanzel-Fukuda and Pfaff, 1989). OMP-immunoreactive cells migrate to the ventrolateral part of the olfactory bulb (De Carlos et al., 1995). Because *slit1* and *slit2* are expressed in cells lining the pathway followed by the migrating cells (the midline mesenchymal cells, the olfactory epithelium, the olfactory bulb, the basal forebrain, and so on), Slit/Robo could be involved in the control of the migration of these cells.

Role of Slits and Robos in axonal branching

Several axon guidance molecules are also branching factors (see for a review Kalil et al., 2000). Slit2 was originally isolated in vertebrate as a branching factor for NGF-responsive sensory axons of the dorsal root ganglia (Wang et al., 1999). It is not known yet whether Slit2 has

as a similar branching activity on other classes of axons, neither is it known whether other slits have branching activities. In the CNS, axonal branching has been mostly studied in the corticopontine projection. In this system, layer V neurons of the motor cortex initially project into the spinal cord and later send axon collaterals to their final target, the basilar pons, by a process of interstitial branching (O'Leary et al., 1990, 1991). Coculture experiments in collagen gels have shown that these axonal branches are attracted toward the pons by a diffusible factor that has not been identified yet (Heffner et al., 1990). We found that during this branching period (occurring between birth and P2 in vivo) layer V neurons express *robo1* and *robo2* mRNAs and that the basilar pons expresses high levels of *slit3*. Therefore, it will be interesting to test directly whether Slit3 can stimulate branch formation in this system.

Slits and Robos function in the adult brain

A surprising result of our study is the clear demonstration that the expression of *slits* and their receptors is up-regulated during postnatal development and maintained at high levels in adult neurons. This up-regulation suggests that the function of these proteins is not restricted to the control of axonal pathfinding and neuronal migration but that they could also be involved in synaptic plasticity. The hippocampus is such a structure where persistent changes in connectivity have been observed and are correlated with modifications of neural activity (Toni et al., 1999). Interestingly, *slit1* and *robo2* expression patterns in the hippocampus change abruptly from P10, when synaptogenesis increases in this system (Steward and Falk, 1991).

In the adult CNS, injured neurons are not able to regenerate their axons. Myelin and proteoglycans are the best identified inhibitory molecules preventing axon regeneration, but chemorepulsive factors have also been proposed to play a role in this process (Pasterkamp et al., 2000). We could not obtain any evidence for *slits* expression in oligodendrocytes or astrocytes, which would argue against a role for these molecules in the inhibition of regeneration, although it could be possible that glial cells express them after a lesion.

CONCLUDING REMARKS

Most neurons simultaneously express *slit* and *robo* genes. It has been shown that there is a promiscuous binding of Slits to the different Robos (Brose et al., 1999; Li et al., 1999; A.C., K.T.N.-B.-C. and M.T.L. unpublished observation). For instance, in *Drosophila*, Slit is able to activate all Robos (Rajagopalan et al., 2000a,b; Simpson et al., 2000a,b). Therefore, our observations suggest that, in many systems, Slits could act in an autocrine manner, but this possibility requires direct testing. Such a coexpression of a diffusible factor and its receptors and a possible autocrine action has been proposed before for Slit2 in the developing spinal cord (Brose et al., 1999; Wang et al., 1999), and for members of the Semaphorin family (Shepherd et al., 1997; William-Hogarth et al., 2000). However, it was shown that, although all secreted semaphorins can bind with similar affinity to the neuropilin-1 (Chen et al., 1997), only a few of them are active on neuropilin-1 expressing axons and that coreceptors (the plexins) are required to specify the response (Takahashi et al., 1999;

Fig. 11 (Overleaf). *robos* and *slits* expression in the developing olivary system. Coronal sections were hybridized with digoxigenin-labeled riboprobes (A,B,D,E,G,H,J,K,M,N) or with ³⁵S-labeled riboprobes (C,F,I,L,O) for *robo1* (A–C), *robo2* (D–F), *slit1* (G–I), *slit2* (J–L), and *slit3* (M–O). A–C: At embryonic day (E) 15 (A), *robo1* is not detected in inferior olivary neurons, and at postnatal day (P) 1 (B) *robo1* expression is still undetectable in this structure. From postnatal day (P) 10 (C), a low level of *robo1* is found in the dorsal accessory olive (arrowheads). A weak *robo1* expression is observed in the hypoglossal (XII), the cuneate (Cu), and gracile (Gr) nuclei from P1. D–F: At E15 (D), *robo2* is strongly expressed in migrating olivary neurons in the tangential migratory stream (short arrows). From P1 (E) to P10 (F), *robo2* is highly detected in the medial and dorsal accessory olive (arrowhead) a large portion of the principal olive (long arrow) and in the medial accessory olive (short arrow). *robo2* is also observed in the hypoglossal nucleus (XII), the spinal trigeminal nuclei (Vs), and the cuneate (Cu) and the gracile (Gr) nuclei. G–I: At E15 (G), *slit1* is detected in the rhombic lip (arrow) and in the floor plate (arrowhead). From P1 (H), *slit1* starts to be detected in the principal olive (PO) and the dorsal accessory olive (arrowhead in H and I). J–L: From E15 (J) to P10 (L), *slit2* is highly expressed in the hypoglossal nucleus (XII), the lateral reticular nucleus (LRN), the area postrema (arrowheads in L), the rhombic lip (arrow in J), in the floor plate at E15 (arrowhead in J), and in the roof plate (arrow in K). M–O: At E15 (M), *slit3* is only detected in the floor plate (short arrow). From P1 (N) to P10 (O), *slit3* is also expressed in the inferior olive (IO) (arrowheads in N), the hypoglossal (arrow in N) and the lateral reticular (LRN) nuclei. Scale bars = 300 μm in A,D,G,J,M, 670 μm in B,C,E,F,H,I,K,L,N,O.

Tamagnone et al., 1999). In mammals, no direct proof has been obtained yet demonstrating the involvement of Robos in mediating all Slit actions. Moreover, Slits are also ligands of the heparan sulfate proteoglycan glypican-1 (Liang et al., 1999; Ronca et al., 2001), which is also expressed in developing neurons (Karthikeyan et al., 1994). It is likely that the slit receptor is a multimeric complex, and that understanding slit/robo function will require identifying and studying the expression pattern of these coreceptors that could modulate slit function. Several recent studies support this idea, as Robos have been shown to interact with the netrin receptor DCC (Stein and Tessier-Lavigne, 2001) and with the chemokine receptor CXCR4 (Wu et al., 2001). We have also shown that the response of sensory axons to Slit2 is modulated by extracellular matrix proteins such as laminin (Nguyen-Ba-Charvet et al., 2001b).

An important limitation to the analysis of slit/robo function in the vertebrate brain is the absence of antibodies allowing to visualize the subcellular location of slit and robo proteins. This is crucial, as in *Drosophila*, a key element in Robo function is the regulation of its expression on the growth cone by transmembrane proteins of the Commissureless family (Comm; Tear et al., 1996; Kidd et al., 1998b; Rajagopalan et al., 2000a; Simpson et al., 2000b). Comm acts posttranscriptionally to maintain Robo expression at a low level on the cell membrane of commissural axons until they have crossed the CNS midline. The exact mechanism of action of Comm is still unknown, and to date no Comm homologues have been identified in vertebrates. If such homologues exist, neurons expressing robo mRNAs could still be unresponsive to Slit. Recently, the phenotype of a Zebrafish mutant of the robo2 homologue, *astray*, has been reported and confirmed that this receptor is crucial for axonal pathfinding at the CNS midline. It is clear that an important step toward the understanding of slit/robo function in mammals will come from the analysis of robo and slit mutants.

ACKNOWLEDGMENTS

K.T.N.-B.-C. is supported by the Fondation de France, V.M. is a recipient of a MENRT fellowship, and M.T.L. is an investigator of the HHMI.

LITERATURE CITED

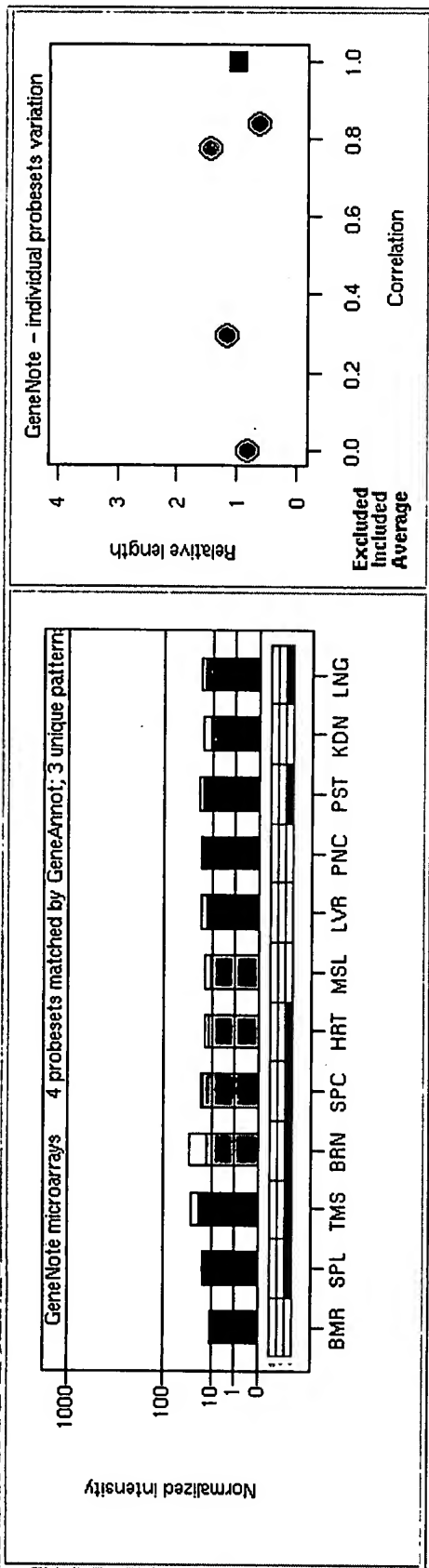
- Alcantara S, Ruiz M, De Castro F, Soriano E, Sotelo C. 2000. Netrin 1 acts as an attractive or as a repulsive cue for distinct migrating neurons during the development of the cerebellar system. *Development* 127:1359–1372.
- Altman J, Bayer SA. 1978. Development of the diencephalon in the rat. I. Autoradiographic study of the time of origin and settling patterns of neurons of the hypothalamus. *J Comp Neurol* 182:945–971.
- Altman J, Bayer SA. 1985. Embryonic development of the rat cerebellum. III. Regional differences in the time of origin, migration, and settling of Purkinje cells. *J Comp Neurol* 231:42–65.
- Altman J, Bayer SA. 1988. Development of the rat thalamus: I. Mosaic organization of the thalamic neuroepithelium. *J Comp Neurol* 275:346–377.
- Battye R, Stevens A, Jacobs JR. 1999. Axon repulsion from the midline of the *Drosophila* CNS requires slit function. *Development* 126:2475–2481.
- Bloch-Gallego E, Ezan F, Tessier-Lavigne M, Sotelo C. 1999. Floor plate and netrin-1 are involved in the migration and survival of inferior olivary neurons. *J Neurosci* 19:4407–4420.
- Brose K, Bland KS, Wang K-H, Arnott D, Henzel W, Goodman CS, Tessier-Lavigne M, Kidd T. 1999. Slit proteins bind Robo receptors and have an evolutionarily conserved role in repulsive axon guidance. *Cell* 96:795–806.
- Brose K, Tessier-Lavigne M. 2000. Slit proteins: key regulators of axon guidance, axonal branching, and cell migration. *Curr Opin Neurobiol* 10:95–102.
- Chen H, Chédotal A, He ZG, Goodman CS, Tessier-Lavigne M. 1997. Neuropilin-2, a novel member of the neuropilin family, is a high affinity receptor for the semaphorins Sema E and Sema IV but not Sema III. *Neuron* 19:547–559.
- Chen J-H, Wen L, Dupuis S, Wu JY, Rao Y. 2001. The N-terminal leucine-rich regions in slit are sufficient to repel olfactory bulb axons and subventricular zone neurons. *J Neurosci* 21:1548–1556.
- Cholley B, Wassef M, Arsenio-Nunes L, Brehier A, Sotelo C. 1989. Proximal trajectory of the brachium conjunctivum in rat fetuses and its early association with the parabrachial nucleus. A study combining in vitro HRP anterograde axonal tracing and immunocytochemistry. *Dev Brain Res* 45:185–202.
- De Carlos JA, Lopez-Mascaraque L, Valverde F. 1995. The telencephalic vesicles are innervated by olfactory placode-derived cells: a possible mechanism to induce neocortical development. *Neuroscience* 68:1167–1178.
- Erskine L, Williams SE, Brose K, Kidd T, Rachel RA, Goodman CS, Tessier-Lavigne M, Mason CA. 2000. Retinal ganglion cell axon guidance in the mouse optic chiasm: expression and function of robos and slits. *J Neurosci* 20:4975–4982.
- Feirabend HK. 1990. Development of longitudinal patterns in the cerebellum of the chicken (*Gallus domesticus*): a cytoarchitectural study on the genesis of cerebellar modules. *Eur J Morphol* 28:169–223.
- Grove EA, Tole S. 1999. Patterning events and specification signals in the developing hippocampus. *Cereb Cortex* 9:551–561.
- Halloran MC, Sato-Maeda M, Warren JT, Su F, Lele Z, Krone PH, Kuwada JY, Shoji W. 2000. Laser-induced gene expression in specific cells of transgenic zebrafish. *Development* 127:1953–1960.
- Heffner CD, Lumsden AG, O'Leary DD. 1990. Target control of collateral extension and directional axon growth in the mammalian brain. *Science* 247:217–220.
- Hohenester E, Tisi D, Talts JF, Timpl R. 1999. The crystal structure of a laminin G-like module reveals the molecular basis of alpha-dystroglycan binding to laminins, perlecan, and agrin. *Mol Cell* 4:783–792.
- Holmes GP, Negus K, BurrIDGE L, Raman S, Algar E, Yamada T, Little MH. 1998. Distinct but overlapping expression patterns of two vertebrate slit homologs implies functional roles in CNS development and organogenesis. *Mech Dev* 79:57–72.
- Hu H. 1999. Chemorepulsion of neuronal migration by Slit2 in the developing mammalian forebrain. *Neuron* 23:703–711.
- Itoh A, Miyabayashi T, Ohno M, Sakano S. 1998. Cloning and expression of three mammalian homologues of *Drosophila* slit suggest possible roles for slit in the formation and maintenance of the nervous system. *Mol Brain Res* 62:175–186.
- Kalil K, Szebenyi G, Dent EW. 2000. Common mechanisms underlying growth cone guidance and axon branching. *J Neurobiol* 44:145–158.
- Karthikeyan L, Flad M, Engel M, Meyer-Puttlitz B, Margolis R, Margolis R. 1994. Immunocytochemical and in situ hybridization studies of the heparan sulfate proteoglycan, glypican, in nervous tissue. *J Cell Sci* 107:3213–3222.
- Kidd T, Brose K, Mitchell KJ, Fetter RD, Tessier-Lavigne M, Goodman CS, Tear G. 1998a. Roundabout controls axon crossing of the CNS midline and defines a novel subfamily of evolutionarily conserved guidance receptors. *Cell* 92:205–215.
- Kidd T, Russell C, Goodman CS, Tear G. 1998b. Dosage-sensitive and complementary functions of roundabout and commissureless control axon crossing of the CNS midline. *Neuron* 20:25–33.
- Kidd T, Bland KS, Goodman CS. 1999. Slit is the midline repellent for the robo receptor in *Drosophila*. *Cell* 96:785–794.
- Kramer SG, Kidd T, Simpson JH, Goodman CS. 2001. Switching repulsion to attraction: changing responses to slit during transition in mesoderm migration. *Science* 292:737–740.
- Li H-S, Chen J-H, Wu W, Fagaly T, Zhou L, Yuan W, Dupuis S, Jiang Z-H, Nash W, Glick C, Ornitz DM, Wu JY, Rao Y. 1999. Vertebrate Slit, a secreted ligand for the transmembrane protein roundabout, is a repellent for olfactory bulb axons. *Cell* 96:807–818.
- Liang Y, Annan RS, Carr SA, Popp S, Mevissen M, Margolis RK, Margolis RU. 1999. Mammalian homologues of the *Drosophila* Slit protein are

- ligands of heparan sulfate proteoglycan Glypican-1 in brain. *J Biol Chem* 274:17885-17892.
- Lopez-Mascaraque L, De Carlos JA, Valverde F. 1996. Early onset of the rat olfactory bulb projections. *Neuroscience* 70:255-266.
- Mori K, Von Campenhausen H, Yoshihara Y. 2000. Zonal organisation of the mammalian main and accessory olfactory systems. *Philos Trans R Soc Lond B* 355:1801-1812.
- Nguyen-Ba-Charvet KT, Brose K, Marillat V, Kidd T, Goodman CS, Tessier-Lavigne M, Sotelo C, Chédotal A. 1999. Slit2-mediated chemorepulsion and collapse of developing forebrain axons. *Neuron* 22:463-473.
- Nguyen-Ba-Charvet KT, Brose K, Ma L, Wang KH, Marillat V, Sotelo C, Tessier-Lavigne M, Chédotal A. 2001a. Diversity and specificity of actions of slit2 proteolytic fragments in axon guidance. *J Neurosci* 21:4281-4289.
- Nguyen-Ba-Charvet KT, Brose K, Marillat V, Sotelo C, Tessier-Lavigne M, Chédotal A. 2001b. Sensory axon response to substrate-bound slit2 is modulated by laminin and cyclic GMP. *Mol Cell Neurosci* 17:1048-1058.
- Niclou SP, Julia L, Raper JA. 2000. Slit2 is a repellent for retinal ganglion cell axons. *J Neurosci* 20:4962-4974.
- Nusslein-Volhard C, Wiechaus E, Kluding H. 1984. Mutations affecting the pattern of the larval cuticle in *Drosophila melanogaster*. I. Zygotic loci on the second chromosome. *Roux Arch Dev Biol* 193:267-283.
- O'Leary DD, Bicknese AR, De Carlos JA, Heffner CD, Koester SE, Kutka LJ, Terashima T. 1990. Target selection by cortical axons: alternative mechanisms to establish axonal connections in the developing brain. *Cold Spring Harb Symp Quant Biol* 55:453-468.
- O'Leary DDM, Heffner CD, Kutka L, Lopez-Mascaraque L, Missias A, Reinoso BS. 1991. A target-derived chemoattractant controls the development of the corticopontine projection by a novel mechanism of axon targeting. *Development Suppl* 2:123-130.
- Pasterkamp RJ, Giger RJ, Baker RE, Hermens WT, Verhaagen J. 2000. Ectopic adenoviral vector-directed expression of Sema3A in organotypic spinal cord explants inhibits growth of primary sensory afferents. *Dev Biol* 220:129-141.
- Paxinos G, Törk I, Tcort LH, Valentino KL. 1991. Atlas of the developing rat brain. San Diego: Academic Press.
- Paxinos G, Watson C. 1986. The rat brain stereotaxic coordinates. San Diego: Academic Press.
- Pini A. 1993. Chemorepulsion of axons in developing mammalian central nervous system. *Nature* 261:95-98.
- Puelles L, Kuwana E, Puelles E, Bulfone A, Shimamura K, Keleher J, Smiga S, Rubenstein JLR. 2000. Pallial and subpallial derivatives in the embryonic chick and mouse telencephalon, traced by the expression of the genes *Dlx-2*, *Emx-1*, *Nkx-2.1*, *Pax-6*, and *Tbr-1*. *J Comp Neurol* 424:409-438.
- Rajagopalan S, Nicolas E, Vivancos V, Berger J, Dickson BJ. 2000a. Crossing the midline: roles and regulation of robo receptors. *Neuron* 28:767-777.
- Rajagopalan S, Vivancos V, Nicolas E, Dickson BJ. 2000b. Selecting a longitudinal pathway: Robo receptors specify the lateral position of axons in the *Drosophila* CNS. *Cell* 103:1033-1045.
- Ringstedt T, Braisted JE, Brose K, Kidd T, Goodman C, Tessier-Lavigne M, O'Leary DM. 2000. Slit inhibition of retinal axon growth and its role in retinal axon pathfinding and innervation patterns in the diencephalon. *J Neurosci* 20:4983-4991.
- Ronca F, Andersen JS, Paech V, Margolis RU. 2001. Characterization of slit protein interactions with glypican-1. *J Biol Chem* 276:29141-29147.
- Rothberg JM, Artavanis-Tsakonas S. 1992. Modularity of the Slit protein characterization of a conserved carboxy-terminal sequence in secreted proteins and a motif implicated in extracellular protein interactions. *J Mol Biol* 227:367-370.
- Rothberg JM, Hartley DA, Walther Z, Artavanis-Tsakonas S. 1988. slit: an EGF-homologous locus of *D. melanogaster* involved in the development of the embryonic central nervous system. *Cell* 55:1047-1059.
- Rothberg JM, Jacobs JR, Goodman CS, Artavanis-Tsakonas S. 1990. Slit: an extracellular protein necessary for development of midline glia and commissural axon pathways contains both EGF and LRR domains. *Genes Dev* 4:2169-2187.
- Rudenko G, Nguyen T, Chelliah Y, Sudhof TC, Deisenhofer J. 1999. The structure of the ligand-binding domain of neuroligin Ibeta: regulation of LNS domain function by alternative splicing. *Cell* 99:93-101.
- Schwanzel-Fukuda M, Pfaff DW. 1989. Origin of luteinizing hormone-releasing hormone neurons. *Nature* 338:161-164.
- Schwartz GA, Kostek C, Bless EP, Ahmad N, Tobet SA. 2001. Deleted in colorectal cancer (DCC) regulates the migration of luteinizing hormone-releasing hormone neurons to the basal forebrain. *J Neurosci* 21:911-919.
- Seeger M, Tear G, Ferres-Marco D, Goodman CS. 1993. Mutations affecting growth cone guidance in *Drosophila*: genes necessary for guidance toward or away from the midline. *Neuron* 10:409-426.
- Shepherd I, Luo Y, Lefcort F, Reichardt L, Raper JA. 1997. A sensory axon repellent secreted from ventral spinal cord explants is neutralized by antibodies raised against collapsin-1. *Development* 124:1377-1385.
- Shipley MT, Ennis M. 1996. Functional organization of the olfactory system. *J Neurobiol* 30:123-176.
- Shu T, Richards LJ. 2001. Cortical axon guidance by the glial wedge during the development of the corpus callosum. *J Neurosci* 21:2749-2758.
- Simpson JH, Bland KS, Fetter RD, Goodman CS. 2000a. Short-range and long-range guidance by slit and its robo receptors: a combinatorial code of Robo receptors controls lateral position. *Cell* 103:1019-1032.
- Simpson JH, Kidd T, Bland KS, Goodman CS. 2000b. Short-range and long-range guidance by slit and its robo receptors: Robo and Robo2 play distinct roles in midline guidance. *Neuron* 28:753-766.
- Sonnenfeld MJ, Jacobs JR. 1994. Mesectodermal cell fate analysis in *Drosophila* midline mutants. *Mech Dev* 46:3-13.
- Sotelo C, Chédotal A. 1997. Development of the olivocerebellar projection. *Perspect Dev Neurobiol* 5:57-67.
- Stein E, Tessier-lavigne M. 2001. Hierarchical organization of guidance receptors: silencing of netrin attraction by slit through a Robo/DCC receptor complex. *Science* 291:1928-1938.
- Steward O, Falk PM. 1991. Selective localization of polyribosomes beneath developing synapses: a quantitative analysis of the relationship between polyribosomes and developing synapses in the hippocampus and dentate gyrus. *J Comp Neurol* 314:545-557.
- Takahashi T, Fournier A, Nakamura F, Wang LH, Murakami Y, Kalb RG, Fujisawa H, Strittmatter SM. 1999. Plexin-neuropilin-1 complexes form functional semaphorin-3A receptors. *Cell* 99:59-69.
- Tamagnone L, Artigiani S, Chen H, He Z, Ming GI, Song H, Chédotal A, Winberg ML, Goodman CS, Poo M, Tessier-Lavigne M, Comoglio PM. 1999. Plexins are a large family of receptors for transmembrane, secreted, and GPI-anchored semaphorins in vertebrates. *Cell* 99:71-80.
- Tear G, Harris R, Sutaria S, Kilomanski K, Goodman CS, Seeger MA. 1996. commissureless controls growth cone guidance across the CNS midline in *Drosophila* and encodes a novel membrane protein. *Neuron* 16:501-514.
- Tessier-Lavigne M, Goodman CS. 1996. The molecular biology of axon guidance. *Science* 274:1123-1133.
- Tole S, Grove EA. 2001. Detailed field pattern is intrinsic to the embryonic mouse hippocampus early in neurogenesis. *J Neurosci* 21:1580-1589.
- Tole S, Christian C, Grove EA. 1997. Early specification and autonomous development of cortical fields in the mouse hippocampus. *Development* 124:4959-4970.
- Toni N, Buchs PA, Nikonenko I, Bron CR, Muller D. 1999. LTP promotes formation of multiple spine synapses between a single axon terminal and a dendrite. *Nature* 402:421-425.
- Vargesson N, Luria V, Messina I, Erskine L, Laufer E. 2001. Expression patterns of Slit and Robo family members during vertebrate limb development. *Mech Dev* 106:175-180.
- Wang KH, Brose K, Arnott D, Kidd T, Goodman C, Henzel W, Tessier-Lavigne M. 1999. Biochemical purification of a mammalian Slit protein as a positive regulator of sensory axon elongation and branching. *Cell* 96:771-784.
- Wassef M, Berod A, Sotelo C. 1981. Dopaminergic dendrites in the pars reticulata of the rat substantia nigra and their striatal input. Combined immunocytochemical localization of tyrosine hydroxylase and anterograde degeneration. *Neuroscience* 6:2125-2139.
- Wassef M, Chédotal A, Cholley B, Thomasset M, Heizmann CM, Sotelo C. 1992. Development of the olivocerebellar projection in the rat: I. Transient biochemical compartmentation of inferior olive. *J Comp Neurol* 323:529-536.
- William-Hogarth LC, Puche AC, Torrey C, Cai X, Song I, Kolodkin AL, Shipley MT, Ronnett GV. 2000. Expression of semaphorins in developing and regenerating olfactory epithelium. *J Comp Neurol* 423:565-578.
- Wu W, Wong K, Chen JH, Jiang ZH, Dupuis S, Wu JY, Rao Y. 1999.

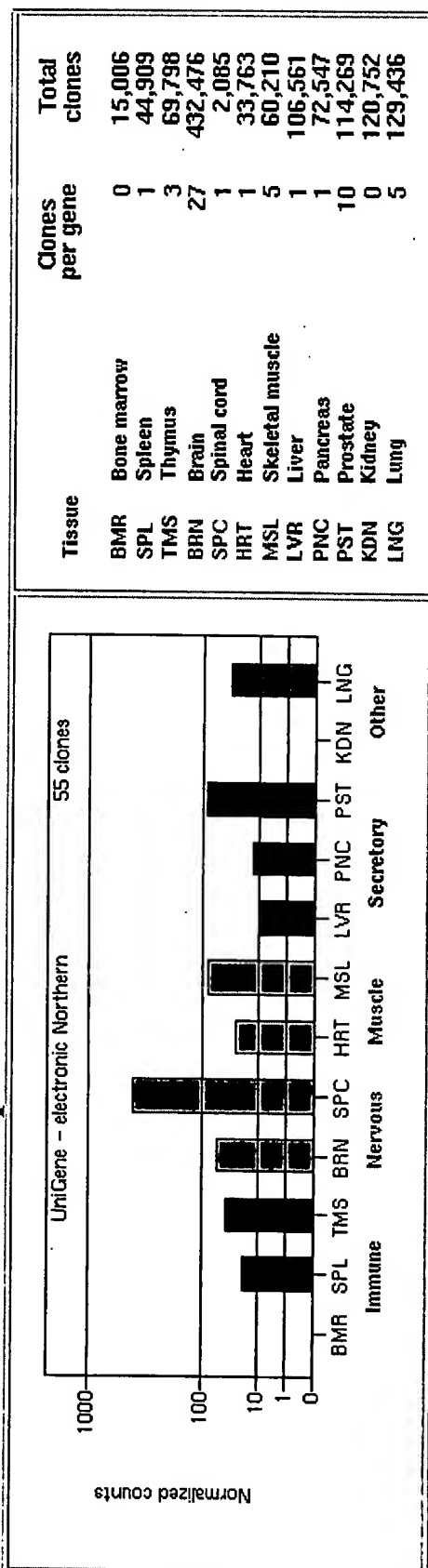
- Directional guidance of neuronal migration in the olfactory system by the protein slit. *Nature* 400:331-336.
- Wu JY, Feng L, Park H-T, Havlioglu N, Wen L, Tang H, Bacon KB, Jiang Z-H, Zhang X-C, Rao Y. 2001. The neuronal repellent Slit inhibits leukocyte chemotaxis induced by chemotactic factors. *Nature* 410:948-952.
- Yee KT, Simon HH, Tessier-Lavigne M, O'Leary DM. 1999. Extension of long leading processes and neuronal migration in the mammalian brain directed by the chemoattractant netrin-1. *Neuron* 24:607-622.
- Yeo SY, Little MH, Yamada T, Miyashita T, Halloran MC, Kuwada JY, Huh TL, Okamoto H. 2001. Overexpression of a slit homologue impairs convergent extension of the mesoderm and causes cyclopia in embryonic zebrafish. *Dev Biol* 230:1-17.
- Yoshihara Y, Kawasaki M, Tamada A, Fujita A, Hayashi H, Kagamiyama H, Mori K. 1997. OCAM: a new member of the neural cell adhesion molecule family related to zone-to-zone projection of olfactory and vomeronasal axons. *J Neurosci* 17:5830-5842.
- Yuan S-SF, Cox LA, Dasika GK, Lee EY-HP. 1999. Cloning and functional studies of a novel gene aberrantly expressed in RB-deficient embryos. *Dev Biol* 207:62-75.
- Zallen JA, Yi BA, Bargmann CI. 1998. The conserved immunoglobulin superfamily member SAX-3/Robo directs multiple aspects of axon guidance in *C-elegans*. *Cell* 92:217-227.
- Zhu Y, Li HS, Zhou L, Wu JY, Rao Y. 1999. Cellular and molecular guidance of GABAergic neuronal migration from an extracortical origin to the neocortex. *Neuron* 23:473-485.

Appendix B

Microarray Expression for ROBO1



Electronic Northern Expression for ROBO1



Microarrays

- **RNA source**

PolyA+ RNA samples from twelve normal human tissues were purchased from Clontech (Palo Alto, CA).

This collection of major human tissues includes:

Bone marrow (catalog number: 6573-1), brain (6516-1), heart (6533-1), kidney (6538-1), liver (6510-1), lung (6524-1), pancreas (6539-1), prostate (6546-1), skeletal muscle (6541-1), spinal cord (6593-1), spleen (6542-1) and thymus (6536-1).

- **Data Normalization**

Arrays were analyzed and expression values, called signal, was calculated for each gene by using Microarray Suit (MAS) version 5.0 software (Affymetrix, Santa Clara, CA) using default parameter settings. Scaling was not done via a MAS 5.0 option. Instead, the intensities of each array were log10 transformed and scaled to a constant reference value (global normalization). This reference value was the mean of all log intensities in all of the tissues.

- **Expression Profiles**

Duplicate measurements were obtained for twelve normal human tissues hybridized against Affymetrix GeneChips HG-U95A-E. The intensity values (shown on the y-axis) were normalized and drawn on a novel scale, which is an intermediate between log and linear scales. This enables displaying several orders of magnitude on the same graph, while emphasizing the differences between them.

- **Aggregate Expression**

The bar graphs represent the averaged expression level calculated for a given gene. The calculation is done by averaging all of the probe-sets individual profiles. The detailed expression profile with the annotation for each individual probe-sets are presented in the table on the given gene web-page.

- **Variation plots**

Multiple probe-sets corresponding to the given gene are included for its tissue vector calculation only if their normalized intensity levels reach a threshold in at least one tissue. The variation of included and excluded probe-sets are visualized in the x-y plane: the x-axis shows Pearson's correlations between individual probe-sets vectors and the average tissue vector; the y-axis shows the relative length of an individual probe-set vector (its scalar length divided by that of the average vector). The average is shown as a black square, while individual probe-sets are depicted as colored circles.

- **Probe set annotation**

The list of probes and their sequences was obtained from the Affymetrix public database

(<http://www.affymetrix.com/index.affx>), wherein each probe-set on Affymetrix HG-U95 is constructed from 16 probes 25

nucleotide long. 16 probes taken from each probe-set were aligned against the mRNA sequences from the most comprehensive public databases using the GeneAnnot algorithm (<http://genecards.weizmann.ac.il/geneannot/>). The alignment was performed using the BLAT algorithm (Kent, W.J. (2002) BLAT--the BLAST-like alignment tool. Genome Res, 12, 656-64.) allowing one mismatch along the sequence. The quality scores of a probe-set are given per specific genes, while taking into consideration the relationships of other genes that were aligned. Specificity and sensitivity parameters describe the quality of each probe-set.

- *Specificity calculation*

If a probe is aligned to a single gene its score will be 1. However, if it is aligned to n genes the value will be $1/n$. The specificity is calculated by the weighted summation of all probe values in the set, divided by the total number of aligned probes in the set.

- *Sensitivity calculation*

Probe set sensitivity is calculated by the summation of the successfully aligned probes divided by the total number of probes in the set (e.g., 16).

Electronic Northern

- *Electronic Northern method*

For the shown set of normal human tissues NCBI's Unigene dataset *Hs.data* is mined for information about the number of unique clones per gene per tissue. Clones are assigned to particular tissues by applying data-mining heuristics to Unigene's library information file *Hs.lib.info*. Electronic expression results were calculated by dividing the number of clones per gene by the number of clones per tissue. They were then normalized by multiplying by 1M, and the obtained normalized counts are presented on the same root scale as the experimental tissue vectors. This scale (shown on the y-axis) is an intermediate between log and linear scales. This enables displaying several orders of magnitude on the same graph, while emphasizing the differences between them.

Appendix C

Expression of *netrin-1*, *slit-1* and *slit-3* but not of *slit-2* after cerebellar and spinal cord lesions

Rosine Wehrle,^{1,2} Emeline Camand,^{1,2} Alain Chedotal,^{1,2} Constantino Sotelo^{1,2} and Isabelle Dusart^{1,2}

¹INSERM-U106/U616, Hôpital de la Salpêtrière, 75013 Paris France

²UMR7102, Université Pierre et Marie Curie, Bat B, 6^{ème} étage, case 12, 9 Quai Saint Bernard, 75005 Paris, France

Keywords: axotomy, mouse, rat, *robo*, *unc5h*

Abstract

To determine whether members of the Netrin-1 and Slit families and their receptors are expressed after central nervous system (CNS) injury, we performed *in situ* hybridization for *netrin-1*, *slit-1*, 2 and 3, and their receptors (*dcc*, *unc5h-1*, 2 and 3, *robo-1*, 2 and 3) 8 days, 2–3 months and 12–18 months after traumatic lesions of rat cerebellum. The expression pattern of these molecules was unchanged in axotomized Purkinje cells, whereas *unc5h3* expression was upregulated in deafferented granule cells. Cells expressing *slit-2* or *dcc* were never detected at the lesion site. By contrast, cells expressing *netrin-1*, *slit-1* and *slit-3*, *unc5h-1*, 2 and 3, and *robo-1*, 2 and 3 (*rig-1*) could be detected at the cerebellar lesion site as soon as 8 days after injury. Expression of *unc5h-2*, *robo-1*, *robo-2*, *slit-1* and *slit-3* at the lesion site was maintained until 3 months, and up to 12–18 months for *unc5h-1* and 3 and *robo-3*. Likewise, in the mouse spinal cord, *netrin-1*, *slit-1* and *slit-3* were also expressed at the lesion site 8 days after injury. Most of the cells expressing these mRNAs were located at the centre of the lesions, suggesting that they are macrophages/activated microglial cells (macrophagic cells) or meningeal fibroblastic cells. The macrophagic nature of most Netrin-1-positive cells and the macrophagic or fibroblastic nature of Robo-1-positive cells were corroborated by double staining. Thus, Netrin-1, Slits and their receptors may contribute to the regenerative failure of axons in the adult CNS by inhibiting axon outgrowth or by participating in the formation of the CNS scar.

Introduction

In the mammalian central nervous system (CNS), adult neurons fail to regenerate their axons after lesion. It is known that this failure is partly due to the presence of axon growth-inhibitory molecules in the local environment of the severed axons in myelin (Filbin, 2003; Schwab, 2004) and in the glial scar (Moon *et al.*, 2001). However, even after neutralization of these inhibitors, the number of severed axons that regenerate is low (Schwab *et al.*, 1993), reflecting either the poor intrinsic ability of central neurons to regenerate and/or the existence of additional inhibitory factors.

One tempting hypothesis is that chemorepellent molecules, which collapse embryonic growth cones and repel developing axons and migrating neurons, could be upregulated at the lesion site and surrounding glial scar after adult CNS injury. Chemotropic molecules have been identified in three gene families, the Semaphorins, the Netrins and the Slits (Culotti & Kolodkin, 1996; Brose & Tessier-Lavigne, 2000). Several class 3 secreted Semaphorins are highly expressed after CNS lesions, suggesting that they could inhibit axonal regeneration (De Winter *et al.*, 2002; Pasterkamp *et al.*, 1998a, b, c, 1999; Pasterkamp & Verhaagen, 2001). In addition, expression of the transmembrane semaphorin, Sema 4D, is upregulated by oligodendrocytes after spinal cord lesions (Moreau-Fauvarque *et al.*, 2003). By contrast, expression of the other members of these chemorepellent families has not yet been analysed

after traumatic lesion in mammalian CNS, the the most commonly used model for axon regeneration studies. Only an increase in *slit-2* mRNA in reactive astrocytes has been reported in the cryo-injured mouse cerebral cortex (Hagino *et al.*, 2003), a model not used to study axon regeneration.

The aim of this study was to determine whether *netrin-1*, *slit-1*, *slit-2* and *slit-3* and their receptors are expressed or upregulated after traumatic injury in the adult CNS of mammals. Netrin-1 has been shown to interact with the transmembrane receptors DCC (Deleted in Colorectal Cancer) and UNC5H (Keino-Masu *et al.*, 1996; Ackerman *et al.*, 1997; Leonardo *et al.*, 1997; Forcet *et al.*, 2002). In parallel, three members of the Roundabout (Robo) family, Robo-1 and 2 and Rig-1/Robo-3 have been shown to bind Slit molecules (Brose *et al.*, 1999). It is known that glial cell reactivity depends on the species and on the site of the lesion. For instance, after a traumatic injury in the CNS, rats develop cavities whereas mice do not (Dusart & Schwab, 1994; Dusart & Sotelo, 1994; Steward *et al.*, 1999; Morel *et al.*, 2002). In mice, astrocytes enter the necrotic area of traumatic cerebellar injury, but they do not enter after traumatic spinal cord injury (Morel *et al.*, 2002; Camand *et al.*, 2004). Owing to these species and location differences, we decided to carry out first a complete longitudinal study (from 8 days to 18 months after a traumatic lesion) in the rat cerebellum. For that purpose, we analysed the expression of *netrin-1*, *slit-1*, *slit-2* and *slit-3* mRNAs and their receptors *dcc*, *unc5h1*, 2 and 3 and *robo-1*, 2 and 3. Thereafter, the results were compared with those obtained with *netrin-1*, *slit-1*, *slit-2* and *slit-3* mRNAs in the mouse spinal cord 8 days after the lesion, the period of maximal expression of chemotropic factors following cerebellar lesions.

Correspondence: Dr I. Dusart, as above.
E-mail: isabelle.dusart@snv.jussieu.fr

Received 21 July 2005, revised 2 September 2005, accepted 5 September 2005

Materials and methods

All procedures were carried out in accordance with guidelines approved by the French Ministry of Agriculture, following European Standards. Twenty-one female Wistar rats (weighing 200 g at the time of lesion, Janvier, Le Genest St Isle, France), 12 female Swiss mice (weighing 20 g at the time of lesion, Janvier) and three *slit-1* knockout (KO) mice (Plump *et al.*, 2002) were used in this study. The rats were anesthetized with chloral hydrate (400 mg/kg i.p.) and the mice with ketamin (146 mg/kg) and xylazin (7.4 mg/kg). After the lesion, animals were returned to their cages and given free access to food and water. The procedures to induce cerebellar and spinal cord lesions were as described previously (Dusart & Sotelo, 1994; Camand *et al.*, 2004).

Lesioned animals were divided into two groups, which were, respectively, prepared for immunohistochemistry (three rats for 8 days and 1 month and three mice with a survival time of 8 days) and *in situ* hybridization (three rats for each of 8 days, 2–3 months and 12–18 months, and three mice with a survival time of 8 days). For controls, 12 nonoperated animals were processed in the same way (three per procedure). The lesioned cerebella and spinal cords were sectioned in the parasagittal plane.

In situ hybridization

cDNA encoding rat *slit-1*, rat *slit-2*, rat *slit-3*, mouse *netrin-1*, rat *dcc* and rat *Unc5h1*, 2 and 3 were as described by Keino-Masu *et al.* (1996), Serafini *et al.* (1996), Leonardo *et al.* (1997) and Marillat *et al.* (2002). The *in vitro* transcription was carried out by using the Riboprobe Gemini System II buffers (Promega, Madison, WI, USA) and probes were labeled with ³⁵S UTP (1000 Ci/mM; Amersham, Arlington Heights, IL, USA) as described in Fontaine & Changeux (1989). *In situ* hybridization was performed on fresh frozen cerebellar and spinal cord sections as described in Wehrle *et al.* (2001). The autoradiographs were analysed via bright- and dark-field microscopy by using a Zeiss Axiophot microscope or a Leica DMR microscope. Some of the slices were counterstained with cresyl violet.

Immunohistochemistry

Rats and mice were anesthetized and perfused through the aorta with 0.12 M phosphate-buffered (pH 7.4) 4% paraformaldehyde. Brains or spinal cords were removed, postfixed for 4 h and cryoprotected in 30% sucrose for 2 days. The cerebella and the spinal cord were cut in the parasagittal plane (24-μm-thick free-floating sections) on a freezing microtome (Leica). Rabbit polyclonal antibody against Netrin-1 (PC364, diluted 1 : 20, Oncogen research Products, Cambridge, UK; Madison *et al.*, 2000) and goat polyclonal antibody against Robo-1 (diluted 1 : 250, R&D Systems Europe, Lille France) were used. Rabbit polyclonal antibodies against fibronectin (diluted 1 : 500, Sigma, St Louis, MO, USA) were applied to reveal the presence of meningeal fibroblasts and non-CNS elements. Isolectin B4 from *Bandeira simplicifolia* coupled to FITC (diluted 0.02 mg/mL; Sigma) was used to visualize microglial cells and macrophages (Streit & Kreutzberg, 1987). The sections were incubated for 1 h in PBS containing 0.25% Triton X-100 (Sigma), 0.2% gelatin (Prolabo, Fontenay-sous-Bois, France) and 0.1% sodium azide (PBSGTA) containing 0.1 M lysine (blocking solution). Then, the sections were incubated overnight at room temperature in the primary antibodies at the dilutions indicated above in PBSGTA. The rabbit polyclonal antibodies against Netrin-1 and fibronectin were visualized with goat

antirabbit antibodies coupled to Cy3 (diluted 1 : 200, Jackson Immunoresearch, West Grove, PA, USA) and donkey antigoat coupled to AMCA (diluted 1 : 50, Jackson Immunoresearch), respectively. The mouse monoclonal antibody against Robo-1 was revealed with donkey antigoat coupled to Cy3 (diluted 1 : 200, Jackson Immunoresearch). Some of the sections were counterstained with Hoechst (bisbenzimidazole, 1 : 1000, Sigma) to label cell nuclei. Finally, the slices were washed several times with PBS, and mounted in mowiol (Calbiochem, La Jolla, CA, USA).

The sections were analysed using a Leica DMR microscope equipped with a coolsnap-fx camera (Princeton Instruments, Evry, France). Images were captured on a Dell computer using Metaview software (Universal Imaging Corporation, West Chester, PA, USA). In some cases, double staining was confirmed on 1-μm-thick confocal sections observed with a Leica confocal microscope (Plateforme d'Imagerie, IFR83). Images were treated and assembled using Adobe Photoshop software version 6.0 (Adobe System, Inc.).

Results

Expression in the cerebellum

In parasagittal sections of rat cerebellum 8 days after lesion, the knife cut only affects the vermis and is easily identified as the narrow gap dividing the lobules into dorsal and ventral portions (Fig. 1A). Under the cut, particularly in the ventral portions, large necrotic areas (Fig. 1A) filled with macrophages and activated microglial cells are generated (Fig. 1B). The narrow gap and these necrotic areas are considered to be the center of the lesion. They are surrounded by a wider zone of reactive astrocytes considered as the periphery of the lesion (Fig. 1C). This area extends throughout the white matter and most of the grey matter of lobules IV and VII, and contains not only reactive astrocytes but also microglial cells, oligodendrocytes and granule cells (Dusart & Sotelo, 1994; Dusart *et al.*, 1999). Two months after the lesion, the center of the lesion is either a cavity or a thin line containing macrophages and activated microglial cells (Fig. 1D and F). These central areas are surrounded by highly activated astrocytes that delineate the glial scar (Fig. 1E and G).

Netrin-1

In the intact adult rat cerebellum, *netrin-1* mRNA is exclusively expressed in interneurons of the molecular layer, Purkinje cells and deep nuclear neurons, as previously described in younger animals (Livesey & Hunt, 1997; Alcantara *et al.*, 2000). Eight days after the lesion, this neuronal expression remains unchanged. By contrast, at the center of the lesion, new cells organized in clusters strongly express *netrin-1* (see Fig. 6A, Table 1), whereas only sparse cells are labeled at the periphery in the glial scar. Two months postlesion, no *netrin-1* expression can be detected at the center of the lesion (Table 1). From this time point onwards, *netrin-1* expression is similar to that observed in the intact cerebellum.

Dcc

Whatever the time after injury, expression of *dcc* was similar to that in the intact cerebellum (i.e. faint labeling of the Purkinje cells), as previously described (Bloch-Gallego *et al.*, 1999; Table 1).

Unc5h-1, 2, 3

In the intact cerebellum, the neurons expressing *unc5h1* are deep nuclear neurons and granule cells (Fig. 2A). *Unc5h2* is detected in granule cells, molecular layer interneurons and glial cells in the white

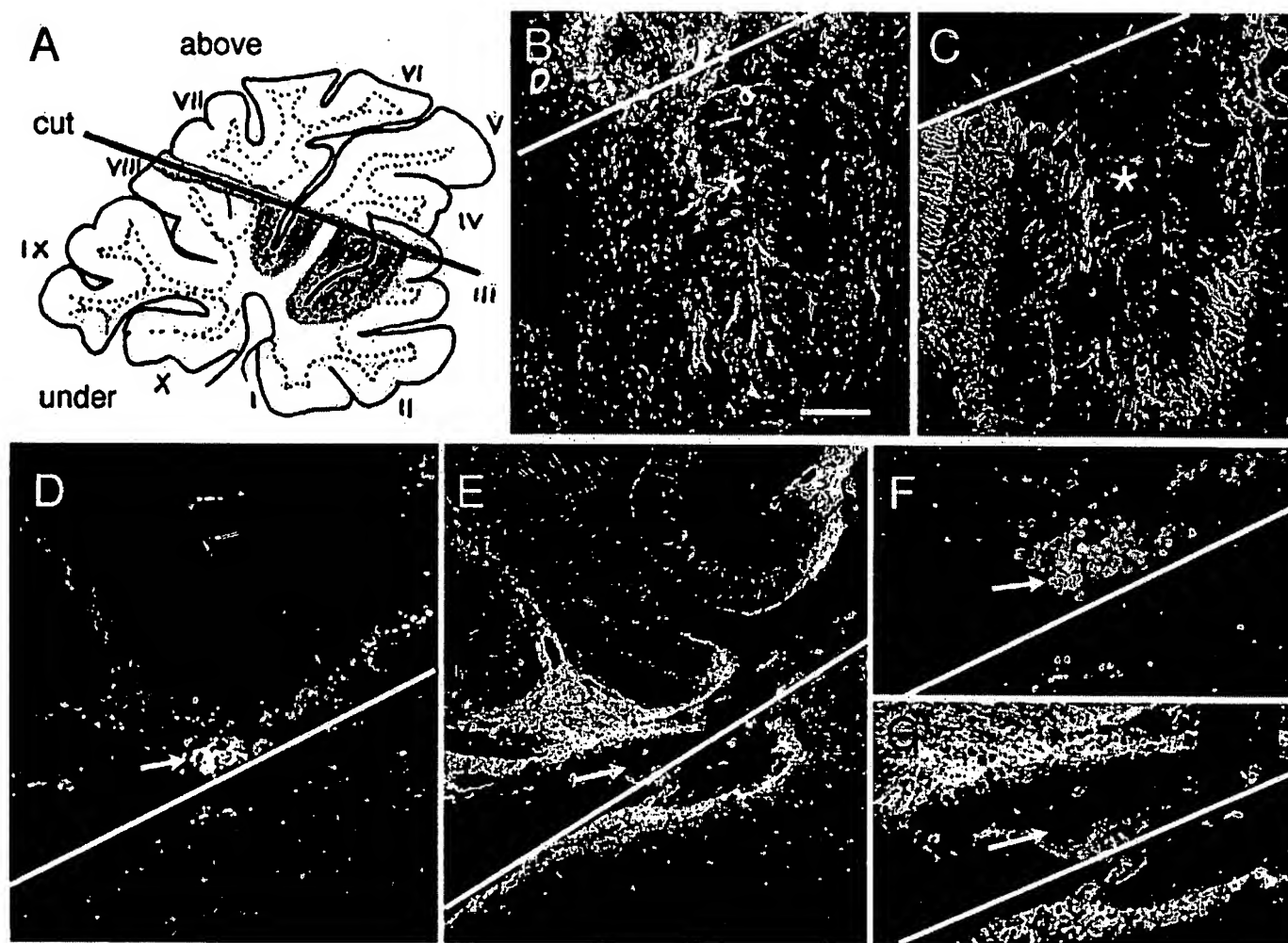


FIG. 1. (A) Schematic representation of a parasagittal section of a lesioned cerebellum. The cut (dark line) delineates the sectioned lobules (IV, V, VI and VII) located above the cut from the nonlesioned lobules (I, II, III, VIII, IX and X) located beneath the cut. The grey areas represent what we term here the lesion center. Asterisks indicate the necrotic areas under the cut. Adapted from Dusart & Sotelo (1994). Parasagittal cerebellar sections at 8 days post lesion (B and C), and 2 months post lesion (D–G) double stained with Isolecithin B4 (B, D and F) and anti-glial fibrillary acidic protein (GFAP) (C, E and G). Note the absence of GFAP immunostaining and the presence of Isolecithin B4-positive cells in the center of the lesion (asterisk indicates as in A the necrotic area). The white lines represent the cuts. Arrows in D–G point to the same area. Scale bar in B, 240 μ m (B–D) and 120 μ m (E and F).

matter (Fig. 2B). Purkinje cells, some cells in the granule cell layer that are presumably Golgi cells, and granule cells in lobule X express *unc5h3* (Fig. 2C). In the transected cerebella, additional cells express *unc5h1*, 2 and 3 at the center of the lesion at 8 days (Fig. 2D). *Unc5h2* expression in these cells is maintained up to 2 months (Fig. 2E), whereas expression of *unc5h1* and 3 is maintained up to 12 months (Fig. 2F, Table 1). At any time after the lesion, *unc5h3* expression can be detected at the center of the lesion and in the granule cells located in the lobules dorsal to the lesion cuts (Fig. 2F).

Slit-1, 2, 3

In the cerebellum, as described previously (Marillat *et al.*, 2002), *slit-1*, 2 and 3 are expressed in neurons of the lateral nucleus, *slit-1* and 2 in the interpositus nucleus, *slit-2* in Purkinje cells of lobules IX and X, and *slit-3* in granule cells. There was no modification of these expression patterns after the lesion (Fig. 3). However, many cells located at the center of the lesion strongly express *slit-1* mRNA at 8 days (Fig. 3A) and 2 months (Fig. 3B) but not after 3 months (Table 1). A few cells, at the lesion center, also express *slit-3* mRNA up to 2 months postlesion (Fig. 3C and D). This additional expression was not detected for *slit-2* transcripts (Table 1).

Robo-1, 2 and 3

In the intact cerebellum, *robo-1* can be detected in Purkinje cells, deep nuclear neurons and fibroblastic cells (Fig. 4A; Marillat *et al.*, 2002). *Robo-2* is expressed in deep nuclear neurons, Purkinje cells and a subpopulation of granule cells located around the fissura prima (Fig. 4B); and finally, *robo-3/rig-1* transcripts are present in granule cells, molecular layer interneurons and deep nuclear neurons (Fig. 4C). Following lesions, many cells strongly express *robo-1*, 2 and 3 at the center of the lesion (Fig. 4D–F). Expression is maintained up to 2 and 3 months for *robo-1* and 2 (Fig. 4E), and up to 12–18 months for *robo-3* (Fig. 4F).

Expression in the spinal cord

In the intact adult mouse spinal cord, cells expressing *netrin-1* mRNA are scattered within the grey and the white matter, and may correspond to motoneurons, and multiple classes of interneurons and oligodendrocytes, respectively (Manitt *et al.*, 2001). As previously reported (Moreau-Fauvarque *et al.*, 2003; Camand *et al.*, 2004), 8 days after a dorsal hemisection of the mouse spinal cord, two lesion areas can be distinguished: the center of the lesion filled with fibroblastic cells,

TABLE 1. Presence of guidance cues at the center of the cerebellar lesion

Molecule	8 days	2–3 months	12–18 months
<i>netrine-1</i>	+	–	–
<i>dcc</i>	–	–	–
<i>unc5h1</i>	+	+	+
<i>unc5h2</i>	+	+	–
<i>unc5h3</i>	+	+	+
<i>slit-1</i>	+	+	–
<i>slit-2</i>	–	–	–
<i>slit-3</i>	+	+	–
<i>robo-1</i>	+	+	–
<i>robo-2</i>	+	+	–
<i>robo-3/rig-1</i>	+	+	+

macrophages and activated microglial cells, and the periphery of the lesion defined by the presence of activated astrocytes, activated microglial cells, oligodendrocytes and polydendrocytes. In addition to the cells encountered in the intact spinal cord, numerous cells with strong *netrin-1* mRNA expression are detected at the center of the lesion (Fig. 5A).

In the intact mouse spinal cord, *slit-1*, *slit-2* and *slit-3* mRNAs are detected in all lamina of the thoracic grey matter but with slightly different repartitions. *Slit-1* expression is much stronger in the dorsal than in the ventral spinal cord (Fig. 5B). Expression of *slit-2* is similar to that of *slit-1*, with the highest level in the ventral region (Fig. 5C). Expression of *slit-3* is similar to that of *slit-2*, but is slightly less

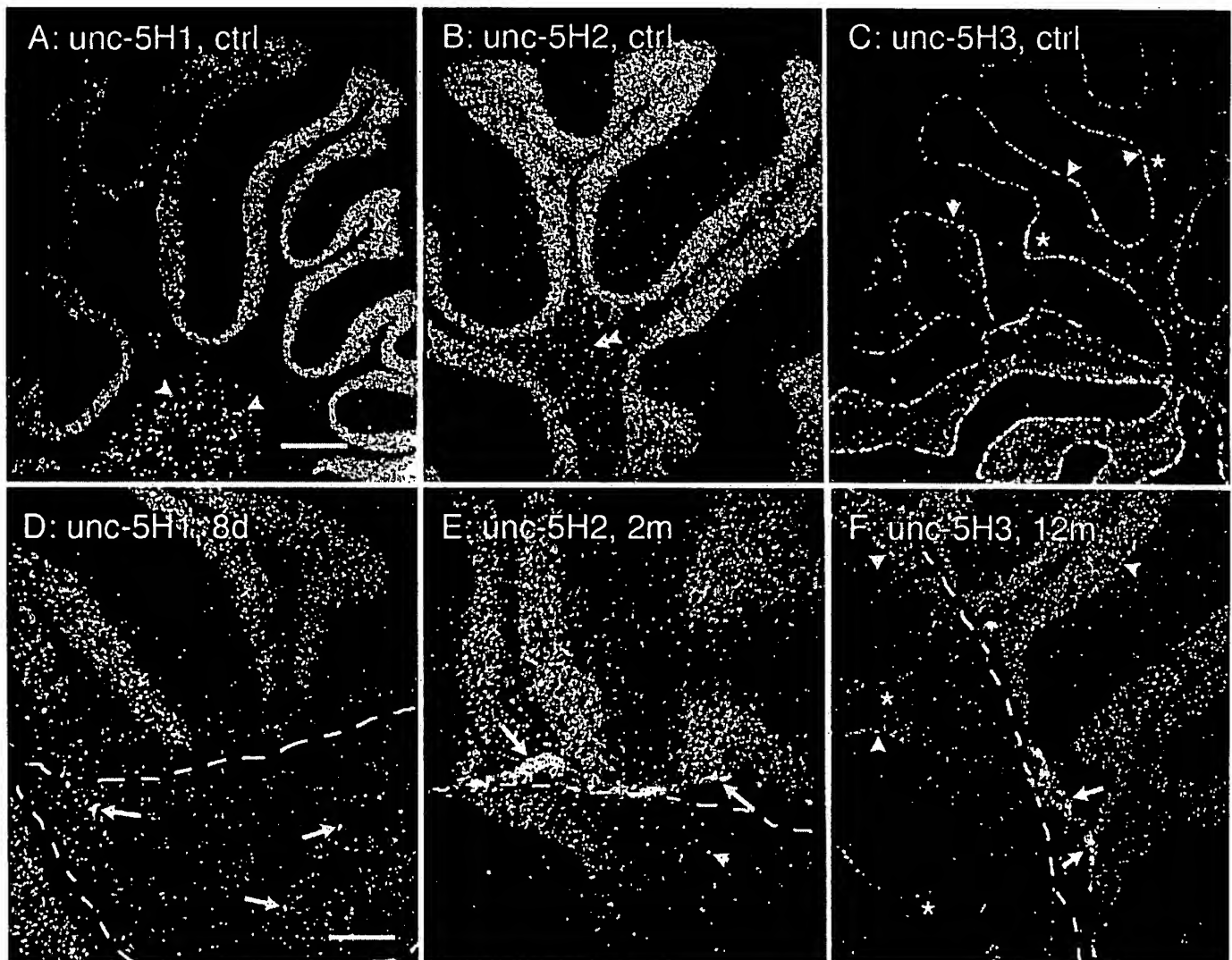


FIG. 2. Expression of *unc5h* in cerebellum. Parasagittal cerebellar sections of control (ctrl, A, B and C), 8 days post lesion (8d, D), 2 months post lesion (2m, E) and 12 months post lesion (12m, F) hybridized with the *unc5h1* (unc-5H1, A and D), *unc5h2* (unc-5H2, B and E) and *unc5h3* (unc-5H3, C, F) antisense probes. (A) Note the presence of *unc-5h1*-labeled granule cells (black asterisk) and deep nuclear neurons (arrowheads). (B) Note the presence of *unc-5h2*-labeled granule cells (black asterisk), and glial cells in the white matter (double arrowhead). (C) Note the presence of *unc-5h3*-labeled Purkinje cells (arrowheads) and that the only labeled granule cells are present in lobules X and IX (black asterisk), whereas granule cells in the other lobules are not labeled (white asterisks). (D) Eight days after lesion (8d), the granule cell neurons are still labeled (black asterisk) and numerous labeled cells (arrows) can be observed at the lesion site (dotted line). (E) Two months after the lesion (2m), in addition to the labeled granule cells (black asterisk), molecular interneurons and glial cells in the white matter (arrowheads), numerous clustered cells are also labeled (arrows) around the cut (dotted line). (F) Note the presence of *unc-5h3*-labeled cells (arrows) around the cut (dotted line) 12 months after the lesion (12m). Interestingly, the granule cells that are located in the sectioned lobules (above the cut) are now labeled (black asterisks), whereas the granule cells in the other lobules are still not labeled (white asterisks). Purkinje cells are still labeled (arrowheads). Scale bar in A, 670 μ m (A and C), 330 μ m (B, D and F) and 250 μ m (E).

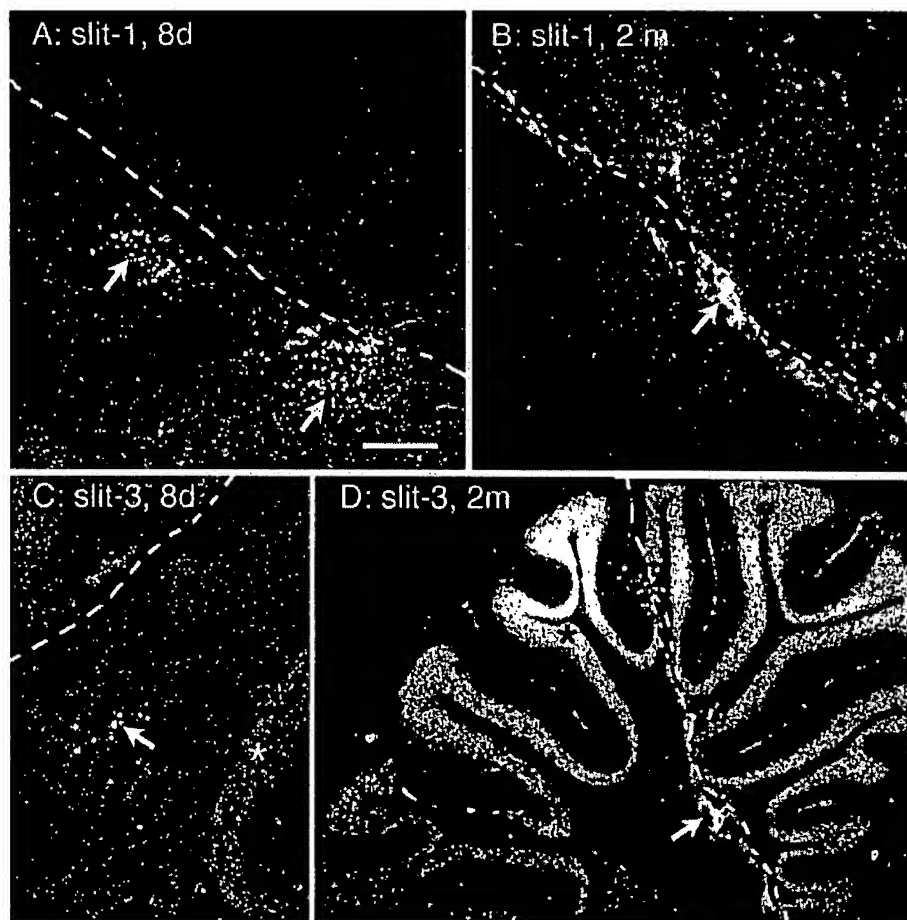


FIG. 3. Expression of *slit-1* and *slit-3* in the lesioned cerebellum. Parasagittal sections of lesioned cerebellum (8 days A and C, 2 months B and D) hybridized with the *slit-1* (*slit-1*, A and B) and the *slit-3* (*slit-3*, C and D) antisense probes. (A) Note the presence of two clusters of numerous heavily labeled cells (arrows) under the knife cut (dotted line). These areas are similar to those represented in Fig. 1A by asterisks. (B) Note the presence of numerous heavily labeled cells (arrow) around the knife cut (dotted line). (C) Note the presence of numerous heavily labeled cells (arrow) under the cut (dotted line). The granule cell layer is labeled (white asterisk). (D) Note the presence of numerous heavily labeled cells (arrow) around the knife cut (dotted line). The granule cell layer is labeled (black asterisk). Scale bar in A, 330 μ m (A–C) and 670 μ m (D).

intense (Fig. 5D). The cresyl violet counterstaining suggests that the cells expressing *slit* mRNAs are neurons and not glial cells, given that they are large and weakly stained by cresyl violet (Fig. 6C).

Eight days after a mouse spinal cord dorsal hemisection, *slit-1* and *slit-3* mRNAs are detected in cells at the center of the lesion (Fig. 5E and F). Here again, as in the cerebellum, expression of *slit-2* was not observed (data not shown). At the center of the lesion, *slit-3* mRNA seems more strongly expressed than that of *slit-1* (compare Fig. 5F with Fig. 5E), whereas in the cerebellum there are more cells expressing *slit-1* than *slit-3* (see above, Fig. 3A and C). We were able to validate our results by performing *slit-1* *in situ* hybridization in a *slit-1* KO mouse with a spinal cord lesion. Indeed, in this case, no *slit-1* mRNA was detected even at the center of the lesion (Fig. 5G). Moreover, in the *slit-1* KO mouse, *slit-2* mRNA was not upregulated (Fig. 5H).

Characterization of the cells

Our *in situ* hybridization results in cerebellar and spinal cord lesions have revealed cells strongly expressing *netrin-1* mRNA in and around the lesion, following a distribution pattern that mimics that of macrophagic and fibroblastic cells (see above). To characterize these cells further, we performed double labeling experiments using an

antibody against Netrin-1 and the Isolectin B4 coupled to FITC. On sections from intact animals, Netrin-1 immunostaining, although faint, corresponds to the labeling observed with *in situ* hybridization: molecular interneurons and Purkinje cells in the cerebellar cortex, some neurons in the grey matter and small cells in the white matter of the spinal cord (data not shown). In both types of lesions, clusters of round Netrin-1-immunoreactive cells are present at the lesion center (Fig. 6D–G). In addition, a mixture of round and ramified cells are observed at the periphery of spinal cord lesions (Fig. 6H–J) and to a lesser extent at the periphery of the cerebellar lesions (data not shown). However, although almost all Netrin-1-immunoreactive cells are double stained with Isolectin B4, only a small fraction of the Isolectin B4-positive cells are Netrin-1 immunoreactive (Fig. 6D–G). Thus, Netrin-1-positive cells belong to a subpopulation of activated microglial cells and macrophages.

In the intact cerebellum, Robo-1 is coexpressed in blood vessels with fibronectin (Fig. 6K, M and N) but not with Isolectin B4 (Fig. 6K, L and N). At the lesion site, in addition to these vascular associated Robo-1-expressing cells, which maintain their fibronectin expression (data not shown), there are other Robo-1-expressing cells that are double stained with Isolectin B4 (Fig. 6O and P). Therefore, as reported above for Netrin-1, only a subpopulation of Isolectin B4-positive cells are Robo-1 immunoreactive (Fig. 6O and P). For

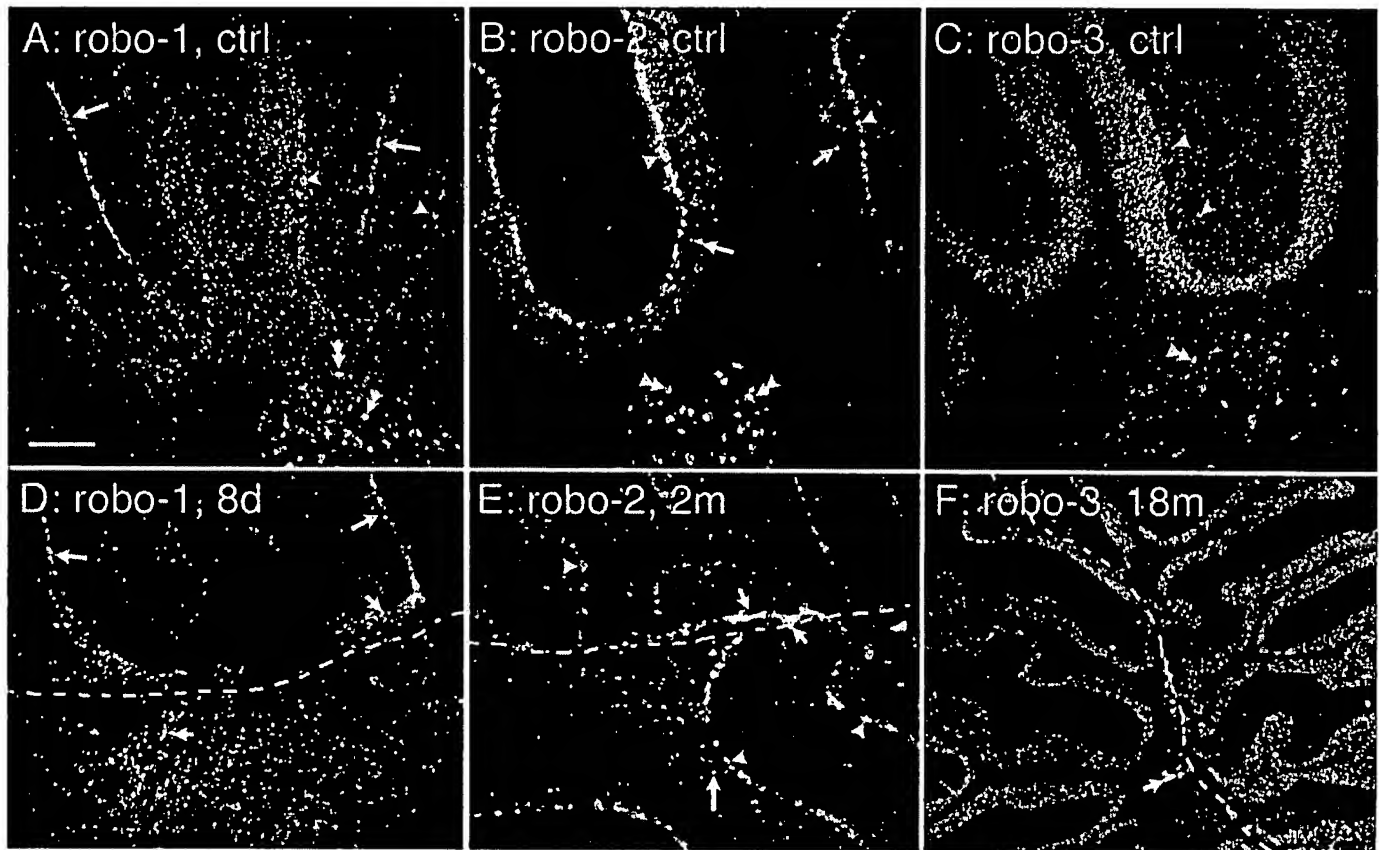


FIG. 4. Expression of *robos* in the cerebellum. Parasagittal cerebellar sections of control (A–C), 8 days post lesion (D), 2 months post lesion (E) and 18 months post lesion (F) hybridized with the *robo-1* (*robo-1*, A and D), *robo-2* (*robo-2*, B and E) and *robo-3/rig-1* (*robo-3*, C and F) antisense probes. (A) Note the presence of strong *robo-1* labeling in the meninges (arrows) and in the deep nuclear neurons (double arrowheads) and of a weak expression in the Purkinje cells (arrowheads). (B) Note the presence of a strong expression of *robo-2* in Purkinje cells (arrowheads), some presumably Golgi cells (arrows) and deep nuclear neurons (double arrowheads). The granule cell layer of some lobules is labeled (black asterisk), but not in other lobules (white asterisks). (C) Note the presence of *robo-3*-labeled granule cells (black asterisk), molecular interneurons (arrowheads) and deep nuclear neurons (double arrowheads). (D) Note the presence of numerous heavily *robo-1*-labeled cells (short arrows) in the continuation of the meninges (long arrows) and under the cut (dotted line). (E) Two months after lesion, numerous heavily *robo-2*-labeled cells (short arrows) can be detected around the cut (dotted line). Note the presence of a strong expression of *robo-2* in Purkinje cells (arrowheads) and in some presumably Golgi cells (arrows). (F) Up to 18 months after the lesion, some heavily *robo-3*-labeled cells (short arrow) can be detected around the cut (dotted line). The white asterisk indicates the labeled granule cells. Scale bar in A, 240 μ m (A–E) and 670 μ m (F).

identification of cells labeled with the other probes and in the absence of specific antibodies, we carried out an analysis on adjacent sections. These were double labeled with Hoechst stain to delineate the different cerebellar layers and with Isolectin B4 (Fig. 6Q), fibronectin (Fig. 6Q) or *robo-1* (Fig. 6R), *slit-1* (Fig. 6S), *slit-3* (Fig. 6T), *rig-1* (Fig. 6U), *dcc* (Fig. 6V), and *unc5h1*, 2 and 3 probes (data not shown). As described previously, no cells expressing *dcc* were detected at the lesion site (Fig. 6V). By contrast, the other mRNA probes always labeled the same cell clusters located at the lesion center (Fig. 6R–U) and containing Isolectin B4-positive cells as well as fibronectin-positive cells (Fig. 6Q). These results suggest that the cells revealed with *slit-1*, *slit-3*, *rig-1*, and *unc5h1*, 2 and 3 *in situ* hybridization are macrophagic or fibroblastic cells. Therefore, the population of macrophages and fibroblastic cells, at the lesion center, seems to be heterogeneous, and composed of several subclasses of specialized cells expressing different chemotropic factors.

Discussion

The aim of this work was to study the expression of chemotropic factors and their receptors following traumatic lesions in the adult rat cerebellum and mouse spinal cord. Expression patterns of these ligands

and receptors were first analysed by *in situ* hybridization in control adult animals. We corroborated the neuronal expressions of *netrin-1*, *dcc*, *unc5h3*, *slits* and *robos* in rat cerebellum, and added new information on the expressions of *unc5h1* and 2 in the cerebellum and of *slits* in the mouse spinal cord. Following lesion, the neuronal expression pattern of most of these molecules remained unchanged, although *unc5h3* expression was upregulated in de-afferented granule cells. More importantly, cells expressing *netrin-1*, *unc5h1*, 2 and 3, *slit-1* and 3, and *robo-1*, 2 and 3 were systematically present at the lesion site (lesion center and close periphery). Their position and the double staining with Isolectin B4 or with anti-fibronectin antibodies suggested that these cells were macrophagic and/or fibroblastic cells. The present results suggest that chemotropic molecules may contribute to inhibition of axon regeneration and glial scar formation.

Neuronal expressions of netrin-1, slits and their receptors, except that of *unc5h3*, are unchanged after traumatic lesions

The expression of chemotropic molecules in the developing CNS has been well documented (Ackerman *et al.*, 1997; Leonardo *et al.*, 1997; Livesey & Hunt, 1997; Bloch-Gallego *et al.*, 1999; Alcantara *et al.*, 2000; Marillat *et al.*, 2002) but much less is known regarding their

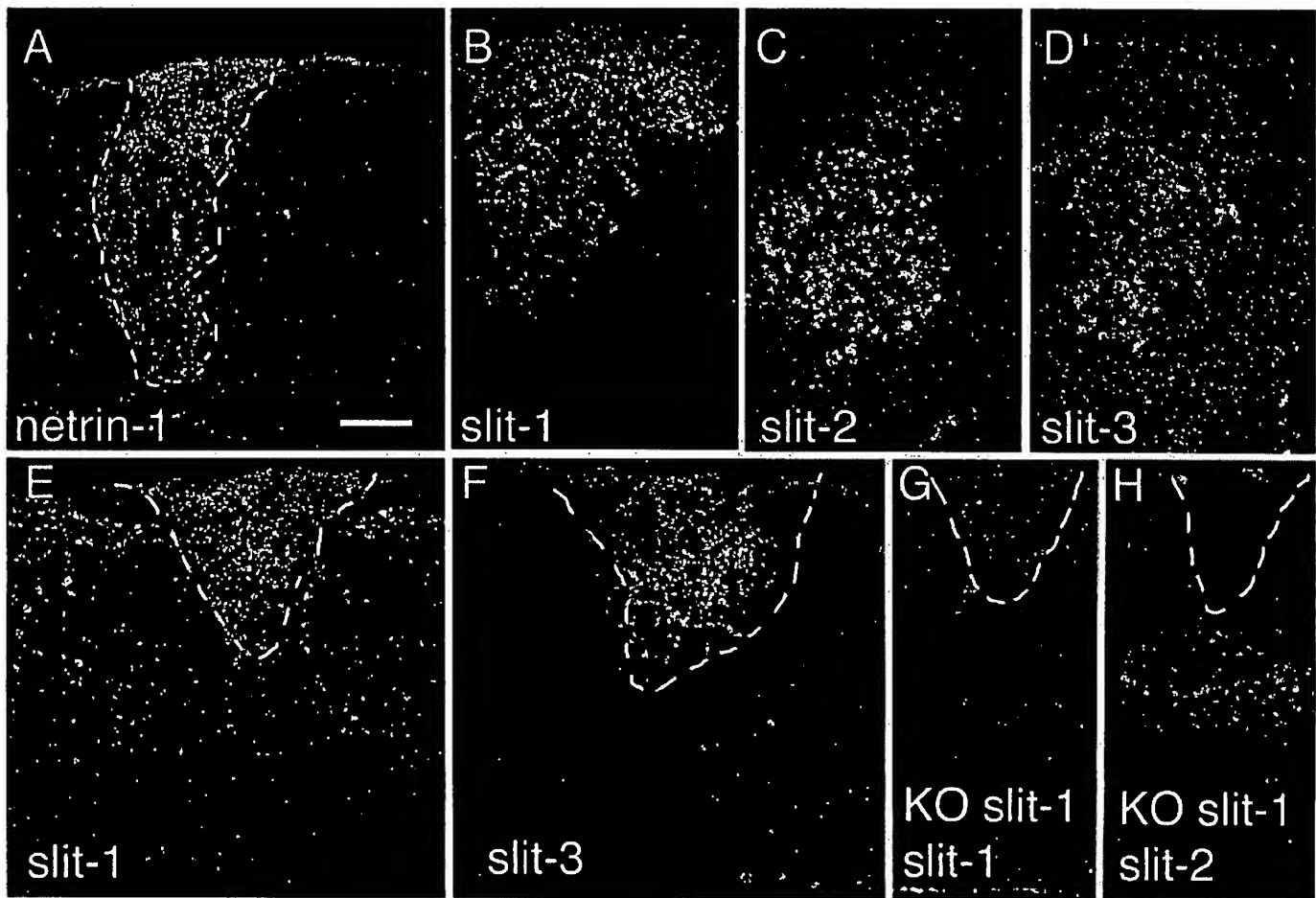


FIG. 5. Expression of *netrin-1* and *slit* mRNAs in the spinal cord. (A) Parasagittal section of sectioned spinal cord, 8 days post lesion, hybridized with the *netrin-1* (*netrin-1*) antisense probe. Note the presence of labeled cells in and around the lesion (dotted line). (B–D) Coronal sections of control spinal cord hybridized with the *slit-1* (B), *slit-2* (C) and *slit-3* (D) antisense probe, illustrating the pattern of expression of the three *slit* mRNAs. (E and F) Parasagittal sections of sectioned spinal cord, 8 days post lesion, hybridized with the *slit-1* (E) and *slit-3* (F) antisense probe. Note the presence of labeled cells within the lesion site (dotted line). The density of the autoradiographic signal is somewhat higher with the *slit-3* than with the *slit-1* antisense probe at the lesion center. (G and H) Parasagittal sections of KO *slit-1* sectioned spinal cord, 8 days post lesion, hybridized with the *slit-1* (G) and *slit-2* (H) antisense probes. Note the total absence of labeled cells in the spinal cord in G and only within the lesion site (dotted line) in H. Scale bar in A, 250 μ m (A) and 350 μ m (B–H).

expression in the adult (Manitt *et al.*, 2001; Marillat *et al.*, 2002). Our work showed that *unc5h1* and 2 are expressed in granule cells and *unc5h1* in deep nuclear neurons, whereas *unc5h2* is expressed in molecular layer interneurons and glial cells in the white matter. In the adult cerebellum, the expression patterns of *slits* and of *robos* are similar to those described by Marillat *et al.* (2002). In the spinal cord, we show here that the three *slits* are most probably expressed with different intensities in neurons. In addition, *slit-1*-expressing cells are detected more predominantly in the dorsal part of the spinal cord, whereas *slit-2* and *slit-3* are more highly expressed ventrally, including presumed motoneurons.

Changes in neuronal expression of chemotropic molecules (with the exception of *unc5h3*, see below) were not detected after lateromedial transection of the cerebellum or dorsal hemisection of the spinal cord. In particular, Purkinje cells do not regulate expression of *netrin-1* or *slits* after axotomy, contrary to what has been reported for other chemotropic molecules and for other neurons such as olfactory neurons (Pasterkamp *et al.*, 1998b; Williams-Hogarth *et al.*, 2000; Astic *et al.*, 2002) and retinal ganglion cells (Petrausch *et al.*, 2000; Ellezam *et al.*, 2001). This difference in the postaxotomy reaction observed for Purkinje cells (no increase of *netrin-1* or of *slit* mRNAs) confirms the diversity of the neuronal responses following axotomy.

Postlesion modifications of the receptors for chemotropic molecules have been reported: *dcc*, *unc5h1* and *unc5h2* are rapidly downregulated after axotomy of retinal ganglion cells (Petrausch *et al.*, 2000; Ellezam *et al.*, 2001). After cerebellar lesion, we did not detect any changes in the neuronal expression of *dcc*, *unc5h1* and 2, *robo-1* and 2, or *rig-1*. However, *unc5h3* expression was upregulated in the granule cells above the lesion site, i.e. in the sectioned lobules. These granule cells were not axotomized by the lesion, but a large proportion of them was deafferented. Indeed, transection of the cerebellar white matter axotomized not only Purkinje cells but also climbing and mossy fibers, the latter being the extracerebellar afferent fibers of the granule cells. Interestingly, *unc5h3* is transiently expressed by granule cells during development (Ackerman *et al.*, 1997), suggesting that after lesion granule cells reinitiate a developmental program.

Netrin-1, unc5hs, slits and robos are expressed by a subpopulation of macrophagic and/or fibroblastic cells

In contrast to the almost complete lack of changes in their neuronal expressions, *netrin-1*, *slit-1* and 3, *robo-1* and 2, *rig-1*, and *unc5h-1*, 2 and 3 transcripts appeared at the lesion center. The position of these

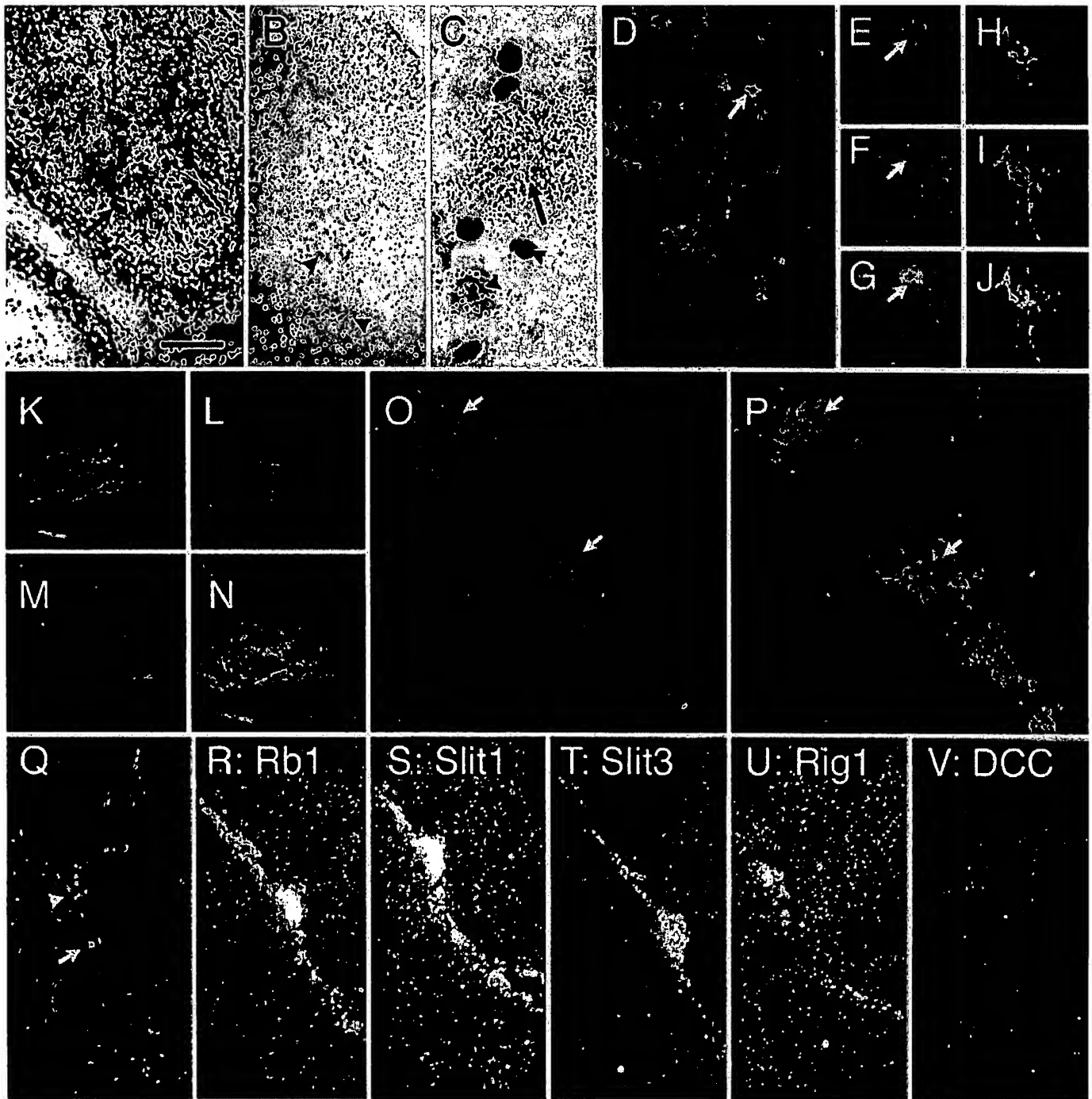


FIG. 6. (A) Parasagittal section of lesioned cerebellum, 8 days post lesion, hybridized with the *netrin-1* antisense probe and counterstained with cresyl violet (CV), illustrating numerous heavily labeled cells (arrow) in a region ventral to the cut, containing a large cell infiltrate, corresponding to the presumptive necrotic area (delineated by a dotted line; area similar to those indicated by asterisks in Fig. 1A). (B) Coronal section of control spinal cord hybridized with the *slit-2* antisense probe and counterstained with CV. Arrowheads point to labeled cells. Low magnification for orientation purposes. (C) Coronal section of control spinal cord hybridized with the *slit-2* antisense probe and counterstained with CV. Note that a large, faintly CV-stained cell highly expresses *slit-2* (arrow), a small, faintly CV-stained cell expresses also *slit-2* (arrowhead) in the ventral horn whereas the small, intensely CV-stained cells (double arrowhead) do not express *slit-2*. (D–J) Double staining, with anti-Netrin-1 in red (D, E, G, H and J) and Isolectin B4 in green (D, F, G, I and J), of macrophagic cells at the center of a cerebellar lesion (D–G) and of microglial cells at the periphery of a spinal cord lesion (H–J) 8 days post lesion. Arrows in D–G point to the same cell. (K–N) Confocal photomicrographs of a cerebellar parasagittal slice 2 months after lesion triple labeled with anti-Robo-1 (red, K and N), Isolectin B4 (green, L and N) and anti-fibronectin (blue, M and N). Note that Robo-1 and fibronectin stainings colocalize (presence of violet in N) whereas Robo-1 and Isolectin B4 stainings do not colocalize (absence of yellow in N). (O and P) Photomicrographs of a cerebellar sagittal slice 2 months after lesion triple labeled with anti-Robo-1 (red, O and P), Isolectin B4 (green, P) and antifibronectin (blue, O and P). Note that cells expressing Robo-1 are also stained with Isolectin B4 (O and P, arrows). (Q–V) Photomicrographs of adjacent sections from a 2-month-old cerebellar lesion stained with (Q) Hoechst (blue), Isolectin B4 (green) and anti-fibronectin (red); (R) *robo-1* antisense probe; (S) *slit-1* antisense probe; (T) *slit-3* antisense probe; (U) *rig-1* antisense probe; (V) *dcc* antisense probe. Note that in all the photomicrographs with exception of V, cells expressing the different mRNAs are present in the same area as those stained with Isolectin B4 (arrowheads in Q) or fibronectin (arrow in Q). Scale bars, 85 μ m (A), 300 μ m (B), 20 μ m (C), 50 μ m (D and K–N), 25 μ m (E–J and O–P) and 250 μ m (Q–V).

newly expressing cells at the center of the lesion suggests that they are not neural cells because neurons, oligodendrocytes and astrocytes were never found at such location. Indeed, our previous work has shown that there are many macrophages or activated microglial cells, as well as endothelial cells and fibroblasts, at the lesion center (Dusart & Sotelo, 1994; Camand *et al.*, 2004).

With regard to astrocytes, our results differ from those recently reported in reactive astrocytes after a cerebral cortical cryolesion, where *slit-2* mRNA expression was described (Hagino *et al.*, 2003). In our two post-traumatic central structures, *slit-2* mRNA was not detected in or around the lesion, and *slit* mRNAs were not detected in astrocytes, suggesting that this discrepancy is probably due to the type of lesion (cryolesion vs. traumatic injury) rather than to its location.

Furthermore, the macrophagic and/or fibroblastic nature of the cells newly expressing chemotropic factors or their receptors is supported by the data reported in this study. In short-term lesions (8 days) these cells were located in the large necrotic region, and were double labeled with anti-Netrin-1 antibodies and Isolectin B4, indicating that they belong to macrophages or activated microglial cells. Similarly, many cells populating the necrotic region and stained with Isolectin B4 or anti-fibronectin antibodies were double labeled with anti-Robo-1 antibodies or, on adjacent sections, labeled for different chemotropic molecules or their receptor mRNAs, suggesting that most of the cells expressing chemotropic factors at the lesion site are macrophagic or fibroblastic cells.

In conclusion, netrin-1 is expressed by a subpopulation of macrophages and ramified microglial cells. Similarly, *slit-1* and 3 and the receptors *unc5h1*, 2 and 3 and *robo-1*, 2 and 3 are also expressed – at least partly – by macrophagic cells, and probably also by fibroblasts, as already demonstrated for Sema-3A (Pasterkamp *et al.*, 1999; Pasterkamp & Verhaagen, 2001). These results suggest that within the scar, different cell types are able to secrete different chemorepellent molecules according to the lesion type.

Potential roles of these molecules in axon regeneration and glial scar formation

It is generally accepted that the failure of axonal regeneration in the mammalian CNS is the combined result of intrinsic neuronal properties and of environmental factors in the vicinity of sectioned axons. Since the classical work of Schwab *et al.* (1993), it has been shown that the adult CNS contains inhibitory molecules preventing axon growth and regeneration. Membrane neurite outgrowth inhibitors have been identified on oligodendrocytes and myelin: Nogo-A, an antigen of the IN-1 antibody (Chen *et al.*, 2000; GrandPré *et al.*, 2000), myelin-associated glycoprotein (McKerracher *et al.*, 1994; Mukhopadhyay *et al.*, 1994), Tenascin-R (Pesheva & Probstmeier, 2000), myelin-oligodendrocyte glycoprotein (Wang *et al.*, 2002) and recently Sema-4D (Moreau-Fauvarque *et al.*, 2003). Chondroitin sulfate proteoglycans have been demonstrated to be major inhibitory molecules of the glial scar (Moon *et al.*, 2001). Furthermore, all secreted class 3 Semaphorins have been detected in the scar after different types of lesions (Pasterkamp *et al.*, 1998b, c; Pasterkamp & Verhaagen, 2001; De Winter *et al.*, 2002). Here we report that, in addition to these inhibitory molecules, a subpopulation of macrophages and activated microglial cells, and probably meningeal cells, express and thus might secrete chemotropic molecules such as Netrin-1, Slit-1 and Slit-3 with a preponderant location at the lesion center. Neuronal expression of the chemotropic receptors is maintained after the lesion and some of them are expressed in Purkinje cells. Thus,

these chemotropic molecules could play a role in the failure of axon regeneration. However, because the number of macrophages expressing chemotropic factors is low and spatially restricted 2 months after the lesion, it is unlikely that these molecules could play a major role in the long-term failure of central axon regeneration.

It is well established that axon guidance molecules are also involved in cell migration. For instance, Netrin-1 and Slits influence the tangential migration of several types of neurons (Bloch-Gallego *et al.*, 1999; Yee *et al.*, 1999; Zhu *et al.*, 1999; Alcantara *et al.*, 2000; Causeret *et al.*, 2002; Marin *et al.*, 2003; Marillat *et al.*, 2004; Nguyen-Ba-Charvet *et al.*, 2004). Slits inhibit leucocyte migration (Wu *et al.*, 2001) and vascular endothelial cell migration (Wang *et al.*, 2003). Likewise, Netrin-1 modulates endothelial cell migration through Unc5h2 (Lu *et al.*, 2004; Park *et al.*, 2004). Thus, it is possible that expression of Netrin-1 and Slits in macrophagic cells at the lesion center is related to control of their migration to the necrotic region and to the neoangiogenesis that occurs after the CNS lesions. Last, DCC and Unc5h belong to a family of 'dependence receptors', so called because they induce apoptosis when unbound to their ligand (Mehlen *et al.*, 1998; Llambi *et al.*, 2001; Mehlen & Mazelin, 2003; Thiebault *et al.*, 2003). Thus, it is possible that the balance between expression of *netrin-1* and *unc5h* regulates the survival of macrophages. Interestingly, Netrin-1 is expressed only during the first 8 days and disappears thereafter in parallel with the decrease in the number of macrophages. The migration of macrophages, their subsequent elimination and the revascularization of the lesioned CNS are related to the process of scar formation, which is essential in determining the outcome of axon regeneration.

We have shown here that the expression of chemotropic factors following traumatic lesion is different in rat cerebellum and in mice spinal cord. For example, *slit-1* is more highly expressed in the cerebellum and *slit-3* in the spinal cord. More importantly, cells newly expressing chemotropic molecules after lesion are found in clusters in the cerebellum whereas they are more uniformly distributed in the spinal cord. It is of note that the scarring process, which involves both activation and migration of glial cells, is also different between rat and mice (Dusart & Schwab, 1994; Dusart & Sotelo, 1994; Steward *et al.*, 1999; Morel *et al.*, 2002; Camand *et al.*, 2004). Thus, we propose that the differences in expression of the Slit molecules at the lesion site between rat cerebellum and mouse spinal cord partly reflect the differences observed in the scarring processes in these two different central regions and species.

Acknowledgements

We thank Dr M. Teissier-Lavigne for the gift of Slit-1 knockout mice, and Richard Schwarzman, Plateforme imagerie IFR83, for his help with confocal microscopy. This work was supported by the Centre National de la Recherche Scientifique (CNRS), Institut National Scientifique pour la Recherche Médicale (INSERM), Institut pour la Recherche sur la Moelle épinière and Fondation pour la Recherche Médicale (FRM). E.C. is supported by La Mission Recherche et Technologie (MRT).

Abbreviations

CNS, central nervous system; DCC, Deleted in Colorectal Cancer; GFAP, glial fibrillary acidic protein; KO, knock-out; Robo, Roundabout.

References

- Ackerman, S.L., Kozak, L.P., Przyborski, S.A., Rund, L.A., Boyer, B.B. & Knowles, B.B. (1997) The mouse rostral cerebellar malformation gene encodes an UNC-5-like protein. *Nature*, **386**, 838–842.

- Alcantara, S., Ruiz, M., De Castro, F., Soriano, E. & Sotelo, C. (2000) Netrin 1 acts as an attractive or as a repulsive cue for distinct migrating neurons during the development of the cerebellar system. *Development*, **127**, 1359–1372.
- Astic, L., Pellier-Monnin, V., Saucier, D., Charrier, C. & Mehlen, P. (2002) Expression of netrin-1 and netrin-1 receptor, DCC, in the rat olfactory nerve pathway during development and axonal regeneration. *Neuroscience*, **109**, 643–656.
- Bloch-Gallego, E., Ezan, F., Tessier-Lavigne, M. & Sotelo, C. (1999) Floor plate and netrin-1 are involved in the migration and survival of inferior olivary neurons. *J. Neurosci.*, **19**, 4407–4420.
- Brose, K., Bland, K.S., Wang, K.H., Arnott, D., Henzel, W., Goodman, C.S., Tessier-Lavigne, M. & Kidd, T. (1999) Slit proteins bind Robo receptors and have an evolutionarily conserved role in repulsive axon guidance. *Cell*, **96**, 795–806.
- Brose, K. & Tessier-Lavigne, M. (2000) Slit proteins: key regulators of axon guidance, axonal branching, and cell migration. *Curr. Opin. Neurobiol.*, **10**, 95–102.
- Camand, E., Morel, M.P., Faissner, A., Sotelo, C. & Dusart, I. (2004) Long-term changes in the molecular composition of the glial scar and progressive increase of serotonergic fibre sprouting after hemisection of the mouse spinal cord. *Eur. J. Neurosci.*, **20**, 1161–1176.
- Causseret, F., Danne, F., Ezan, F., Sotelo, C. & Bloch-Gallego, E. (2002) Slit antagonizes netrin-1 attractive effects during the migration of inferior olivary neurons. *Dev. Biol.*, **246**, 429–440.
- Chen, M.S., Huber, A.B., van der Haar, M.E., Frank, M., Schnell, L., Spillmann, A.A., Christ, F. & Schwab, M.E. (2000) Nogo-A is a myelin-associated neurite outgrowth inhibitor and an antigen for monoclonal antibody IN-1. *Nature*, **403**, 434–439.
- Culotti, J.G. & Kolodkin, A.L. (1996) Functions of netrins and semaphorins in axon guidance. *Curr. Opin. Neurobiol.*, **6**, 81–88.
- De Winter, F., Oudega, M., Lankhorst, A.J., Hamers, F.P., Blits, B., Ruitenberg, M.J., Pasterkamp, R.J., Gispens, W.H. & Verhaagen, J. (2002) Injury-induced class 3 semaphorin expression in the rat spinal cord. *Exp. Neurol.*, **175**, 61–75.
- Dusart, I., Morel, M.P., Wehrle, R. & Sotelo, C. (1999) Late axonal sprouting of injured Purkinje cells and its temporal correlation with permissive changes in the glial scar. *J. Comp. Neurol.*, **408**, 399–418.
- Dusart, I. & Schwab, M.E. (1994) Secondary cell death and the inflammatory reaction after dorsal hemisection of the rat spinal cord. *Eur. J. Neurosci.*, **6**, 712–724.
- Dusart, I. & Sotelo, C. (1994) Lack of Purkinje cell loss in adult rat cerebellum following protracted axotomy: degenerative changes and regenerative attempts of the severed axons. *J. Comp. Neurol.*, **347**, 211–232.
- Ellezam, B., Selles-Navarro, I., Manitt, C., Kennedy, T.E. & McKerracher, L. (2001) Expression of netrin-1 and its receptors DCC and UNC-5H2 after axotomy and during regeneration of adult rat retinal ganglion cells. *Exp. Neurol.*, **168**, 105–115.
- Filbin, M.T. (2003) Myelin-associated inhibitors of axonal regeneration in the adult mammalian CNS. *Nat. Rev. Neurosci.*, **4**, 703–713.
- Fontaine, B. & Changeux, J.P. (1989) Localization of nicotinic acetylcholine receptor alpha-subunit transcripts during myogenesis and motor endplate development in the chick. *J. Cell Biol.*, **108**, 1025–1037.
- Forcet, C., Stein, E., Pays, L., Corset, V., Llambi, F., Tessier-Lavigne, M. & Mehlen, P. (2002) Netrin-1-mediated axon outgrowth requires deleted in colorectal cancer-dependent MAPK activation. *Nature*, **417**, 443–447.
- GrandPre, T., Nakamura, F., Vartanian, T. & Strittmatter, S.M. (2000) Identification of the Nogo inhibitor of axon regeneration as a Reticulon protein. *Nature*, **403**, 439–444.
- Hagino, S., Iseki, K., Mori, T., Zhang, Y., Hikake, T., Yokoya, S., Takeuchi, M., Hasimoto, H., Kikuchi, S. & Wanaka, A. (2003) Slit and glypican-1 mRNAs are coexpressed in the reactive astrocytes of the injured adult brain. *Glia*, **42**, 130–138.
- Keino-Masu, K., Masu, M., Hinck, L., Leonardo, E.D., Chan, S.S., Culotti, J.G. & Tessier-Lavigne, M. (1996) Deleted in Colorectal Cancer (DCC) encodes a netrin receptor. *Cell*, **87**, 175–185.
- Leonardo, E.D., Hinck, L., Masu, M., Keino-Masu, K., Ackerman, S.L. & Tessier-Lavigne, M. (1997) Vertebrate homologues of *C. elegans* UNC-5 are candidate netrin receptors. *Nature*, **386**, 833–838.
- Livesey, F.J. & Hunt, S.P. (1997) Netrin and netrin receptor expression in the embryonic mammalian nervous system suggests roles in retinal, striatal, nigral, and cerebellar development. *Mol. Cell Neurosci.*, **8**, 417–429.
- Llambi, F., Causseret, F., Bloch-Gallego, E. & Mehlen, P. (2001) Netrin-1 acts as a survival factor via its receptors UNC5H and DCC. *EMBO J.*, **20**, 2715–2722.
- Lu, X., Le Noble, F., Yuan, L., Jiang, Q., De Lafarge, B., Sugiyama, D., Breant, C., Claes, F., De Smet, F., Thomas, J.L., Autiero, M., Carmeliet, P., Tessier-Lavigne, M. & Eichmann, A. (2004) The netrin receptor UNC5B mediates guidance events controlling morphogenesis of the vascular system. *Nature*, **432**, 179–186.
- Madison, R.D., Zomorodi, A. & Robinson, G.A. (2000) Netrin-1 and peripheral nerve regeneration in the adult rat. *Exp. Neurol.*, **161**, 563–570.
- Manitt, C., Colicos, M.A., Thompson, K.M., Rousselle, E., Peterson, A.C. & Kennedy, T.E. (2001) Widespread expression of netrin-1 by neurons and oligodendrocytes in the adult mammalian spinal cord. *J. Neurosci.*, **21**, 3911–3922.
- Marillat, V., Cases, O., Nguyen-Ba-Charvet, K.T., Tessier-Lavigne, M., Sotelo, C. & Chédotal, A. (2002) Spatiotemporal expression patterns of slit and robo genes in the rat brain. *J. Comp. Neurol.*, **442**, 130–155.
- Marillat, V., Sabatier, C., Failli, V., Matsunaga, E., Sotelo, C., Tessier-Lavigne, M. & Chédotal, A. (2004) The slit receptor RIG-1/Robo3 controls midline crossing by hindbrain precerebellar neurons and axons. *Neuron*, **43**, 69–79.
- Marin, O., Plump, A.S., Flames, N., Sanchez-Camacho, C., Tessier-Lavigne, M. & Rubenstein, J.L.R. (2003) Directional guidance of interneuron migration to the cerebral cortex relies on subcortical Slit1/2-independent repulsion and cortical attraction. *Development*, **130**, 1889–1901.
- McKerracher, L., David, S., Jackson, D.L., Kottis, V., Dunn, R.J. & Braun, P.E. (1994) Identification of myelin-associated glycoprotein as a major myelin-derived inhibitor of neurite growth. *Neuron*, **13**, 805–811.
- Mehlen, P. & Mazelin, L. (2003) The dependence receptors DCC and UNC5H as a link between neuronal guidance and survival. *Biol. Cell*, **95**, 425–436.
- Mehlen, P., Rabizadeh, S., Snipas, S.J., Assa-Munt, N., Salvesen, G.S. & Bredesen, D.E. (1998) The DCC gene product induces apoptosis by a mechanism requiring receptor proteolysis. *Nature*, **395**, 801–804.
- Moon, L.D., Asher, R.A., Rhodes, K.E. & Fawcett, J.W. (2001) Regeneration of CNS axons back to their target following treatment of adult rat brain with chondroitinase ABC. *Nat. Neurosci.*, **4**, 465–466.
- Moreau-Fauvarque, C., Kumanogoh, A., Camand, E., Jaillard, C., Barbin, G., Boquet, I., Love, C., Jones, Y., Kikutani, H., Lubetzki, C., Dusart, I. & Chédotal, A. (2003) The transmembrane semaphorin Sema4D/CD100, an inhibitor of axonal growth, is expressed on oligodendrocytes and upregulated after CNS lesion. *J. Neurosci.*, **23**, 9229–9239.
- Morel, M.P., Dusart, I. & Sotelo, C. (2002) Sprouting of adult Purkinje cell axons in lesioned mouse cerebellum: 'non-permissive' versus 'permissive' environment. *J. Neurocytol.*, **31**, 633–647.
- Mukhopadhyay, G., Doherty, P., Walsh, F.S., Crocker, P.R. & Filbin, M.T. (1994) A novel role for myelin-associated glycoprotein as an inhibitor of axonal regeneration. *Neuron*, **13**, 757–767.
- Nguyen-Ba-Charvet, K.T., Picard-Riera, N., Tessier-Lavigne, M., Baron-Van Evercooren, A., Sotelo, C. & Chédotal, A. (2004) Multiple roles for slits in the control of cell migration in the rostral migratory stream. *J. Neurosci.*, **24**, 1497–1506.
- Park, K.W., Crouse, D., Lee, M., Karnik, S.K., Sorensen, L.K., Murphy, K.J., Kuo, C.J. & Li, D.Y. (2004) The axonal attractant Netrin-1 is an angiogenic factor. *Proc. Natl Acad. Sci. USA*, **101**, 16210–16215.
- Pasterkamp, R.J., De Winter, F., Giger, R.J. & Verhaagen, J. (1998a) Role for semaphorin III and its receptor neuropilin-1 in neuronal regeneration and scar formation? *Prog. Brain Res.*, **117**, 151–170.
- Pasterkamp, R.J., De Winter, F., Holtmaat, A.J. & Verhaagen, J. (1998b) Evidence for a role of the chemorepellent semaphorin III and its receptor neuropilin-1 in the regeneration of primary olfactory axons. *J. Neurosci.*, **18**, 9962–9976.
- Pasterkamp, R.J., Giger, R.J., Ruitenberg, M.J., Holtmaat, A.J., De Wit, J., De Winter, F. & Verhaagen, J. (1999) Expression of the gene encoding the chemorepellent semaphorin III is induced in the fibroblast component of neural scar tissue formed following injuries of adult but not neonatal CNS. *Mol. Cell Neurosci.*, **13**, 143–166.
- Pasterkamp, R.J., Giger, R.J. & Verhaagen, J. (1998c) Regulation of semaphorin III/collapsin-1 gene expression during peripheral nerve regeneration. *Exp. Neurol.*, **153**, 313–327.
- Pasterkamp, R.J. & Verhaagen, J. (2001) Emerging roles for semaphorins in neural regeneration. *Brain Res. Brain Res. Rev.*, **35**, 36–54.
- Pesheva, P. & Probstmeier, R. (2000) The yin and yang of tenascin-R in CNS development and pathology. *Prog. Neurobiol.*, **61**, 465–493.
- Petrasch, B., Jung, M., Leppert, C.A. & Stuermer, C.A. (2000) Lesion-induced regulation of netrin receptors and modification of netrin-1 expression in the retina of fish and grafted rats. *Mol. Cell Neurosci.*, **16**, 350–364.

- Plump, A.S., Erskine, L., Sabatier, C., Brose, K., Epstein, C.J., Goodman, C.S., Mason, C.A. & Tessier-Lavigne, M. (2002) Slit1 and Slit2 cooperate to prevent premature midline crossing of retinal axons in the mouse visual system. *Neuron*, **33**, 219–232.
- Schwab, M.E. (2004) Nogo and axon regeneration. *Curr. Opin. Neurobiol.*, **14**, 118–124.
- Schwab, M.E., Kapfhammer, J.P. & Bandtlow, C.E. (1993) Inhibitors of neurite growth. *Annu. Rev. Neurosci.*, **16**, 565–595.
- Serafini, T., Colamarino, S.A., Leonardo, E.D., Wang, H., Beddington, R., Skarnes, W.C. & Tessier-Lavigne, M. (1996) Netrin-1 is required for commissural axon guidance in the developing vertebrate nervous system. *Cell*, **87**, 1001–1014.
- Steward, O., Schauwecker, P.E., Guth, L., Zhang, Z., Fujiki, M., Inman, D., Wrathall, J., Kempermann, G., Gage, F.H., Saatman, K.E., Raghupathi, R. & McIntosh, T. (1999) Genetic approaches to neurotrauma research: opportunities and potential pitfalls of murine models. *Exp. Neurol.*, **157**, 19–42.
- Streit, W.J. & Kreutzberg, G.W. (1987) Lectin binding by resting and reactive microglia. *J. Neurocytol.*, **16**, 249–260.
- Thiebaut, K., Mazelin, L., Pays, L., Llambi, F., Joly, M.O., Scoazec, J.Y., Saurin, J.C., Romeo, G. & Mehlen, P. (2003) The netrin-1 receptors UNC5H are putative tumor suppressors controlling cell death commitment. *Proc. Natl Acad. Sci. USA*, **100**, 4173–4178.
- Wang, K.C., Koprivica, V., Kim, J.A., Sivasankaran, R., Guo, Y., Neve, R.L. & He, Z. (2002) Oligodendrocyte-myelin glycoprotein is a Nogo receptor ligand that inhibits neurite outgrowth. *Nature*, **417**, 941–944.
- Wang, B., Xiao, Y., Ding, B.B., Zhang, N., Yuan, X., Gui, L., Qian, K.X., Duan, S., Chen, Z., Rao, Y. & Geng, J.G. (2003) Induction of tumor angiogenesis by Slit-Robo signaling and inhibition of cancer growth by blocking Robo activity. *Cancer Cell*, **4**, 19–29.
- Wehrle, R., Caroni, P., Sotelo, C. & Dusart, I. (2001) Role of GAP-43 in mediating the responsiveness of cerebellar and precerebellar neurons to axotomy. *Eur. J. Neurosci.*, **13**, 857–870.
- Williams-Hogarth, L.C., Puche, A.C., Torrey, C., Cai, X., Song, I., Kolodkin, A.L., Shipley, M.T. & Ronnett, G.V. (2000) Expression of semaphorins in developing and regenerating olfactory epithelium. *J. Comp. Neurol.*, **423**, 565–578.
- Wu, J.Y., Feng, L., Park, H.T., Havlioglu, N., Wen, L., Tang, H., Bacon, K.B., Jiang, Z., Zhang, X. & Rao, Y. (2001) The neuronal repellent Slit inhibits leukocyte chemotaxis induced by chemotactic factors. *Nature*, **410**, 948–952.
- Yee, K.T., Simon, H.H., Tessier-Lavigne, M. & O'Leary, D.M. (1999) Extension of long leading processes and neuronal migration in the mammalian brain directed by the chemoattractant netrin-1. *Neuron*, **24**, 607–622.
- Zhu, Y., Li, H.-S., Zhou, L., Wu, J.Y. & Rao, Y. (1999) Cellular and molecular guidance of GABAergic neuronal migration from an extracortical origin to the neocortex. *Neuron*, **23**, 473–485.

Appendix D

santa cruz biotechnology, inc.

Log In | My Account | View Order | Wish List | Help? |



The Power of Question

Product Search

Welcome! 0 Items in Cart

Search Browse our Catalog 

Advanced S

HOME

WHAT'S NEW?

SUPPORT

COMPANY

SHOP

home » Neurobiology » robo Antibody / robo Antibodies

robo Antibody / robo Antibodies

PRODUCT NAME	CATALOG #	ISOTYPE	EPITOPE	APPLICATIONS
robo1 (N-20) Antibody	sc-16611	goat IgG	N-terminus (h)	WB, IF
robo1 (I-20) Antibody	sc-16612	goat IgG	N-terminus (h)	WB, IP, IF
robo1 (H-200) Antibody	sc-25672	rabbit IgG	1452-1651 (h)	WB, IP, IF
Robo1 (dN-19) Antibody	sc-19715	goat IgG	internal (Dm)	WB, IF
Robo1 (dP-20) Antibody	sc-19716	goat IgG	internal (Dm)	WB, IF
robo2 (C-20) Antibody	sc-16615	goat IgG	internal (h)	WB, IF
robo2 (H-100) Antibody	sc-25673	rabbit IgG	1281-1380 (h)	WB, IP, IF
robo2 (D-16) Antibody	sc-31605	goat IgG	internal (h)	WB, IF
robo2 (G-20) Antibody	sc-31606	goat IgG	internal (h)	WB, IF
robo2 (K-18) Antibody	sc-31607	goat IgG	C-terminus (h)	WB, IP, IF
Robo2 (dN-20) Antibody	sc-19718	goat IgG	N-terminus (Dm)	WB, IF
Robo2 (dC-20) Antibody	sc-19720	goat IgG	C-terminus (Dm)	WB, IF
robo3 (C-14) Antibody	sc-46493	goat IgG	C-terminal (h)	WB, IF
robo3 (N-17) Antibody	sc-46495	goat IgG	N-terminal (h)	WB, IF
robo3 (C-18) Antibody	sc-46496	goat IgG	C-terminal (h)	WB, IF
Robo3 (dN-20) Antibody	sc-19721	goat IgG	N-terminus (Dm)	WB, IP, IF
robo4 (C-20) Antibody	sc-46497	goat IgG	C-terminus (h)	WB, IP, IF
robo4 (D-19) Antibody	sc-46498	goat IgG	internal (h)	WB, IF
robo4 (N-17) Antibody	sc-46499	goat IgG	N-terminus (h)	WB, IF
robo4 (S-16) Antibody	sc-46500	goat IgG	internal (h)	WB, IF

robo Antibody / robo specific siRNA gene silencers are also available. These include: robo1 siRNA (h): sc-42252, robo2 siRNA (h): sc-42254, robo2 siRNA (m): sc-42255, robo3 siRNA (h): sc-44498, robo3 siRNA (m): sc-44499, and robo4 siRNA (m): sc-44501.



Copyright ©, 2006-2007, Santa Cruz Biotechnology, Inc. All Rights Reserved. LEGAL